RNI: DELENG/2005/15153
Publication: 15th of every month
Posting: 19th/20th of every month at NDPSO

No: DL(E)-01/5079/14-16
Licensed to post without pre-payment U(E) 28/2014-16
Rs.150

ISSN 0973-2136

www.mycoordinates.org

Coordinates

Volume XI, Issue 06, June 2015

THE MONTHLY MAGAZINE ON POSITIONING, NAVIGATION AND BEYOND

A stand-alone positioning method

Application of a multi-sensor approach to near shore hydrography

Gain perspective in real-world GNSS simulation

The GNSS simulator in the R&S®SMBV100A vector signal generator
Expensive, inflexible simulation of GNSS scenarios is a thing of the past. Now you can easily and cost-effectively test your satellite receivers under realistic conditions.

- Comes with a variety of predefined environment models such as "rural area", "urban canyon", "bridge" and "highway"
- Allows flexible configuration of realistic user environments including atmospheric modeling, obscuration, multipath, antenna characteristics and vehicle attitude

The R&S®SMBV100A generates all relevant communications and broadcasting standards such as LTE, HSPA+, WLAN, HD Radio™ and FM stereo.

To find out more, go to
www.rohde-schwarz.com/ad/smbv-gnss

R&S®SMBV-GNSS

ROHDE&SCHWARZ

© airpano.com

STANDARDISED, CONSISTENT DATA COLLECTION AND TRANSFER IS POSSIBLE.

As a utility professional, gathering consistent data in the field and getting that same data back to the office is critical. Now you don't have to deal with varying pen and paper notes prone to data entry errors. With **Trimble® TerraFlex™ software**, you can quickly collect reliable, standardised information with easy-to-create customisable templates on any smart device or professional-level handheld. Field data is automatically synced to a central server back at the office so you can send and receive updates in real-time, even with existing data—all without leaving the job at hand. Whether you are inspecting field assets, carrying out damage assessments, or performing routine safety and maintenance jobs, Trimble TerraFlex workflows give you confidence in the reliability of your collected utilities data so you can act quickly.

Trimble InSphere

TerraFlex is part of Trimble InSphere™, a cloud based platform of software, data and services to streamline workflows for geospatial enterprises.

FREE TRIAL! Discover how TerraFlex mobile solutions can work for utility organisations at www.trimble.com/terraflex

© 2015, Trimble Navigation Limited. All rights reserved. Trimble and the Globe & Triangle logo is a trademark of Trimble Navigation Limited, registered in the United States and in other countries. InSphere and TerraFlex are trademarks of Trimble Navigation Limited. All other trademarks are the property of their respective owners. GEO-060 (04/15)

Trimble

In this issue

Coordinates Volume 11, Issue 06, June 2015

Articles

Application of a multi-sensor approach to near shore hydrography Andrew Waddington 8 **Hydrographic survey of river Drava branches** Dino Dragun, Ana Gavran and Vedran Car 15 **Determining the maritime baseline for marine cadastre** Robin Seet, David Forrest and Jim Hansom 19 **On the transformation of time system in relativity based on SOFA and .NET** Shenquan Tang, Jianan Wei and Erhu Wei 24 **A stand-alone positioning method for kinematic applications** M Halis Saka, Reha Metin Alkan and Alişir Özperçin 37 **Assessing the Quality of an UAV-based Orthomosaic and Surface Model of a Breakwater** Maria João Henriques, Ana Fonseca, Dora Roque, José Nuno Lima and João Marnoto 40

Columns

My Coordinates Editorial 6 **News** Snippets 47 GNSS 50 Imaging 54 UAV 55 LBS 55 Galileo update 56 GIS 58 Industry 59 **Old Coordinates** 48 **Mark your calendar** June 2015 to December 2015 62

This issue has been made possible by the support and good wishes of the following individuals and companies Ana Fonseca, Ana Gavran, Andrew Waddington, Alişir Özperçin, David Forrest, Dino Dragun, Dora Roque, Erhu Wie, João Marnoto, Jianan Wie, Jim Hansom, José Nuno Lima, M Halis Saka, Maria João Henriques, Reha Metin Alkan, Robin Seet, Shenquan Tang and Vedran Car; Antcom, CHC, HiTarget, Javad, Micorsoft Vexcel, Navcom, Pentax, Spirent, Riegl, Rohde & Schwarz, Trace Me, Trimble, and many others.

Mailing Address
A 002, Mansara Apartments
C 9, Vasundhara Enclave
Delhi 110 096, India.
Phones +91 11 22632607, 98102 33422, 98107 24567
Fax +91 11 22632607

Email
[information] talktous@mycoordinates.org
[editorial] bal@mycoordinates.org
[advertising] sam@mycoordinates.org
[subscriptions] iwant@mycoordinates.org

Web www.mycoordinates.org

Coordinates is an initiative of CMPL that aims to broaden the scope of positioning, navigation and related technologies. CMPL does not neccesarily subscribe to the views expressed by the authors in this magazine and may not be held liable for any losses caused directly or indirectly due to the information provided herein. © CMPL, 2015. Reprinting with permission is encouraged; contact the editor for details.

Annual subscription (12 issues)
[India] Rs.1,800 [Overseas] US$100

Printed and published by Sanjay Malaviya on behalf of Coordinates Media Pvt Ltd
Published at A 002 Mansara Apartments, Vasundhara Enclave, Delhi 110096, India.
Printed at Thomson Press (India) Ltd, Mathura Road, Faridabad, India

Editor Bal Krishna
Owner Coordinates Media Pvt Ltd (CMPL)
Designed at Spring Design (ajay@springdesign.in)

This issue of Coordinates is of 64 pages, including cover.

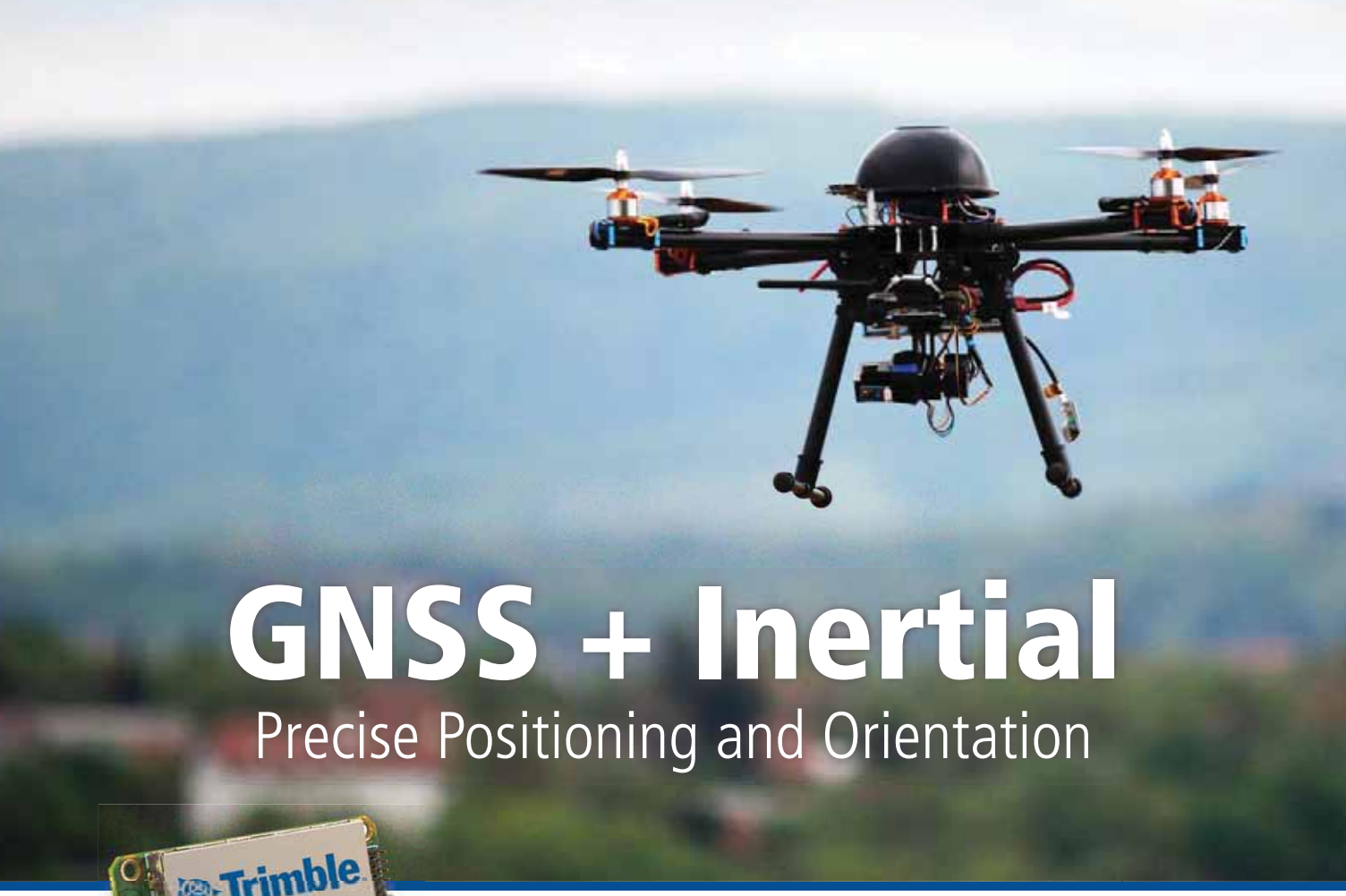

GNSS + Inertial

Precise Positioning and Orientation

60mm x 67mm

THE TRIMBLE BD935-INS — A PRECISON GNSS + INERTIAL MODULE DELIVERING RTK AND ORIENTATION IN REAL TIME

The BD935-INS is a compact module that integrates triple frequency GNSS and MEMS Inertial sensors to provide precise real-time position and attitude.

FOR HIGH-PERFORMANCE, PRECISE POSITIONING IN A COMPACT, MOBILE-READY DESIGN

- 336 Channels
- GPS, GLONASS, Galileo and BeiDou
- Integrated 3-D MEMS Sensors
- 100Hz RTK Position and Orientation
- Also available in IP67 enclosure

The BD935-INS module features a high accuracy GNSS receiver for precise position and an integrated MEMS inertial sensor package for 3-D orientation to serve applications requiring position and attitude. The GNSS + Inertial combination delivers more stability and robustness than GNSS alone.

Trimble

Trimble GNSS OEM

InTech.trimble.com

© Copyright 2014, Trimble. All rights reserved. All other trademarks are the property of their respective owners. TPC103 (05/15)

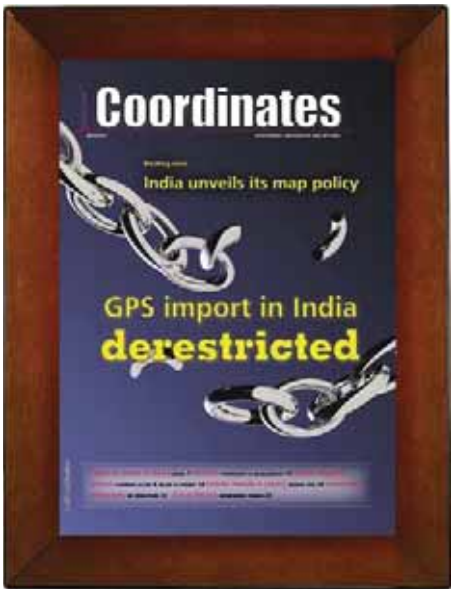

It has been ten years now

This issue of Coordinates takes us into 11th year.

Exactly ten years before, in June 2005

We came out with the first issue.

With a desire to explore the domain

And contribute in the process

By widening the awareness,

Raising issues, Initiating debates

Indulging in discussions and expanding the knowledge.

And if we could do

Even a little of 'our bit'

It was because of the support

Of our readers, authors and advertisers.

We shall continue our journey

with the same passion, enthusiasm and commitment

Bal Krishna, Editor
bal@mycoordinates.org

ADVISORS Naser El-Sheimy PEng, CRC Professor, Department of Geomatics Engineering, The University of Calgary Canada, George Cho Professor in GIS and the Law, University of Canberra, Australia, Professor Abbas Rajabifard Director, Centre for SDI and Land Administration, University of Melbourne, Australia, Luiz Paulo Souto Fortes PhD Associate Director of Geosciences, Brazilian Institute of Geography and Statistics -IBGE, Brazil, John Hannah Professor, School of Surveying, University of Otago, New Zealand

HI-TARGET Surveying the world, Mapping the future

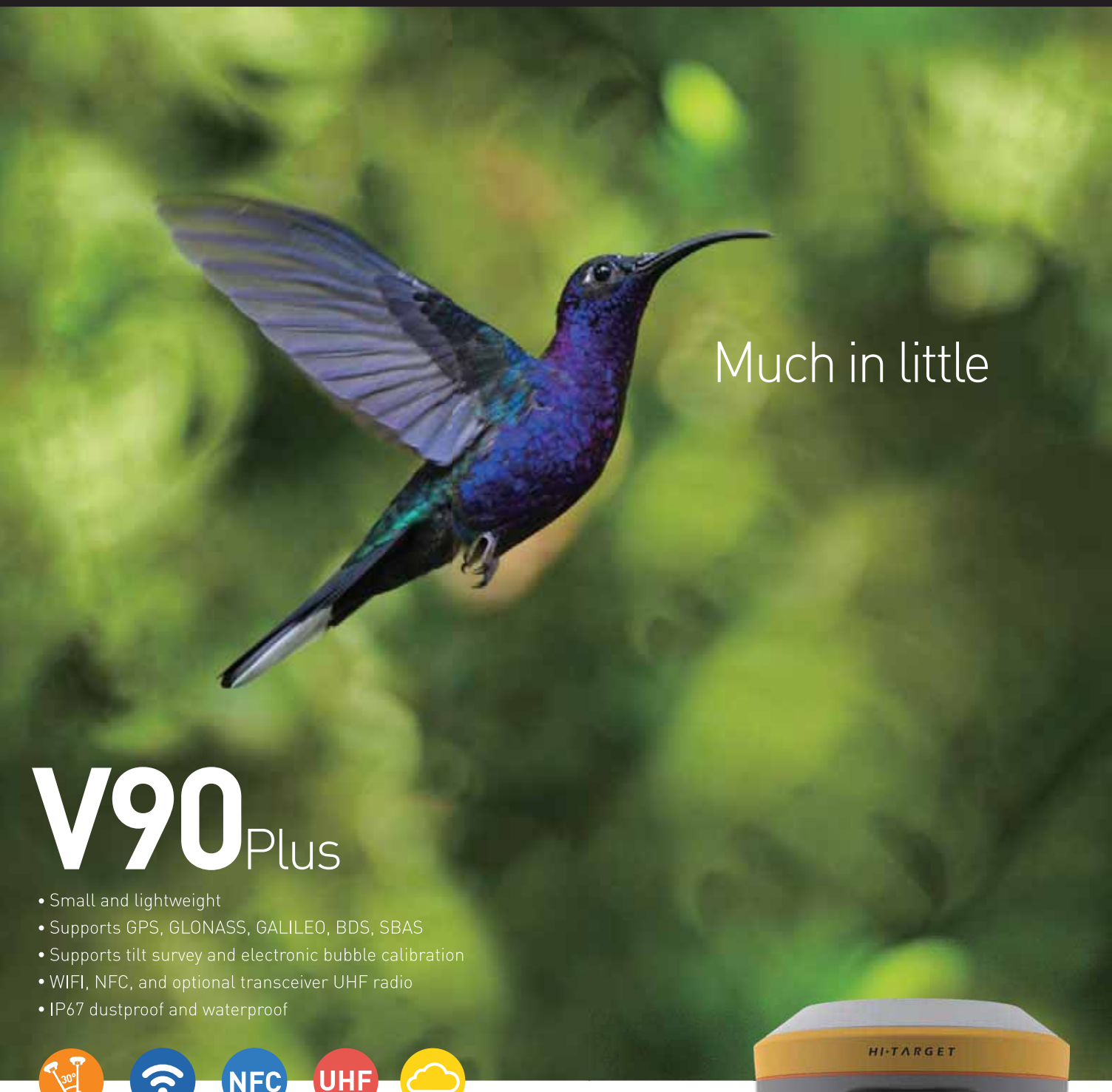

Much in little

V90 Plus

- Small and lightweight
- Supports GPS, GLONASS, GALILEO, BDS, SBAS
- Supports tilt survey and electronic bubble calibration
- WIFI, NFC, and optional transceiver UHF radio
- IP67 dustproof and waterproof

www.hi-target.com.cn info@hi-target.com.cn

FC CE IP67

Application of a multi-sensor approach to near shore hydrography

A cost-benefit analysis

Andrew Waddington
Director,
LW Partners Ltd, UK

Geospatial data in the nearshore region provides information that underpins development and contributes directly to the infrastructure of the area both offshore and on land

The shallow water coastal environment characterises the critical interface between activities at sea and on land. Much of the economic activity at sea that is now being recognised as the Blue Economy takes place 'out there', away from our focus of attention on land. But all of it, at some stage, in order to be relevant to our lives, comes to the shore, and in doing so it passes through the shallow water coastal environment. This is the bit of the maritime world that most of us can associate with and are, at least, aware of. This is also the zone where growth in the Blue Economy and expansion from the land into the sea meet, and where there is potential conflict of interests and increasing pressure in terms of resources, one of which is space.

In order to manage and regulate a space it is first necessary to have some idea of what that space consists of. This is a given on land and yet seems not to be at sea. Some of this is because there really has been no requirement to manage or control the space at sea apart from in a fairly 1 or 2 dimensional fashion. Traditional navigation was a significant driver and has created the historical emphasis for hydrography to be concentrated on safety of shipping. This has largely been the reason why there are some areas well surveyed at sea and others almost not at all. The main factors for safe navigation have been the draught of ships, the main trade routes and entry and exit from ports. This has driven the survey requirement and, as long as we know there is enough water for a ship going about its normal business not to run into danger that has sufficed.

This is similarly the case with explorations for minerals and gas at sea. The purpose of the surveys has been to meet the needs of the resources being mined or drilled, including some very precise work for rig siting and pipeline laying, but essentially the requirement away from these specifics has been simply to know that there is nothing adjacent to or around the area of interest that is going to interfere with the mineral extraction itself.

Appreciation of the more macro nature of the ocean environment started in practical terms with weather forecasting. The weather does have the ability to impact the sorts of specific areas mentioned above and much of the oceanographic work that has gone on in the past century is related to understanding the impact of the oceans on weather patterns so that they can be factored in to the more specific operations of shipping, mineral extraction and coastal design.

But even here, the scale of the events as we understand them means that our understanding of the oceanographic space itself tends to be on a scale that limits it application to uses appropriate to that scale.

So what's changed? Mostly it is twofold: the improvement in our understanding and awareness of the interdependence of the land and sea environment in the nearshore region, and the increasing pressures that are being put on this same region by developments that are

Figure 1: Nearshore processes (AAM Pty Ltd)

taking place mainly on land. These two factors have been the major reason why there has been a large increase in interest in managing and regulating the nearshore region, and consequently why it is becoming increasingly important to improve our understanding of the space that we are operating in.

The role of hydrography in environmental management

The role of the nearshore region in environmental management is well understood. The days of discarding untreated waste into the sea are thankfully largely behind us and regulation of dumping is now almost universal. Similarly there is a clear understanding of the impact of agricultural and industrial practices on the nearshore environment and there is a growing willingness, often backed-up by regulation, to control the chemicals that run-off from land and factory into rivers and seas.

Regulation has created a requirement to understand the flow of water, whether contaminated or not, and its interaction

Figure 2: The nearshore environment (Commons Licence)

with the larger body of water in the nearshore region and even its connection with the wider oceans. Much of this can be done by modelling the fluid flows based on tidal streams, currents and wind but the models themselves are heavily influenced by factors such as the underlying shape of the area on which the model is run and the friction that results from interaction of the fluids with the base of the model. In the real world, the model has to make an allowance for the real shape of the seafloor and also the makeup of the seabed in material terms because there is a considerable difference in the friction and drag associated with the varying seabed materials: fluid mud, sand or rock.

This is where hydrography has a major role in environmental management. By providing the information on the space in which the environmental management has to take place, the outputs from models can be improved and the environment itself monitored more directly. This input of terrain model, seabed texture and classification can also be combined with detailed measurement of water flow at specific locations, analysis of the water itself and mapping of the benthos in order to build a complete picture of the environment being managed. The outcome is better informed decision making and hopefully regulation that is effective, understood and enforceable.

The role of hydrography in civil engineering

Hydrography in civil engineering introduces challenges of scale at the opposite end to the environmental role. Changes in shipping design, particularly propulsion systems, and in materials as well as in attitudes towards risk and risk mitigation mean that the standards currently required in civil engineering projects on land, particularly where there is the potential for harm to life or the environment, are increasingly expected and called for at sea.

Furthermore, improvements in acoustic and visualisation technology in hydrography offer savings in term of cost and time over traditional engineering measurement in the marine environment. It is now possible to visualise in 3D underwater using acoustic systems.

The role of hydrography in economic and social development

The Blue Economy has the potential to provide extraordinary resources. The expansion of mineral extraction offshore and of renewable energy are just two examples of the emerging importance of the Blue Economy where the relevance of hydrography is already established.

Figure 3: Civil engineering in the nearshore (AAM Pty Ltd)

It is in the nearshore region however that the importance is most pronounced and probably least appreciated.

The nearshore region represents the area where all of these factors, including shipping patterns and leisure activities, combine to produce the most pressure on resources, particularly space. Whilst there are some temporal elements that reduce the squeeze in this area, such as tides and daylight, the limiting factor to using these areas optimally is the limitations of space, in all 3 dimensions.

A cost-benefit analysis – valuing infrastructure spend

Applying appraisal principles to hydrographic projects in support of energy, transport, flood risk and coastal erosion and communications.

Situation – there is demand for a new anchorage and landing point for cruise passengers in the SW Pacific islands. Currently a major cruise operator visits the island as part of their cruise cycle, visiting the island around every few days and staying for a day in the main town, which is served by a harbour with a jetty big enough for a cruise liner.

The cruise operator has identified a bay that they would like to use to land their passengers. The purpose is to provide the passengers with access to a picturesque bay with a beach so that the cruise experience is advanced. The cruise ship needs to be able to anchor, lower her boats and take passengers to the beach. A jetty would be beneficial.

Like much of the island, the bay is poorly surveyed and, although the cruise ship has entered and exited the bay safely in the past, the safety of such activities would be enhanced by a survey of the bay.

Social, economic and environmental considerations - the potential of a survey in the bay goes beyond the one dimensional view given above. There is more to hydrography than just a navigational chart.

a. Measurement, regulation and control of environmental impact – benthic mapping, modelling, pollution monitoring, disaster mitigation, pollution control
b. Spin-off industries / activities – aquaculture, non-cruise tourism, diving
c. Secondary anchorage
d. Traffic and demand management
e. Climate change impact mitigation
f. Regulatory compliance

The requirement is to get all stakeholders involved so that the benefit can be fully articulated.

A mechanism for assessing and presenting the value of nearshore hydrography

a. Consider existing data sources – charted depths, echo sounder information from visiting ships, local knowledge, crowd-sourced data, tidal data
b. Consider current shipping traffic patterns
c. Consider forecast shipping traffic patterns – without the survey / with the survey
d. Consider contribution of survey to other infrastructure projects
e. Consider contribution of survey to environmental projects
f. Consider contribution of survey to regulatory responsibilities
g. Consider contribution of survey to other industries

The decision to plan and undertake the survey should not be done in isolation nor should it focus exclusively on the needs of shipping. As many stakeholders as possible should be involved so that the full requirement and the benefits are identified and articulated. It may even be possible to identify additional sources of funding for the survey. These stakeholders may include:

- Local planning authorities
- Tourism
- Aquaculture
- Environmental agencies
- Nearshore resource extraction
- Pipeline and cable routes
- Local fishermen
- Port operators
- Defence and security authorities, and
- the Leisure industry, as well as the national charting authority.

Hydrographic surveys should be considered as part of the infrastructure of a country and should be thought of in terms that include the wider impact of traditional infrastructure, the interdependence of infrastructure networks, and the risk of infrastructure failure.

Options

Do nothing - There will be no initial investments costs but costs in other areas (eg the main port) may rise as usage increases, causing congestion in the port, and also the existing road / port infrastructure. Ships will only visit on an ad hoc basis meaning the local economy misses out on potential increased revenue from tourism. The cruise operators may decide to go elsewhere.

Do minimum - Use existing data to establish a safe entry and exit. A low cost option which may meet existing low demand. Possibility of congestion as the available space and facilities are limited.

NEW

LT500 Series

Ultimate GIS Mapping Solution

- **Multiple Models**
  Covering Centimeter to Sub-meter accuracies

- **High-end Specifications**
  From its blazing fast processor to its 4-constellation 3-frequency GNSS RTK engine the LT500 Series is the most capable handheld available

- **Cost-effective**
  Complete units including software starting under $3,000 bring high-performance GNSS handhelds to all users

- **More Options**
  Laser Plummet, eCompass, eBubble/Gyro, Accelerometer, RFID, 1/2D Barcode Scanner, WiFi BGN, Bluetooth, USB, Camera w/Flash, Phone and Data Modem

www.chcnav.com

Limited survey – approaches, anchorage and boat lane survey. There will be some reduction in navigation risk and the possibility that more ships will visit the bay. Navigable water will only be confirmed in those areas where the survey has been carried out. Costs will be quite high and the needs of only one sector will have been met. The fundamental capacity constraints will remain.

Full MBES survey – The investment cost will be very high but the whole of the bay will be mapped to a very high standard allowing safe navigation and optimising the use of space for multiple applications. This sort of investment should fit into a wider affordability strategy for all infrastructure development in the region and cannot be considered in isolation. It is very unlikely that nautical charting alone will justify this level of expenditure and the quality of the survey data is likely to be in excess of that required by non-nautical charting applications.

Multi-sensor survey – The various stakeholders are likely to have different requirements in terms of accuracies and coverage; nautical charting will require IHO Order 1a or Special Order accuracies which will drive the requirement towards a multibeam survey. This level of accuracy is unlikely to be required by fishermen and leisure users however and their needs may well be met by bathy LiDAR or lines of singlebeam data. The needs of aquaculture, benthic mapping, climate change and pollution assessment/ mitigation and regulatory requirements may even be met by satellite observations. Although these methods aren't capable of the accuracies and object detection of MBES, and will not work at all in some conditions, they are much cheaper than MBES and produce data more quickly over a wider area. Approaching the survey of the bay in this fashion will have a lower initial investment cost than the MBES survey and yet the same benefits from the perspective of the stakeholders will be realised. Concentrating high effort into the areas where it is most needed, whilst also providing data at the appropriate level of detail across the whole of the bay offers the potential to meet multiple requirements, serve the needs of several applications and provide a more balanced cost-benefit ratio.

Valuing the risk of infrastructure failure

Societies and economies are dependent upon their infrastructure to provide the mechanisms that keep industries working, societies interacting and countries developing, whether it be the simple process of individuals getting to work, food getting to market or capital projects providing impetus to growth and job creation. For island communities and for economies with a maritime component the infrastructure extends well offshore and the failure to provide a safe and reliable offshore infrastructure can result in disruption and loss of output as a failure of terrestrial based infrastructure. In order to properly assess the benefits that can be derived from a hydrographic survey it is also necessary to consider the risks implicit in not conducting the survey.

Figure 4: Costa Concordia (Rvongher)

Figure 5: Oil slick in the Gulf of Mexico (US Navy)

In order to assess the impact of not providing adequate hydrographic data it is necessary to consider the severity of an event, the probability of it occurring and the impact of the event on the society or economy. If a ship has an incident and blocks the approach channel to the main port it will have a serious impact on the functioning of that port as other traffic may be prevented from entering or leaving harbour. It may take some time to clear an obstruction eg. Costa Concordia, during which time the port is effectively closed to major traffic.

A fuel spill may cause damage to nearby marine ecosystems which will in turn affect the industries that are based on them eg. the Deepwater Horizon incident in 2010 in the Gulf of Mexico, and this may have significant implications for the parent company or the related industry, as with BP and oil production in the Gulf of Mexico.

In cost-benefit terms the risk associated with the infrastructure failure is measured by looking at the impact of these sorts of incidents and the probability of them happening as a result of that failure. In this case, the survey provides additional resilience into the infrastructure system that can be assessed by considering to what extent the probability of the incident occurring is reduced, how the additional information derived from the survey may mitigate the failure should it occur, and by how the impact of such an event may be reduced by the survey either directly or indirectly.

Placing a value on some of these things is very difficult and the value may vary from place to place and even time to time because the value will depend on the economic and social weight/importance placed by the society on the assets that could be put at risk. The effects of climate change provide a good example of this, where a rise in sea level in one

place may mean only the need to build a higher sea wall, while in another the same increase in mean sea level could submerge a whole island-based society.

Assessing the benefits of hydrography

A more complete understanding of the nearshore environment can bring a number of benefits to be considered. The most obvious one is that based in traditional nautical charting which can improve safe navigation for ships and, when combined with good navigation skills and equipment, and sound seamanship, will reduce the risk of groundings and collisions occurring.

Unfortunately it is not possible to prevent incidents happening for other reasons such as mechanical failure, weather impacts or human error. However, once an incident has occurred a good knowledge of the hydrography in an area can mitigate the impact of an event in the following ways:

- Assisting the safe conduct of a rescue effort
- Containing related pollution
- Enabling a recovery
- Permitting traffic management (diversion)
- Predicting the most probable short term and long term impact on the ecosystem

All of which will assist with the management and mitigation of the event and its aftermath. Good decision making is based on good and reliable information, especially in a crisis, and the provision of geospatial data is integral to the provision of good information.

A multi-sensor approach

One of the common issues with value for money is over-specifying the requirement. In an attempt to gather high specification data, a standard is set requiring an MBES survey for a shipping channel. A requirement could be density and accuracy allowing delineation of contours at 1m intervals. This is logical until the area reaches depths of less than, say, 10m. At this point requirement exceeds reality, as many ships won't go there (unless there is plenty of tide). Effort and budget is expended chasing an unrequired standard and looking at only one aspect of hydrography or assuming that the job is best done by only one system type.

The GEBCO system (General Bathymetric Chart of the Oceans – www.gebco.net) is the origin of a Global Base Layer. It represents a basic level of information but is a significant step up from no data at all. Its limitations are known, however it forms the first stage of spatial decision making. GEBCO is also the original concept of crowd sourcing and yet technology, particularly in terms of data logging and position fixing, has made huge advances and suitable quality controlled crowd sourced data has the potential to contribute in a very big way to filling in the white space on charts. In the case presented here, the cruise ships that have already been in and out of the bay will have echosounder readings and position information that could contribute significantly to navigation safety at virtually no cost.

Satellite derived bathymetry currently has the ability to provide good quality depth data in very shallow and optically clear water. The uncertainty associated with the technology and the apparent errors in deeper water mean that its application is currently limited but it is a very cost effective method of obtaining depths in very shallow water in specific conditions. When combined with other data in the same area such as crowd sourced bathymetry or bathymetric LiDAR, the depths derived from satellite observations can be tuned to give a more complete and accurate picture of the sea floor.

The potential of satellite data is growing and improving. Although currently limited in depth and with uncertainties that exceed IHO order 1, it is a useful planning and risk reduction tool. Satellite data gathering is passive, repeatable and relatively cheap and will meet the requirements for environmental applications and most low level modelling requirements in very shallow water.

Satellite data can also identify areas where LiDAR bathymetry can 'tighten' the solution or provide Order 1 if required. This adds redundancy to the data as some areas will now be covered using independent systems,

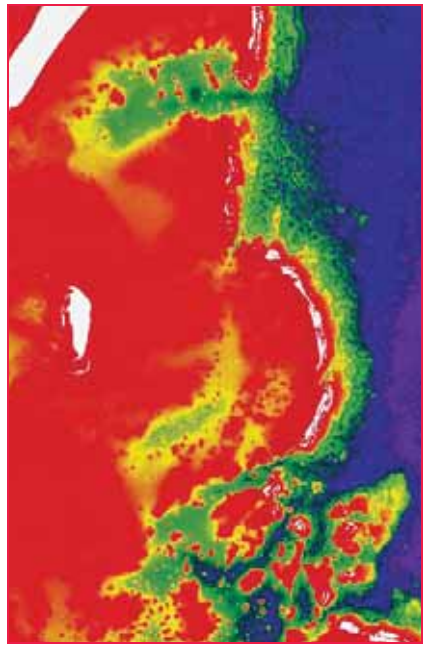

Figure 6: Satellite derive bathymetry in the SW Pacific

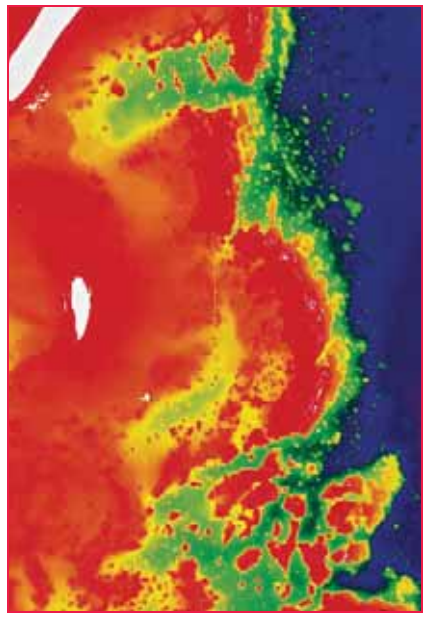

Figure 7: Bathymetric LiDAR over the same area

reducing the measurement uncertainties in these more important areas.

Bathymetric LiDAR is generally limited to depths of less than 50m (more commonly 20-30m) but achieves IHO Order 1, offering an economic alternative to MBES, particularly in shallow water where echo sounding may be inefficient or dangerous. Many modelling processes are better suited to lower resolution datasets.

LiDAR offers an IHO Order 1 compliant product in coastal areas at a price around half that of an MBES survey and will meet the needs of most applications outside high definition navigation surveys. It is ideal for the shallow waters of the bay considered in our study and can also inform the areas suitable for the shipping channel, anchorage area and approaches to be surveyed with mutibeam.

With Order 1 requirements met using LiDAR, and the very shallow and land area covered with satellite, MBES can be employed where it is actually needed. It is relatively slow and expensive in shallow water, which is a good reason to employ it only in those locations where it is really needed.

Valuing the wider benefits of hydrography

As with most infrastructure spending and investment, the benefits of hydrography extend into social and environmental effects which are difficult to measure and evaluate. For example, better charted information may mean that a ship does not have to have all her engines available for rapid manoeuvre which implies reduced CO2 emissions, improved air quality, less noise pollution and less wear on the ships machinery. Ships' boats landing passengers in the bay may also have a positive effect on economic activity in the area itself, facilitating the creation of new jobs and spreading the benefits of the cruise industry further across the island.

It also represents increased resilience in the infrastructure. A safe anchorage and landing point would permit multiple ship visits to the island without increasing congestion in the port, and offers an alternative visit location should the port be rendered temporarily unsuitable by weather or other incident. The survey in the bay represents an extension of the existing infrastructure network and assets and is likely to have an impact on the rest of the network, perhaps in terms of more traffic throughout the network.

Infrastructure development is recognised as being a major driver of both commercial and residential economic development and investment in the infrastructure in the nearshore should be considered in the same way. Planning strategically, involving multiple stakeholders and applying the appropriate technologies, creates an opportunity to add significant value in a particular location when infrastructure is considered as part of wider development.

Conclusion

At the coastal margin, depths become critical for navigation, the environmental impact of humans is significant and the effects of onshore and offshore processes need to be fully understood. The coastal margin is where routine human activity is most influenced by, and affects, the hydrography. Geospatial data in the nearshore region provides information that underpins development and contributes directly to the infrastructure of the area both offshore and on land.

The importance of considering the coastal region as a whole is growing and it is no longer efficient to consider hydrographic surveys as a single dimension activity in support of safe navigation. In order to fully appreciate the benefits and costs of hydrographic surveys, they have to be considered as an integral part of the strategic planning process for infrastructure development and spending. Only then can the real contribution of hydrography be assessed and the right investment decisions reached.

A multi-sensor approach to surveys, blending data from different sources and at the appropriate levels of accuracy and cost, makes it possible to model the coastal margin more completely and to meet the needs of different users in specific areas; regional satellite mapping; project aerial survey; targeted acoustic survey. This approach offers real cost and time savings and allows a cost benefit analysis to be carried out that is appropriate to the needs of the multiple end users. It is a vast improvement over no data, historic data unlikely to be improved upon due to available budgets, or the prohibitive costs of trying to do everything with MBES.

Bibliography

Greenland A, 2013, Hydrographic Risk Assessment for maritime Safety, A presentation at the FIG SIDS Symposium 2013, Land Information New Zealand (LINZ), http://www.fig.net/pub/fiji/ppt/ts1b/ts1b_Greenland.pdf

HM Treasury, 2011, Valuing infrastructure spend, Supplementary guidance to the Green Book, www.hm-treasury.gov.uk, London

International Federation of Surveyors (FIG), 2011, Report on the Economic Benefits of Hydrography, FIG Publication No 57, International Federation of Surveyors (FIG), Copenhagen

International Federation of Surveyors (FIG), 2006, Administering Marine Spaces: International issues, FIG Publication No 36, International Federation of Surveyors (FIG), Copenhagen

International Hydrographic Organisation (IHO), 2008, IHO Standards for Hydrographic Surveys, Special Publication No 44, Monaco, International Hydrographic Bureaux

Patreiko D & Holthus P, 2013, The Shipping Industry and Marine Spatial planning; a Professional Approach, the Nautical Institute, London http://www.nautinst.org/en/forums/msp/

Quadros N, 2013, Bathymetry Acquisition - Technologies and Strategies. Investigating shallow water bathymetry acquisition technologies, survey considerations and strategies, Prepared for the Commonwealth Government of Australia DCCEE, Cooperative Research Centre for Spatial Information (CRCSI)

Waddington A, 2013, A Layered Approach, Hydro International, Issue 7 October 2013, p20-23, Geomares Publishing, Lemmer

All images were provided by AAM Pty Ltd or are in the public domain. The paper was presented at FIG Congress 2014, Kuala Lumpur, Malaysia 16-21 June 2014

Hydrographic survey of river Drava branches

The hydrographic survey described in this paper is a contribution to the draft guide for the revitalization and improvement of watercourses and flood forecasting

Dino Dragun
Senior Hydrographic Surveyor, GEOxyz International Surveys, Zwevegem, Belgium

Ana Gavran
Head of the Hydrographic Department, MIG Ltd., Slavosnki Brod, Croatia

Vedran Car
CEO, Cadcom Ltd., Zagreb, Croatia

The hydrographic survey described in this paper is part of the draft guide for revitalization and improvement of watercourses and flood forecast upgrading for the better defense against the increasingly frequent flooding. It is also an important component of the process to establish good environmental water quality through morphological monitoring of the river branches. Majority of the branches are covered in lush vegetation, forming an important habitat for flora and fauna, a vital part of our ecosystem.

Drava river, located in Central Europe, has a total catchment area of 42 000 m^2. It rises in the South Tyrol in Italy, while the Danube flows by the settlement Aljmaš in Croatia, and its total length is 725 km. The total height difference of river Drava in Croatia is 105 m, and the length of the flow is 323 km. Its slope is approximately 0.03%. With the flow of water, the substantial sediment of sand and gravel characterizes the river. Downstream of the river Mura, the Drava River carries about 40,000 m3 of sediment annually. Under normal conditions, transport of sediment in the river is balanced, which means that the sediment removed is replenished with the same amount from upstream. With sediment moving from the source to the river mouth, there is lateral erosion that feeds sediment from the riverbank.

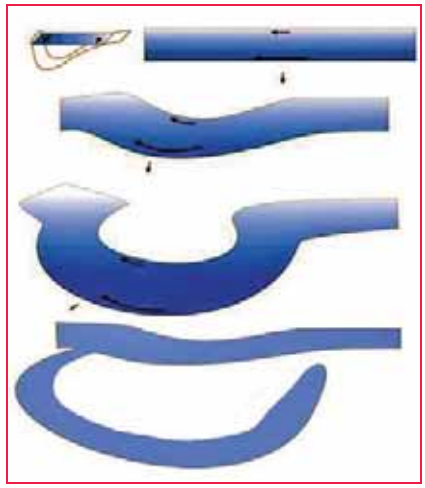

Figure 1: River processes – branch formation

Along the riverbank where the water is deeper, and thus faster, there is increased riverbank erosion. On the other side of the river, the water flows slowly and leads to the deposition of sediment. The consequence of this action on the river channel leads to more twists until the big curve (meander), when the river finally breaks through and creates a parallel short channel. Eventually, a longer branch because of its lower slope and slower flow becomes covered with sediment and forms a separate river stream (figure 1). The Drava River's branches are some of the last remaining river ecosystems of Europe and home to numerous endangered habitats and species. With the deteriorating river health and many species facing severe risk of extinction, these rivers deserve special attention and protection measures. (Grlica 2008)

It is important to mention that the construction of hydropower plants, river channeling and sediment exploitation has lead to a 'lack of sediment' in the river. It means that Drava River removes more sediment than replenished from upstream. Therefore, river sediment is taken from the riverbed, which is increasingly deepening each year with the annual average dents troughs on the river being 2.6 cm/year.

Furthermore, a flood in 2012 was caused by a large water wave on the Drava River that was responsible for more than 15 million

Figure 2: Locations of the five Drava River's branches (Source: Google Maps)

Figure 3: Survey of the Drava River branches

Euros in damage. In 2013, floods were a regular occurrence and caused substantial damage. This clearly indicates the importance of improving the forecasting system and morphological monitoring of the Drava riverbed. In addition, according to prognostic meteorological models, we expect an even greater intensity and frequency of the water waves appearance. The results of this survey will be used to upgrade these processes and records and will become an integral part of the main implementation plan for flood control.

Hydrographic survey of Drava river branches

Taking into account the above information along with the goal of quality hydrographic surveying and determining the morphology of the riverbed and river banks of Drava, we performed extensive office and field preparation for the demanding field work by using modern methods of measurement and data processing. Given that it is the very beginning of the research on the river branches and their design elements do not exist, we designed it as part of the preparatory works. Hydrographic surveys were performed at five branches on the Drava River: Right bank branch near Legrad (length of 3 km), Right bank branch near Komatnica (length of 5.7 km), Left bank branch near Križnica (length of 13.5 km), Right bank branch near Čađavica (length of 5.0 km) and Right bank branch near Višnjevac (length of 5.5 km). The total number of surveyed and processed cross sections in this project is 581. Locations of the branches are shown in the figure 2.

A geodetic survey was performed using a satellite positioning system (GNSS) and where this was not possible, terrestrial measurements were performed with total stations (tachometric method). Specificity of the bathymetric measurement is the integration of the different measurement systems, in order to determine coordinates of the echo sounder and depths in real time. For this purpose, we used single-frequency Sonarmite echo sounder (235 kHz) and Topcon Base and Rover GNSS RTK System. Software package Hypack Max, which is used in this hydrographic survey, automatically transforms coordinates from WGS84 datum to Croatian Terrestrial Reference System (HTRS96/TM). All devices are connected to a laptop PC and integrated in the abovementioned software Hypack Max.

> The ultimate goal of this project is to establish a mathematical model, which is going to be used to analyze the possibility of establishing a system for flood forecasting and simulation occurrence of flood waves.

A base station (Figure 3) was set up above the existing geodetic points along Drava River, while the rover and echo sounder (immersed 0.32 m in the water) were placed on the construction of the side of the vessel. By placing a RTK antenna and echo sounder in the vertical plane, the presence of lateral offset in the position of the echo sounder calculating was avoided. The main challenge was a hydrographic survey of small depths in the river branches, where the bottom of the river branch is covered with plants and vegetation. For this reason, we had a large number of redundant measurements, in order to ultimately obtain reliable and accurate depth information. Since bathymetry is performed using acoustic method, it is necessary to measure the sound velocity in water, which depends on temperature and water depth, ranged between 1,422 m/s and 1,437 m/s. During the hydrographic survey, due to the large amount of precipitation, the water level of the river increased and hydrographic survey of the branches was significantly impeded. We experienced extremely unfavorable conditions during the survey of Drava River, including submerged piers, sedge and other vegetation, and a large water wave that significantly raised the water level of the river and its branches.

When questioned about the accuracy of survey data, there are three errors that affect

Figure 4: Right bank branch near Legrad

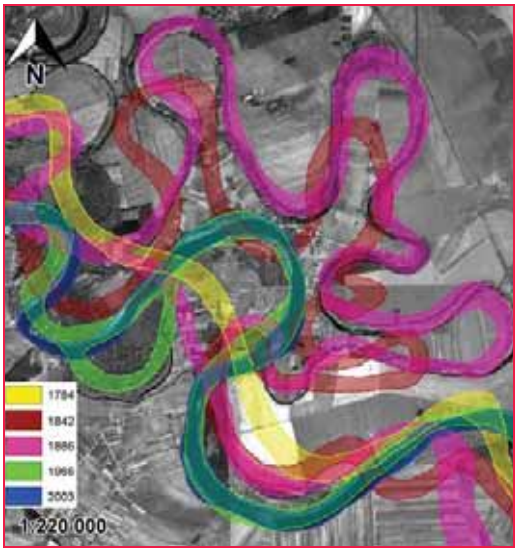

Figure 5: Changing the position of the Drava River during the years (near Križnica)

the accuracy and validity of this survey: GNSS measurement's error, bathymetric error and echo sounder positioning error. According to statistical analysis of the survey results (distribution of measurements, the standard deviation of the mean error), the reliability of hydrographic survey and required centimeter accuracy are confirmed and satisfied (s vertical= 2.8 cm, s horizontal= 2.3 cm). The following are some of the main branches features, as a result of the survey analysis.

Right bank branch near Legrad

In this narrow river, there is not enough space to create large deep meanders, less slope and this slows down the flow. But, it is possible to create short inlets and river branches that are quickly overwhelmed with new sediment deposits. Maximum surveyed depth in this river branch is 8.16 m and its position is shown in figure 4.

> The damage from floods and droughts are a much higher expense than the investment to prevent the damage from the natural disasters

Right bank branch near Komatnica

Inflow of water into this branch comes out of Drava River and Gliboliki stream. The western part of the branch (to the mouth of the creek) is steeper and the surface is gravel, while the eastern part of the branch is tilted lower and the surface is sand. The nearby hydroelectric plant caused permanent changes in the water level, which required extra vigilance during this survey. The maximum surveyed depth in Right bank branch near Komatnica is 5.66 m.

Left bank Branch near Križnica

At a length of 13.5 km, the left bank branch near Križnica is the longest branch of these five branches. The research of this survey, in agreement with long-term professional research, has undoubtedly demonstrated the necessity to ensure the dressing of fresh water from Drava River in order to reduce the impact of eutrophication and siltation intensity. The river has changed its course due to various regulatory interventions implemented in the 1820s. These interventions were implemented without a comprehensive plan and had almost no theoretical scientific basis. Further interventions in the period between 1842 and 1966 were designed to shorten the waterway and to improve the protection of the surrounding area from flooding. Finally in 1966, adequate access to regulatory procedures was performed. However, there is still room for better river channel management, which is discussed in this paper. All of the above resulted in the formation of the Left bank branch near Križnica (magenta color in figure 5), which among the other branches, is the subject of this hydrographic survey.

Right bank branch near Čađavica

This branch was created after making an artificial ditch, which shortened Drava River by 1.8 km. It was found that while diverting water into the new channel, there was a significant slowdown in the old water channel, and thus an appreciable deposition of sand, which resulted in raising the bottom of the old riverbed. In contrast with the ditch, the speed of water flow increased considerably, and there has been increased riverbed erosion and falling water levels. The result of these actions over time will completely interrupt the flow of water in this branch, and it will gradually heal the forest. Maximum depth in Drava River channel is 9.77 m, while in the branch it is 6.90 m.

Right bank branch near Višnjevac

The branch near Višnjevac part of the former course of river Drava in the 60s and 70s to mid-and high water represented the branch total length of 4.66 km.

A system derived from hydraulic engineering was introduced to stabilize the riverbank and control the junction of the right bank and Drava river. However, this caused a deposition of sediment on a low bank and the connection of the branch with low water levels was disabled. Maximum depth in this branch, according to highest water level is 4.34 m, while maximum depth in Drava River channel is 4.95 m.

Revitalization, flood control and morphological monitoring

Revitalization can be easily defined as a return to the situation as close as possible to an unchanged ecosystem. The problems of the branches water systems are mainly

Figure 6: Dried up river branch

Figure 7: Flood in the upper course of the Drava River, November 2012

linked to the supply of nutrients (nitrogen and phosphorus), sediments and other organic pollutants carried from agricultural areas, and the absence of adequate sources of fresh water. The overload of water with nutrients and poor water-flow are preventing development of swamp flora that additionally slows down the water current.

Eutrophication is a global problem. In the world, there are 415 eutrophic ecosystems, and that number is growing as a result of growing human population and increased pollution. From the hydrologic point of view, the river branch is characterized by very small flows and unsteady water regime. Ultimately, all this leads to a reduction in the volume of water or its complete disappearance (figure 6) in the river channel. This results in reducing the number of specimens of fauna and further settling of all pollutants. Actions and parameters that provide revitalization progress are: water surface management by digging canals and clearing forest vegetation, silt removing, marsh vegetation cleaning and the construction of hydraulic structures, reducing the difference of water level between river channel and river branch.

As noted above, every year, at least one of the rivers in Croatia has recorded the emergence of new extreme value. Meteorological models in future, expect even greater changes (Figure 7). This is just another example of why we need to work systematically to improve the system of hydro-meteorological forecasting. Output data of this survey provides information of the river channel configuration and of maximum volume of water that a river channel can accept. In Croatia, there are natural retentions such as Lonjsko polje and Kopački rit, where part of the floodwaters can be stored. A simple and effective project that is being implemented, 'Development of the system for the prediction of floods on the river Drava' will contain a database that can be used to create digital mathematical model of flood forecasting. Databases will inter alia contain the following information: the amount of water discharged by the hydroelectric plants, amount of rainfall and melting snow in the Alps, geoinformatic and hydraulic models for Drava's hydrographic stations, morphological monitoring data obtained by hydrographic survey, etc.

The ultimate goal of this project is to establish a mathematical model, which is going to be used to analyze the possibility of establishing a system for flood forecasting and simulation occurrence of flood waves. Outputs of this survey show that due to digging canals, water level in branches decreases, therefore branches could affect water from the Drava River. The construction and upgrading of flood protection is a complex and lengthy process, but that does not mean it should be pushed aside. Ultimately, the damage from floods and droughts are a much higher expense than the investment to prevent the damage from the natural disasters.

Conclusion

The areas that we have displayed have the characteristics of high biodiversity, and water surfaces of the branches represent the potential for tourism and recreational purposes. The performed hydrographic survey is a contribution to various studies, such as: revitalization, forecast systems improving and morphological system monitoring with the purpose of creating better hydrologic and ecologic conditions and the preservation of these undeniably important habitats.

References

Bukša, Ž. (2012): Stanje i planovi u sustavu obrane od poplava, Informativno-stručni časopis Hrvatskih voda, broj 201., 2012. 6.-11.

Grlica, I. (2008): Studija biološke raznolikosti rijeke Drave, Staništa – strme obale i sprudovi, dio 1, Interreg IIIB Cades projekt - Zeleni pojas, 2007.

Grlica, I. (2008): Studija biološke raznolikosti rijeke Drave, Dravske mrtvice i odvojeni rukavci 2. dio, Interreg IIIB Cades projekt - Zeleni pojas, 2008.

De Jong, C.D., Lachapelle, G., Skone, S., Elema, I.A. (2002): Hydrogrpahy, Vereniging vor Studi-en Studetnenbelange te Delft, Delft, 2002.

Pribičević B., Medak D., Đapo A. (2010): Integracija suvremenih geodetsko-hidrografskih mjernih metoda u krškim područjima Republike Hrvatskem, Ekscentar, br. 12, str. 58-63

Determining the maritime baseline for marine cadastre

The primary aim of this research is to develop a methodology to efficiently determine the baseline by acquiring an integrated terrestrial Digital Terrain Model (DTM) using DGPS and a marine DTM based on near-shore bathymetry and tidal data, in order to derive the location of the baseline at a particular time

Robin Seet
Assistant Director, Geodesy Section, Department of Survey and Mapping Malaysia (JUPEM), Kuala Lumpur, Malaysia

Dr David Forrest
Senior University Teacher, School of Geographical and Earth Sciences, University of Glasgow, UK

Dr Jim Hansom
Reader, School of Geographical and Earth Sciences, University of Glasgow, UK

Malaysia has a marine jurisdiction of approximately 574,000 kilometres^2 (CheeHai & Fauzi, 2006) and is looking to implement a marine cadastre. To do this, the low-water line needs to be determined. This research investigates an efficient method to determine the low-water line and subsequently investigates Malaysia legislation and coastal policies and their effect on the maritime baseline, and finally makes recommendations regarding the management policies for a maritime baseline.

Methods

The method applied in this research requires near-shore Digital Terrain Modal (DTM), bathymetric DTM and tidal information to be obtained in order to derive a low-water line (Figure 1).

Site Selection

Kames Bay, Millport, Scotland was identified as the case study area. It has both a steep rocky section at its sides and a low angled sandy section. It is also the site of a fully instrumented tide gauge allowing cross-calibration of tidal characteristics to the DTMs. This case study area is comparable with parts of the Malaysian coastline, making the tested methodology easily transferable.

Data Acquisition

The DGPS and echo sounding fieldwork was carried out to acquire a terrestrial DTM and a bathymetric DTM of Kames Bay on June 7, 8, 2012, across a spring tide at Millport. The land elevation data was collected using a Leica GPS1200 and a Leica Smartnet with a GS08 Antenna. The bathymetric data was collected using a 5.5m rigid-inflatable boat (RIB) vessel with a 0.4m draught carrying a SONARLITE echosounder linked to a Leica Smartnet rover. The data produced a large overlapping area (MHWS-MLWS) of approximately 150 m from the two sets of DTM (Figure 2).

Determining the low-water lines

Data Analyses

Spatial and statistical analyses were carried out to validate the DTMs generated from the fieldwork by extracting the cell values of the land topography and bathymetry data at each DGPS point to compare with DTMs from ASTER, SRTM and NEXTMap. The following analyses were made with the assumption that the DGPS DTM produced here is of a higher level of accuracy (standard deviation

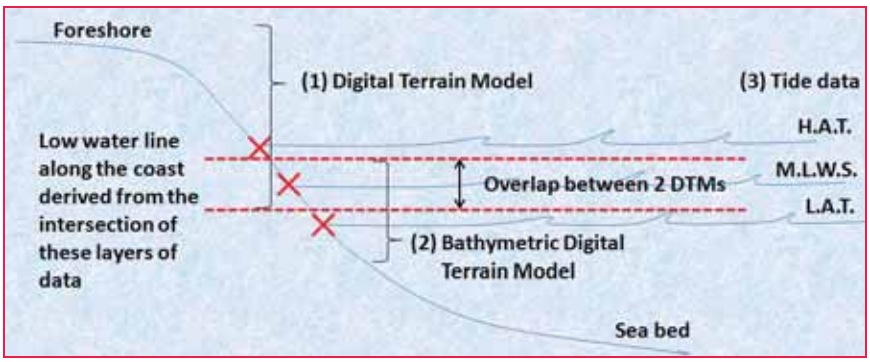

Figure 1: Concept of research methodology used here

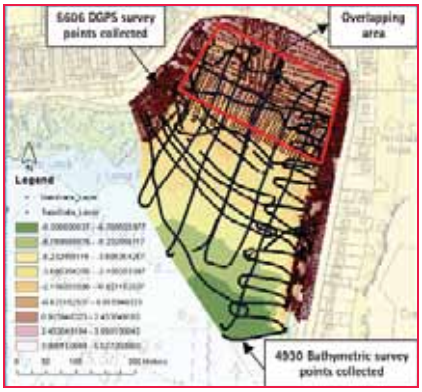

Figure 2: DGPS and bathymetric surveys carried out at Kames Bay

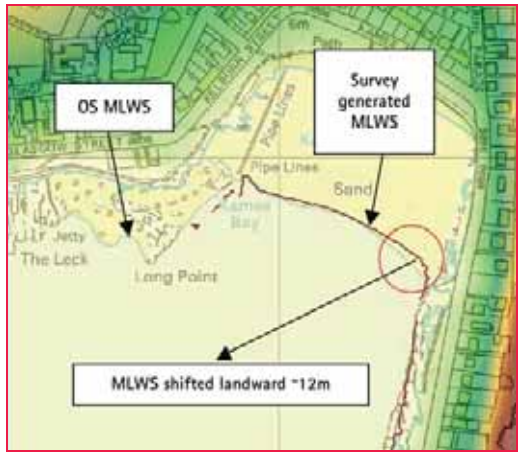

Figure 3: Comparison of the generated MLWS with the current MLWS shown on OS map

of each DGPS height point collected averaged ~ 8mm) than other DTMs and will be used as a reference dataset against which comparisons will be made.

Table 1 shows that the DGPS and bathymetric data have a strong relationship with a relatively high correlation and low RMSE. The high correlation between the DGPS values and echo sounding elevations in the area of overlap provides a high confidence in the echo sounding results further offshore, where the measurements using other data sources could not be validated. Meanwhile, among the third party DTMs, NEXTMap which has the highest resolution is significantly more precise and accurate than ASTER and SRTM. However, despite the reasonably good correlation with NEXTMap, its data does not extend beyond the low-water line region, implying that the time of data collection was not the most appropriate for this purpose, thus limiting its usability.

Despite their global availability, analysis shows that neither the ASTER nor SRTM datasets are a suitable use for determining the marine baseline. Although not analysed here, marine LIDAR shows much more promise at covering extensive areas of coastline with the required accuracy, but with significant costs involved.

Generation of Low-water Lines

Mean Low Water Spring (MLWS) & Lowest Astronomical Tide (LAT) were subsequently generated from the DGPS and bathymetric DTMs using the tidal height information obtained from the UK National Oceanography Centre. Generally in the beach area, the DGPS survey was able to cover the foreshore from HAT to a little beyond MLWS; meanwhile the bathymetric survey was able to cover the foreshore from MLWS to seaward of LAT, but less so in the rocky area.

The generated MLWS location was then compared to the MLWS location shown on Ordnance Survey (OS) raster map and it showed an almost identical line with a slight shift landward ~12m at the southeast of Kames Bay (Figure 3).

The LAT generated from the bathymetric DTM was then compared to the 1:12,500 Leisure Chart 5610.1 (published in 2005). The LAT line generated indicated that the seabed which was once shallower (depth value 07 and 09) in the northwest and southeast of Kames Bay has retreated landward by approximately ~72m and ~94m, respectively (Figure 4). This suggests that changes have occurred in the mobile near the shore. The UK Hydrographic Office (UKHO) confirmed that the LAT line represented on the admiralty chart was surveyed by HMS Gulnare in May 1940 and that information has not been superseded (Hannaford, pers comm, 2012). Admiralty charts adopted LAT as chart datum from 1968 (Burningham & French, 2008), yet the current LAT line shown in Chart 5610.1 has not been revised since the 1940 survey. This suggests that particular sections of Kames Bay have been eroding at an average rate of more than 1m per year over the last 72 years (1940-2012). This is not an unusual rate of movement within the lower intertidal on the Scottish coast, mostly driven by sea level change and dwindling sediment supply (Hansom, 2010).

Table 1: Statistics of comparisons between DGPS DTM and various DTM (metres)

DTM	Δ Min	Δ Max	Mean	RMSE	Correlation*
ASTER	-22.1048	-1.4641	-8.8831	10.2105	0.1715
SRTM	-20.9902	3.6871	-8.5072	10.4047	0.2279
NEXTMap	-2.6784	3.7714	0.8319	1.2910	0.5660
Bathymetric	-1.8032	3.1258	0.1461	0.3918	0.8732

Note: The correlation is between the original data values rather than the 'difference'.

Table 2: Heights of low-water lines in CD and ODN

Millport's low-water datum heights prediction (2008-2026):	In Chart Datum (metres)	In Ordnance Datum Newlyn(metres)
MLWS	0.440	-1.180
LAT	-0.040	-1.660

(National Oceanography Centre, 2012)

Sea-level change rates and future estimates

One of the concerns brought about by global warming is sea-level rise. According to the United Kingdom Climate Projection (UKCP09) produced by Department for Environment, Food and Rural Affairs (DEFRA) for a 95% high estimate emissions scenario for Millport, in 2025, the change in relative sea level

SPIRENT

Precision At All Price Points

So much depends on the fidelity & precision of your testing

GSS6700
Powerful, flexible & scalable simulation for commercial applications

GSS9000
World-leading multi-frequency GNSS RF Simulation for R&D and performance tests

GSS6300M
Flexible, "one box" test for receiver integration, applications, manufacturing and aftercare

GSS6425
Iterate live tests in the lab. Simple, portable tool to record and replay real world RF, video and CAN data

GPS GALILEO SBAS IRNSS QZSS BEIDOU GLONASS

Fidelity + Precision = Spirent

For Sales Enquiries, please contact our Distributor:
M/s Janus G-13, Unitech South City-I, Gurgaon 122001 India
+91 124 4086641 prashant.mehra@januscorp.in www.januscorp.in

SPIRENT +44 1803 546325
globalsales@spirent.com | www.spirent.com/positioning

SPIRENT FEDERAL SYSTEMS +1 800 785 1448
info@spirentfederal.com | www.spirentfederal.com

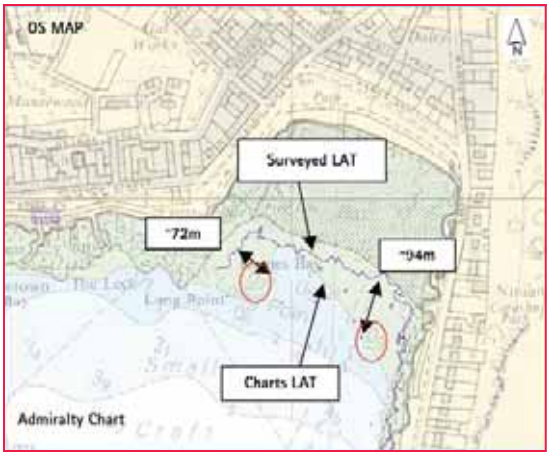

Figure 4: Shift noticed in LAT location when compared to Admiralty Chart

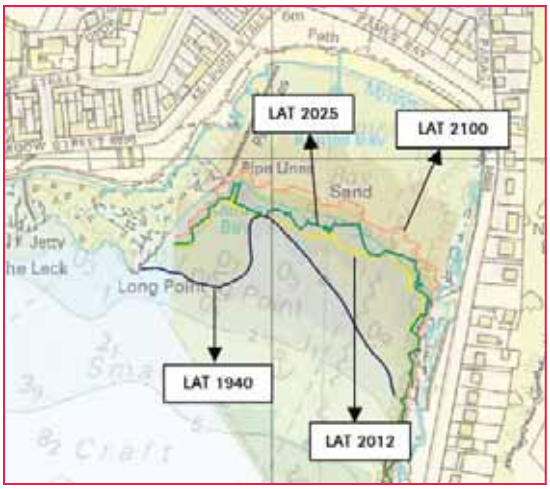

Figure 5: The shift of LAT position from 1940 to 2100 based on historical data, current survey data and 95% estimates in the high emissions scenario projected by UKCP09

(RSL) is ~0.152 m; and in 2100, the RSL will be ~0.714 m (DEFRA, 2012). Provided nothing has changed in the mobile nearshore, the shift of LAT position from 1940 to 2100 is show in Figure 5.

Environmental and economy impact of a receding low-water line

In addition to the implications to the marine cadastre of a shifting baseline over time, the movement of LAT has important environmental consequences. It is well known that the landward movement of MHWS (Mean High Water Springs), otherwise known as coastal erosion, is ongoing as a result of sea level rise and sediment deficiencies on coasts worldwide. What is less obvious is the often unseen and unrecorded landward movement of LAT that results in loss of coastal intertidal habitat as well as loss of intertidal sediments and thus, a steepening of the intertidal zone (Hansom, 2010). Changes to the gradient and sediment composition of the intertidal may ensue since deeper water will promote enhanced wave activity, the result of which may be an elevated erosion and flooding risk and calls for artificial coast protection structures as well as accelerated loss of intertidal habitat.

Marine cadastre in Malaysia

Marine cadastre in Malaysia emphasises on the accurate spatial determination of marine parcels within its international maritime boundaries. However, its implementation is still at a rudimentary stage. One of the prerequisite of marine cadastre is to clearly identify its spatial extent within Malaysia's marine jurisdiction. Therefore, the effective determination of maritime baseline which defines the outer limits of individual state (*negeri*) maritime jurisdiction is of paramount importance.

For a land cadastre, the boundary marks depicting the limit of the cadastre parcels are surveyed and demarcated on the ground. Its physical location is static, although its geographical coordinates might change due to a shift in horizontal land datum caused by natural phenomena such as earthquakes. Such events only result in the recalculation of new coordinate values for the boundaries of a land cadastre parcel without physically shifting the parcels, or altering their existing limit. Compared to land cadastre, a marine cadastre boundary is delimited (not demarcated) from the low-water line and generally there is no physical evidence, only mathematical evidence left behind (Carrera, 1999). However, the dynamism of the coastline determined by, among other things, sea level, waves, currents, winds, and the added issues of coastal erosion and deposition over time, may all cause the baseline to migrate over time. To avoid spatial uncertainty, constant determination may be thus required.

The Malaysia federal-local states' maritime boundary has not been defined and even the maritime boundary between local states has yet to be agreed upon. In addition, no maritime baseline has been officially declared for the country, and this has an effect on the level of jurisdiction exercisable between different maritime zones. The technical issues related to a shifting baseline and how it impacts marine parcels or maritime rights within a maritime zone have thus not been addressed.

The dilemma of Malaysia's marine cadastre baseline

Currently, there is a legislative gap on the issues concerning the maritime baseline. Five Acts define the maritime limit of Malaysian waters but no single policy or guideline is in place that addresses or even acknowledges the shifting nature of the maritime baseline. The closest legislation to the safeguarding of maritime baseline currently is the 'Guidelines on Erosion Control for Development Projects in the Coastal Zone (DID Guidelines 1/97)', but its primary aim is prevention of erosion along the coastline and does not address the complications associated with a shifting maritime baseline or the actions needed to deal with it. Institutionally, many activities that occur in the coastal areas are administered and enforced by a variety of agencies or departments under various ministries or state authorities. No single agency has overall authority over all maritime matters. Likewise, the technical difficulties facing the determination and visualisation of a maritime baseline, coupled with coastal dynamism that threatens baseline stability, has made it impossible to efficiently govern the low-water line

without putting in place a proper mechanism involving all stakeholders.

The absence of an articulate policy on maritime baseline conservation has also caused ambiguity in the limits of federal – state maritime zones and thus, subjects it to unwarranted disturbance. Therefore, as part of this research, a draft proposal for a national maritime baseline policy is presented that might guide how the maritime baseline is to be managed and sustained. In addition, a series of recommendations for Malaysia have been made in order to apply the maritime baseline determination method shown in this research, and how to overcome various issues regarding the maritime baseline for Marine Cadastre implementation.

Acknowledgements

We thank Mr Brian Johnston, Mr Kenny Roberts and Dr Anne Dunlop from University of Glasgow for the survey carried out in Kames Bay, Millport

References

Burningham, H. & French, J. (2008) Marine Estate Research Report: Historical changes in the seabed of the greater Thames estuary.

Carrera, G. (1999) Lecture notes on Maritime Boundary Delimitation. University of Durham, U.K.

CheeHai, T. & Fauzi, A. (2006) A National Geocentric Datum and the Administration of Marine Spaces in Malaysia FIG ed. *Administering Marine Spaces: International Issues*, (36).

Department for Environment Food and Rural Affairs (2012) UK Climate Projections: User Interface [Internet]. Available from: <http://ukclimateprojections-ui.defra.gov.uk/ui/start/start.php> [Accessed 12 November 2012].

Hannaford, G. (2012) Email correspondence with UKHO regarding LAT changes at Millport.

Hansom, J.D. (2010) Coastal Steepening in Scotland. Scottish Natural Heritage Commissioned Research Report, Battleby, Perth. 100pp.

National Oceanography Centre (2012) Chart Datum & Ordnance Datum [Internet]. Available from: <http://www.pol.ac.uk/ntslf/tides/datum.html> [Accessed 15 March 2012].

Seet, Robin,Forrest, D., Hansom, J. D. (2012) Determining the maritime baseline: development of a universal methodology.In: *7th ABLOS Conference 2012: UNCLOS in a Changing World, International Hydrographic Bureau (IHB)*.Monaco.

Seet, Robin, Forrest, D., Hansom, J. D. (2012)Determining the maritime baseline: development of a universal methodology. In: *2013 CASLE Conference: Management of Land and Sea Resources – What's New?* Glasgow (UK).

On the transformation of time system in relativity based on SOFA and .NET

According to assembly of the transformation of time system in relativity provided by Standards Of Fundamental Astronomy (SOFA), the definition of time system in relativity and its transformation are investigated. The mixed programming technology between .NET language and FORTRAN language are used to analyze the transformation process of assembly and to realize interface of transformation of time system

Shenquan TANG
Master Candidate, School of Geodesy and Geomatics, Wuhan University, Wuhan, China

Jianan WEI
Bachelor, Faculty of Built Environment, University of New South Wales, Kensington 2052, NSW, Austrailia

Erhu WEI
Professor, Ph.D, Ph.D supervisor, School of Geodesy and Geomatics, the Key Laboratory of Geospace Environment and Geodesy, Ministry of Education, Wuhan University, Wuhan, China

Time originally determined by the standard clock is called proper time, and the time calculated under the relativistic framework is called coordinate time. The time conversion calculated under the relativistic framework comes to precession, nutation, and polar motion correction models which calculate complexly and are more difficult to write a program, so the IAU gives 'Standards of Fundamental Astronomy' (SOFA) to achieve the computational model. Currently, SOFA has two versions of FORTRAN and C. FORTRAN, as an old programming language by virtue of its powerful computing capability, is still used in some scientific computing and engineering projects. However, FORTRAN runs under DOS unfriendly interface that makes its operation less convenient. C# language that has recently emerged under .NET platform makes up for the lack of FORTRAN. With the rapid development of its technology and user-friendly interface, C# has been widely used in the windows platform.

In this paper, the advantages of FORTRAN's efficient algorithms and C#'s friendly interface are combined. The mixed programming based on FORTRAN and C# is researched, and relativistic frame time conversion system has been studied by analyzing the SOFA assemblies.

Time system in relativity

Terrestrial Time (TT)

Temps Dynamigue Terrestre (TDT), based on the International Atomic Time (TAI), is geocentric coordinate time, whose second length is the same as TAI. The relationship between them is [1]:

$$\mathrm{d}(\mathrm{TAI}) = \sqrt{1 - \frac{2U_{Geo}}{c^2}}\,dt \qquad (1)$$

$$\mathrm{TDT} = \mathrm{TAI} + 32.184\mathrm{s} \qquad (2)$$

In the 21st IAU meeting, Temps Dynamigue Terrestre (TDT) was formally changed to Terrestrial Time (TT). According to the relationship between proper time τ and TT, after ignoring items $O(c^{-4})$, the relationship between the two under post-Newtonian accuracy is [2] :

$$\begin{aligned} \mathrm{d}\tau^2 &\approx \left[1 - \left(\frac{2W}{c^2} + \frac{v^2}{c^2}\right)\right]\frac{d(TT)^2}{(1-L_G)^2} \qquad (3)\\ &= [1 - \left(\frac{2W}{c^2} + \frac{v^2}{c^2}\right)](1 + 2L_G)\,\mathrm{d}(TT)^2 \\ &= \left[1 - \left(\frac{2(W - W_G)}{c^2} + \frac{v^2}{c^2}\right)\right]\mathrm{d}(TT)^2 \end{aligned}$$

where W is contained gravitational potential and perturbation celestial TGP measuring sites' phase function in the Earth center of mass reference frame; v is the observer dimensional velocity in the non-rotating earth's center of mass reference frame; and W_G is geoid gravity position.

$$L_G = \frac{W_G}{c^2} = 6.969290134 \times 10^{-10} \quad (4)$$

Temps Coordinate Geocentrigue (TCG)

Temps Coordinate Geocentrigue is the time basis of Geocentric Celestial Reference System (GCRS) that is set by IAU. Its function is to switch TDT from geoid to center of the earth under the relativistic framework, and the relationship between the two is:

$$d(TT) = (1-L_G)d(TCG) \quad (5)$$

where L_G is similar to formula (4).

Temps Coordinate Barycentrigue (TCB)

Temps Coordinate Barycentrigue is the time basis of Barycentric Celestial Reference System (BCRS). It is suitable for assumption that the observation station is still in the solar system (especially on the sun) and regardless of other factors. The calculation of TCB includes the time variable of planetary movement around the sun and the preparation of the planetary ephemeris time.

Temps Dynamigue Barycentrigue (TDB)

The result of the equations of motion of major planets comes from numerical integration of its argument just coordinate time, so people look at the TDB as coordinate time whose precise definition depends on the solar system CMCS coordinates and choice of metric. Its role is solving planetary motion around the sun and the preparation time motion equation system ephemeris used.

Mixed programming of SOFA and .NET

Development environment and principle introduction

The development environment of mixed programming is Visual Studio 2013; Intel Visual FORTRAN 2013 is embedded in .NET platform. Generally,

> The mixed programming is used to solve examples. It can be seen that the result of the positive sequence call and reserve call of SOFA function library are identical

the executable code under control of the Common Language Runtime (CLR) is called the managed code. The code outside the runtime library is called unmanaged code. FORTRAN program in VS (Visual Studio) platform is unmanaged code, so the standard package handling services are used to generate dynamic link library DLL. Unmanaged code calling schematic is shown in Figure 1.

Realization of mixed programming

Firstly, a Dynamic-link Library (DLL) is created in IVF (Intel Visual Fortran). In order to be called by C#, the relativistic framework on time functions in SOFA library is added to the project.

Modify description of FORTRAN routines.

As FORTRAN and C# are two different languages, there are some differences in grammar and sentence structure between them. To achieve the call of DLL of FORTRAN in .NET platform, some modifications must be done:

(1) FORTRAN language is not case sensitive. When the compiler extracts function from a DLL, the function name will automatically be converted to all uppercase, as the .NET platform can't find functions of FORTRAN source code. The ALIAS (alias) property should be used in the routine which specifies the export function name. Here in the iau_CAL2JD function of SOFA library function as an example (the same below), a line of code is added in a statement after the implicit none:

```
!DEC$ ATTRIBUTES ALIAS: 'iau_CAL2JD':: iau_CAL2JD
```

(2) When a DLL is created, the DLLEXPORTS property must be used in FORTRAN code to add an export declaration, which is a necessary step of importing routine. A line of code after implicit none is added:

```
!DEC$ ATTRIBUTES DLLEXPORT :: iau_CAL2JD
```

(3) C# arrays start at 0 and its execution order is row column. FORTRAN arrays start at 1 and its execution order is column row. When performing the array parameter passing, the first element of the array is passed through to achieve the purpose of passing the first address of the array.

(4) Data for the value type in C# is directly stored in the stack. FORTRAN defaults type is a reference type. The address of the reference parameters is stored on the stack. The numerical value is stored in the heap. When stating or calling a function in C#, the ref keyword is used to modify parameters and make it to be a reference type.

The .NET call instructions:

When SOFA library DLL has been generated, it should be copied to the project directory Debug, then FORTRAN DLL can be called in C# project program and some statements should be made in the program.

(1) First of all, references of dynamic link library operations class should be added in C# using System. Runtime.Interopserviers.

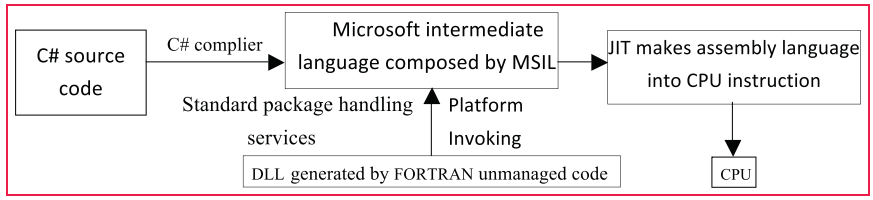

Figure 1: Platform invoking of unmanaged code

(2) .NET platform Dlllmport property is used for C# language to access all API of WIN32 platforms. Property of SetLastError and CharSet are set to true. By setting property of CallingConvention to Stdcall, unity between the two will be achieved.

(3) When a SOFA function is called under .NET platform, it must be declared that the function is achieved from outside program module. Here the extern keyword should be used to modify the method name. The method must be called in public and static form.

Time system conversion under the relativistic framework

The latest version of the SOFA library (as of October 2014) has a total of 186 subprograms. The subprograms at present comprise 131 'astronomy' routines supported by 55 'vector/matrix' routines, available in both Fortran77 and C implementations [4]. The 'astronomy' library comprises 131 routines. The areas addressed include calendars, time scales, ephemerides, precession-nutation, star space−motion, star catalog transformations and geodetic/geocentric transformations. The 'vector−matrix' library, comprising 55 routines, contains a collection of simple tools for manipulating the vectors, matrices and angles used by the astronomy routines. This paper uses the two parts functions of SOFA to achieve the time system conversion under the framework of the relativistic [5].

TT and TCG conversion

The relativistic effects into Equation (5) can be obtained [6]:

$$TCG - TT = \frac{\omega_0}{c^2}\Delta t = L_G \Delta t \qquad (6)$$

where $\Delta t = t_i - t_0$, $W_0 = 62636856.0 m^2/s^2$, t_i for a certain time; t_0 as the starting time for January 1, 1977 0h, which is corresponding to Julian Day JD = 2443144.5, corresponding to simplify Julian Day MJD = 43144.0. The starting time of TCG is specified as TCG = TT, the formula (6) can be written as:

$$\mathrm{TCG} - \mathrm{TT} = L_G\left(\mathrm{MJD} - 43144.0\right)\times 86400\mathrm{s} \qquad (7)$$

When SOFA library is used for time system conversion, the function iau_DTF2D should be called to convert the time to SOFA internal format at first (the details of function, please refer to the literature [7], the same below). Then iau_UTCTAI function should be called to convert UTC to TAI. iau_TAITT function is called to convert TAI to TT. iau_TTTCG function is called to convert TT to TCG. In this way, the conversion between TT and TCG has been indirectly achieved.

TT and TDB conversion

TDB is coordinate time. In literature [2], there is the following relationship between TDB and TT:

$$TDB = TT + \frac{P(TT) - P(TT_0)}{(1 - L_B)} + \frac{1}{C^2}V_E\left(X - X_E\right) + \frac{1}{C^4}\left(3U_{ext}\left(X_E\right) + \frac{V_E^2}{2}\right)V_E \times \left(X - X_E\right) \qquad (8)$$

where the meaning of TT_0 and t_0 in formula (6) is identical. P (TT) is given by the 'FBL' analytical model, using numerical integration methods to calculate. U_{ext} represents Newton potential of all solar system objects except earth (calculated at geocentric). V_E, X_E represent respectively geocentric orbital velocity vector and the position vector of the Barycentric Celestial Reference System (BCRS). X is the position vector of BCRS. TDB is indirectly calculated by calculating difference between the TDB and TT in SOFA function library. At first, function iau_DTDB is called to find difference between the two. It is the most complicated to calculate UT. UT = UT1-UT = + 0.3341 can be checked on the official line from the IERS. hen, iau_UTCUT1 function is called to convert UTC to UT1.

$$\mathrm{UT} = \mathrm{MOD}\left(\mathrm{MOD}\left(\mathrm{UT11},1\right) + \mathrm{MOD}\left(\mathrm{UT12},1\right)\right) \qquad (9)$$

where MOD is the function that strives for the remainder of the FORTRAN language. And then, DTR = iau_DTDB function is called to calculate the difference between the TT and TDB, where U, V can be calculated in two ways: (1), by relations of converting geodetic coordinate system and the meridian plane Cartesian coordinates [8].

$$x = \frac{a\cos B}{W},\ \mathrm{y} = \mathrm{N}\left(1 - e^2\right)\sin B \qquad (10)$$

where $\mathrm{W} = \sqrt{1 - e^2 \sin B^2}$ (The first basic latitude function), $\mathrm{N} = \frac{a}{W}$, here

Table 1: The results of the example time conversion

Time System	PART	Result of transformation
TT	TT1 TT2	2456956.5 0.62577759259259258
TCG	TCG1 TCG2	2456956.5 0.6257872190119953
	TDB1	2456956.5
TDB	TDB2	0.62577758671328887
	TCB1	2456956.5
TCB	TCB2	0.625991754962097
UT	0.12500386689814813	
DTR	-0.00050797184121735	
x	5471.991159432665	unit: km
y	3265.8935166539759	
U	5471.9911594326748	
V	3265.8935166539429	
	TDB1	2456956.5
TDB	TDB2	0.62577758671328887
	TT1	2456956.5
TT	TT2	0.62577759259259258
	TCG1	2456956.5
TCG	TCG2	0.6257872190119953
difference	0.000	

Table 2: The value of Paris, Lhasa, Wuhan three stations of TDB, TCB

City	PART	Result of transformation
Paris	TDB2	0.62577759205940842
	TCB2	0.62599176030821668
Lhasa	TDB2	0.62577759334426453
	TCB2	0.62599176159307279
Wuhan	TDB2	0.62577758671328887
	TCB2	0.625991754962097
difference	0.000	

the WGS-84 ellipsoid is taken and x, y represent respectively U and V.

(2), by calling iau_GD2GC function to calculate the U, V.

$$U = \sqrt{XYZ(1)^2 + XYZ(2)^2},\quad V = XYZ(3) \tag{11}$$

Finally, function iau_TTTDB is called to calculate the TDB.

TT and TCB conversion

TT and TCB have no direct geometrical linear relationship, conversion of which can be achieved by the intermediate variable TDB. In previous section, a conversion relationship is given between TT and TDB. If the conversion relationship between TDB and TCB is given, TT and TCB conversion can be successfully achieved. There is the following relationship between TDB and TCB [9]:

$$\begin{aligned} TCB - TDB &= (TCB - TCG) + (TCG - TT) - (TDB - TT) \\ &= L_C(TT - TT_0)(1 - L_B)^{(-1)} + L_G(TT - TT_0) \\ &= L_B(MJD - 43144.0) \times 86400s + p_0 \end{aligned} \tag{12}$$

where L_C is the long-term coefficient, L_G is the same in formula (3), $L_B = L_C + L_G = 1.550519767772 \times 10^{-8} \pm 2 \times 10^{-17}$, $p_0 \approx 6.55 \times 10^{-5} s$. First iau_TTTDB and iau_TDBTCB functions are called in SOFA function library. Finally, TT and TCB conversion can be achieved.

TCB and TCG conversion

According to movement rules under the major planets orbit perturbations of the earth centroid trajectory, and considering the geocentric orbital velocity and gravity of the sun and other planets as well as the full potential of GR dimensional transformation, the following conversion relationship exists between TCG and TCB:

$$TCB - TCG = c^{-2}\left\{\int_{t_0}^{t_i}\left[\frac{v_e^2}{2} + U_{ext}(X_e)\right]dt + v_e(X - X_e)\right\} + O(c^{-4}) \tag{13}$$

where t_i is a certain time of TCB, t_0 is consistent with the January 1, 1977 TAI time. The meaning of U_{ext}, V_e, X_e and X are the same as the one in formula (8). After ignoring items $O(c^{-4})$, the relationship between the two under post-Newtonian accuracy is:

$$\begin{aligned} TCB - TCG = {} & L_C(MJD - 43144.0) \times 86400s \\ & + 0.00168s \times \sin M + \frac{V_E}{c^2}(X - X_0) \\ & + 0.000014s \times \sin 2M \end{aligned} \tag{14}$$

where the meaning of L_C is as same as

Table 3: the Julian day converted to calendar time

Time System	Translate to calendar time
TAI	October 26, 2014
	15h0m35.000011324882507s
TT	15h1m7.1839848160743713s
TCG	15h1m8.0157244205474854s
TDB	15h1m7.1835020184516907s
TCB	15h1m25.687646269798279s
TDB	15h1m7.1835020184516907s
TT	15h1m7.1839848160743713s
TCG	15h1m8.0157244205474854s
difference	0.000

the one in formula (13), the meaning of V_E, X as in formula (14) and M represent the mean anomaly.

In SOFA library, the conversion between TCB and TCG can also be conducted indirectly. In turn, calling iau_TCBTDB, iau_TDBTT and iau_TTTCG three functions, the indirect conversion between TCB and TCG can be achieved.

Examples of conversion

This example uses Wuhan October 26, 2014, 15:00 (UTC) as the initial data (the same below). The value of TT, TCG, TDB, and TCB are calculated and the self-consistency of time conversion is analyzed under the framework of the relativistic. According to the calculated results, subtraction is done and difference items will be got. The result is shown in Table 1.

The order for time conversion is UTC->TAI->TT->TCG, TT->TDB->TCB. And then TT, TCG, TDB, TCB can be obtained. In turn, the reverse calculation function is used to calculate TCB-> TDB-> TT-> TCG, and then TDB, TT, TCG will be got conversely. Table 2 shows the results of TT, TCG and TDB obtained by positive sequence, which is exactly the same as the reverse results obtained. So the differential item is 0 that indicates the self-consistency of the transitions between the various time systems as very good. When solving TDB, the difference of x and Y, or of U and V is small, which indicates that both methods can be applied. In seeking TCB and TDB time system conversion value, the calculation involves the longitude and latitude. Here we take three sites of Paris, Lhasa and Wuhan, and October 26, 2014, 15:00 (UTC) time as initial time; TDB and TCB are solved respectively. Because TT does not involve solving the latitude and longitude, here the fractional part of the day time that is only listed to avoid repetition.

In Table 2, TDB and TCB of three stations appear different, which is because long-term coefficient of the provisions of IAU and TDB in formula (8) has been removed, which is a direct result of TT. And TDB unit length is inconsistent. After solving TCB through TDB, it will make a difference. In order to make a more intuitive feel of the self-consistency about time conversion under relativistic framework, the calculated Julian date is converted to calendar time. The conversion results of which are shown in Table 3. It can be seen that the time conversion has a good self-consistency.

Conclusions

This paper systematically describes the conversion between the TT, TCB, TDB, TCB-time system under the framework of the theory of relativity, and gives & explains some of the functional relationship between them. Then, the implementation of principle of mixed programming is discussed, and so are the considerations in detail.

Finally, the mixed programming is used to solve examples. It can be seen that the result of the positive sequence call and reserve call of SOFA function library are identical. And the differential item is 0, which well illustrates the good self-consistency of time conversion under relativistic framework based on SOFA function library.

Acknowledgments

This research was funded by the national '863 Project' of China (No. 2008AA12Z308) and National Natural Science Foundation of China (No. 41374012).

References

[1] Huang Tianyi, Xu Bangxin. Time Scales in Relativity [J]. PROGRESS IN ASTRONOMY, 1989, 7 (1):49-50.
[2] ZHANG Han-wei, MA Guo-qiang, etc. The Definition and Application of Concorning Time in the Framework of Relativity [J]. Journal of Institute of Surveying and Mapping. 2004, 21 (3):161-162.
[3] ZHOU Zhen-hong, REN Hui, etc. Fortran DLL component being integrated into Microsoft .NET framework [J].Engineering Journal of Wuhan University. 2005, 38 (4):101-102.
[4] WEI Erhu, CHANG Liu, etc. Transformation Between ICRS and ITRS Based on SOFA [J]. Journal of Geomatics. 2012, 37 (1):31-32.
[5] Han Chunhao. Time Measurement Within the Framework of Relativity [J]. PROGRESS IN ASTRONOMY. 2002, 20 (2): 109-111.
[6] IERS Conventions(2003), D.D.McCautly & Petit(eds.), Frankfurt and Main, (2004)
[7] International Astronomical Union. SOFA TimeScaleandCalenderTools[EB/OL].[2012-12-24].
[8] Kong Xiangyuan, Guo Jiming, Liu Zongquan .Foundation of Geodesy [M].WUHAN: WUHAN UNIVERSITY PRESS, 2010.
[9] IERS.IAUinformationbuller[EB/OL]. [20040801].http://hpiers.Obspm.fr/eoppc/bul/bulb/explanatory.html.
[10]Zhenghang LI, Erhu WEI, et al. Space Geodesy [M], WUHAN: WUHAN UNIVERSITY PRESS, 2010.

RTK V6+
six engines plus one support

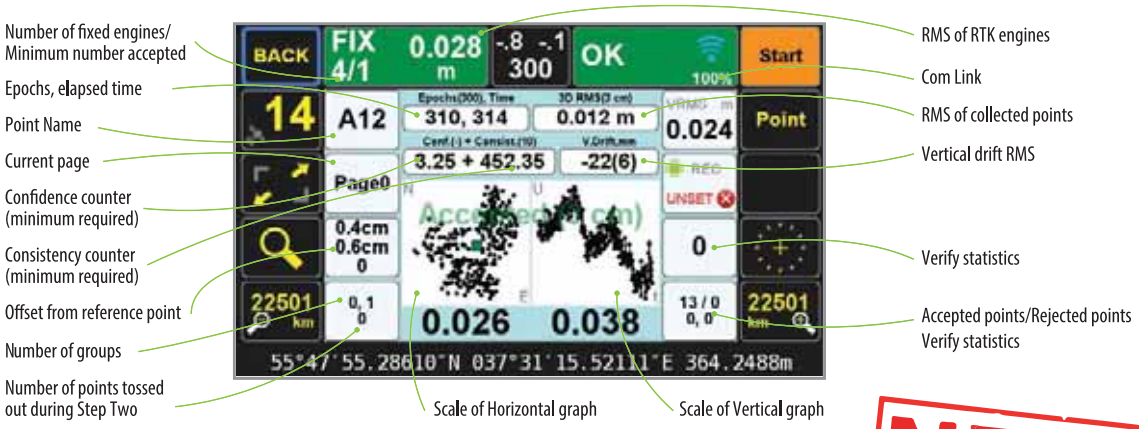

NEW

Auto Verify... Auto Validate...

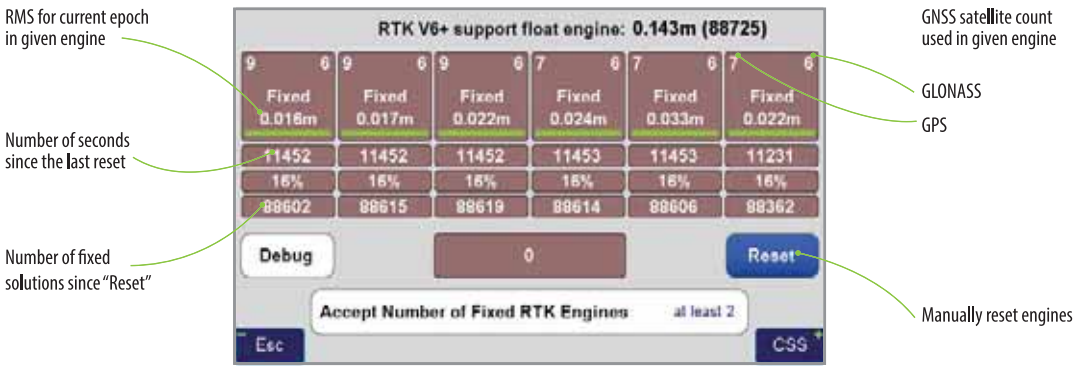

This vigorous, automated approach to verifying the fixed ambiguities determined by TRIUMPH-LS gives the user confidence in his results and saves considerable time compared to the methods required to obtain minimal confidence in the fixed ambiguity solutions of other RTK rovers and data collectors on the market today. The methods required by other systems are not nearly so automated, often requiring the user to manually reset the single engine of his rover, storing another point representing the original point and then manually comparing the two by inverse, all to achieve a single check on the accuracy of the fixed ambiguities. Acquiring more confidence requires manually storing and manually evaluating more points. Conversely, J-Field automatically performs this test, resetting the multiple engines, multiple times (as defined by the user), provides an instant graphic display of the test results, and produces one single point upon completion.

Read details inside and compare with other receivers that require Multiple Point survey, Manual Evaluation, Single Engine, and Single Ambiguity Check per Point.

With TRIUMPH-LS you need Single Point survey, Automated Evaluation, Multiple Engines, and Multiple Ambiguity Checks per Point.

VB-RTK

Reliable, Fast, Accurate, Less Cost

Get on the Grid with VB-RTK. For over a decade American surveyors have been using the National Geodetic Survey's Online Positioning User Service. Surveyors employing RTK have been a significant share of the user segment of OPUS.

A significant share of OPUS users are surveyors using RTK. Often a surveyor will set up his base on a new, unknown position and allow an autonomous (or standalone) position to be used for the base coordinates. While he is performing his RTK work with fixed vectors between his base and rover, he stores data at the base to be submitted at a later time to OPUS. Once he is finished with his work, he downloads this file to his computer, converts the file if necessary, and submits it to OPUS. He then receives an email response back with a precisely determined coordinate for his base station. He then must take this coordinate, relate the coordinate to his project coordinate system, and then translate the work from the autonomous (or standalone) position he used in the field to this new coordinate. This procedure can produce excellent results and anchors the survey to the NSRS. The down side to this is that there are several steps that must be carefully observed and each of these error prone steps costs time.

With J-Field data collection software, Javad has been automating many tasks that surveyors have been doing for years, making the tasks more efficient and reducing sources of potential error. One example, "**Verify RTK with V6 Resets**", is being recognized by surveyors across the country as the most accurate and efficient way to confidently determine RTK positions. Rather than taking a shot, manually resetting (or dumping) the receiver and taking a second shot for comparison, Verify RTK does this automatically with a user defined number of reset iterations.

Javad has continued this automation philosophy by dramatically simplifying the process of translating a survey from an autonomous base position to precise geodetic coordinates with **VB-RTK (Verify Base – RTK)**. Using the Javad GNSS, Data Processing Online Service (DPOS), which is powered by the proven Javad GNSS Justin processing engine. **This multi-level process is done in J-Filed completely automatically.**

Once an RTK session has been completed, the user returns to his Javad base receiver and presses "Stop Base" on the Triumph-LS. **At this point, the raw data file that has been recording at the base during the session, is wirelessly downloaded from the base to the Triumph-LS. When the download is complete, the user returns to his office and connects the Triumph-LS to the internet.**

When internet connection is made, the file is automatically transmitted to one of the Javad GNSS servers for post processing. Once data and ephemerides are available for the session, **DPOS** processes the file and returns results to the waiting Triumph-LS. This all takes within minutes.

Once results are returned, the new coordinates for the base are shown related to your coordinate system (including localization systems).

If the user is not satisfied with the results of the DPOS solution and wants it revert back to the

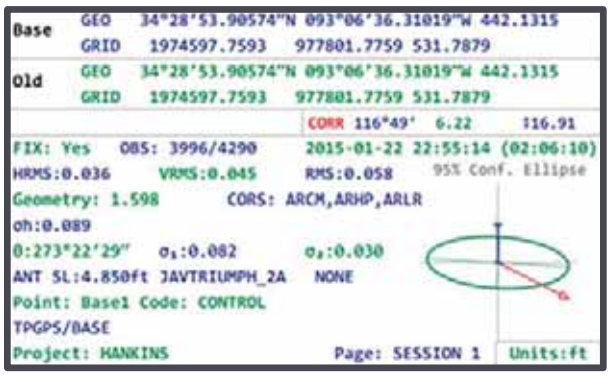

Concepts Behind RTK Verification

Fundamental in the determination of GNSS solutions is calculating the correct number of full wavelengths (so-called ***fixing ambiguities***) in order to figure out the distances from the satellites to the receiver. In doing Real Time Kinematic (RTK) surveying, we need it fast and we need it to be correct.

Multipath, the reflections of GNSS signals from ground and nearby objects and structures create their own indirect measurements from the satellites to the GNSS receiver. It's as if your measuring tape is bent around an obstacle such as a tree instead of a free and clear line of sight between two points. No calculator is going to improve this result.

TRIUMPH-LS has sophisticated hardware to distinguish between the direct and indirect signals and remove most of the indirect signals. It also reports the amount of indirect signal that has been removed. The worst case is when the receiver doesn't see the direct signal at all; e.g., the satellite is behind a building, but it's still receiving the signal reflected off of the nearby structure. It is the task of the RTK engines to isolate such indirect signals and then exclude them from the calculations.

If too many of the signals are affected by severe multipath or indirect signals, no solution may be found. Remember, indirect signals are analogous to the bent measuring tape! When you're preforming RTK surveying, observe your environment and come to recognize that the structures around you are like mirrors for GNSS signals.

The other aspect impacting the veracity of a fixed solution is when there are weak GNSS signals. Frequently, weak signals are due to their penetration directly through tree canopy.

While **TRIUMPH-LS** can't move the obstacles that are creating multipath out of the way, its sophisticated hardware has advanced multipath reduction sub-system, its tracking software is designed to handle even the weakest signals, and its **J-Field** software provides reliable RTK solutions like no other system with its **Automatic RTK Verification System** (patent pending). J-Filed also has ample tools to demonstrate the reliability of the solution or warn against questionable results. You can readily see that without such tools other systems can provide you wrong and misleading solutions.

J-Field uses six RTK engines (Figure 1) running in parallel plus a support engine to monitor and aid the six engines. Each engine uses a different criteria and mathematical method tailored to resolve ambiguities in different conditions. These six parallel engines not only verify robust solutions but also maximize the possibility of providing solutions in all conditions.

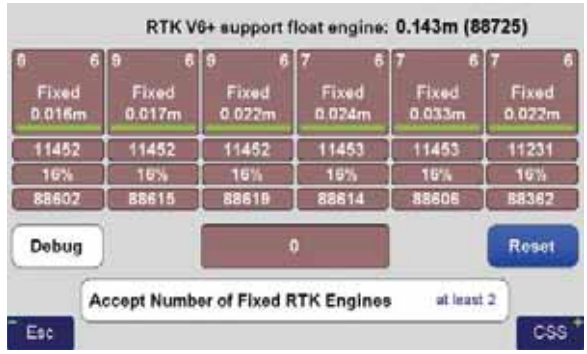

Figure 1 *V6+ six RTK Engines*

User Defined Verification Tools

J-Field provides the option for you to specify the **Minimum Number of Fixed RTK Engines** in verifying solutions **N** times before a position is automatically accepted where **N** is a user defined value.

J-Field employs two metrics to evaluate the performance of its RTK system of six engines: **1) Confidence Counter, and 2) Consistency Counter.** (Figure 2)

Figure 2 *Verify Settings*

Confidence Counter

This metric is incremented each time an engine is reset, ambiguities are recalculated, and the solution is in agreement with the previous ones (as defined by the **Confidence Guard (CG)**, default value 5 cm) is achieved. The Confidence Counter increments by 1, 1.25, 1.5, 1.75, 2.0, and 2.5 depending on the number of reset engines that fix in that epoch.

Consistency Counter

The Consistency Counter is incremented each time a solution is in agreement with the previous ones (as defined by the Confidence Guard) irrespective of engines being reset or not. The Consistency Counter is incremented by 0.0, 0.1, 0.25, 0.5, 1.0 and 1.5 depending on the number of fixed engines used in that epoch. Note that one fixed engine gets no credit and 6 fixed engines gets a **Consistency Credit** of 1.5.

Using these Confidence and Consistency verification tools, J-Field has two options to achieve reliable RTK solutions: **1) Verify With Automatic RTK Engines Resets** and **2) Verify Without Automatic RTK Engines Resets.**

Verify with Automatic RTK Engines Resets

This method has two steps: **1) Confidence Building** and **2) Smoothing and verifying**.

• Step One

In Step One, fixed engines are reset and solutions are collected into groups. Each group contains all the epochs located within a specified radius (the CG value) from its center and new groups are created as necessary so that all epochs fall into at least one group. Each group has its own Epoch Counter, Confidence Level and Elapsed Time. A point may fall into more than one group. The current best group is shown within [ ] and others within ( ). Step One continues until a group reaches the Confidence Level. (Figure 3)

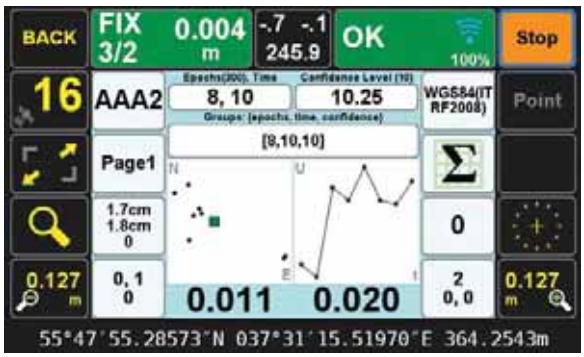

Figure 3 *End of Step one*

• Step Two

In Step Two, engines are not reset and solutions which are inside the CG of the selected group are added to that group for the remaining number of epochs that user has requested (Epoch Number, EN). Solutions that are outside the CG of the selected group, will be ignored but counted and on each such epoch, the RTK engines will reset. If the number of ignored points reaches 30% of EN, the whole process will restart. J-Field has 6 parallel RTK engines. You can specify the minimum number of engines required to be fixed to provide an epoch solution in Step Two. If the number of groups exceeds the Max Group the process restarts at Step One. This is to reduce the possibility of creating too many groups and rare false solutions in difficult environments. (Figure 4)

In both steps the Consistency Counter is also incremented as mentioned earlier.

You can manually reset all RTK engines via the V6-RTK engines screen (Figure 1), or assign this reset function to any one of the U1 to U4 hardware

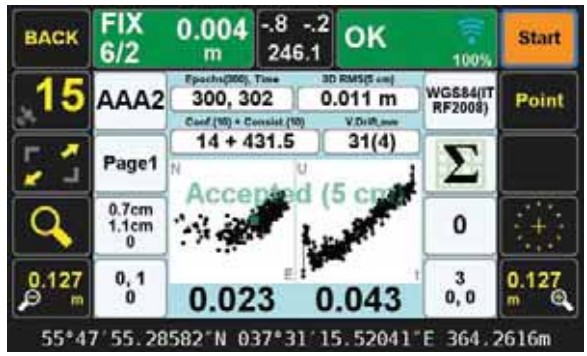

Figure 4 *End of Step 2*

buttons in front of the TRIUMPH-LS for easy access.

Verify without Automatic RTK Engines Resets:

In this method we don't force the RTK engines to reset but rely mostly on the Consistency Counter. There will be only one group as selected by the first epoch. Solutions that are not within the Guard band of the current average will be thrown out. If more than 30% of solutions are thrown out, the process will restart.

The horizontal and vertical graphs presented in both approaches also help the surveyor to evaluate the final solution. The linear drift of the vertical solution and its drift RMS are also shown above the vertical graph. A high linear drift (more than few centimeters) reveals severe multipath or, in rare cases, a wrong ambiguity fix. Pay close attention to the vertical drift and the horizontal and vertical scatter plots of epochs. Consider the scatter plots as doctors examine X-rays to determine anomalies.

The desired **Confidence Level** and **Consistency Level** are user selectable. Default values are 10. These parameters along with the desired number of epochs must be reached before a solution is provided.

In either case there is also a **Validate** option which, when selected, will reset all engines at the end of the collection and continues with 10 more epochs to validate if the solution is within the desired boundary of the Confidence Guard. (Figure 2) Minimum number of engines for the Validation

Figure 5 *How to Start*

Figure 6 *How to Stop*

Phase is user selectable.

In either case, if Auto-Accept is activated, the position will be automatically accepted if the RMS of the final solution is less than what user has selected in the Auto-Accept screen. (Figure 6)

You can also use **Auto-Restart** if you want to monitor structures or test the RTK system unattended. (Figure 6)

Screen Shots of Action Screen

Action Screen shows detailed information about each point collected. Screen shots can automatically be attached to each point and saved at the end of each collection (Figure 7). In **Verify with Automatic**

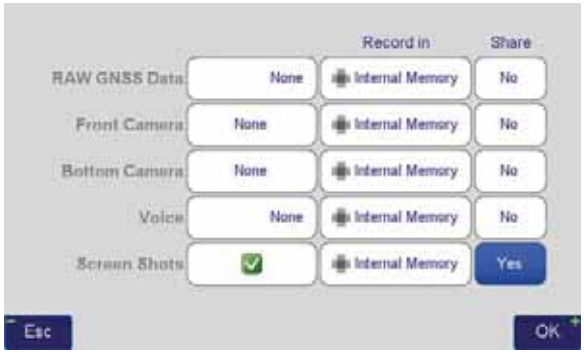

Figure 7 *What to record screen*

RTK Engines Resets screen shots at the end of both Step One and Step Two are saved (Figures 3 and 4). In Action screen there are 8 white boxes that selected items can be viewed on them.

Review Screen

View cluster of all points. Select the desired point to see its point cluster (Figure 8). Click the icons to see additional details about that point (Figure 9) including the distance and direction to the current point (Figure 10).

The effects of multipath, ionosphere, orbit, and other sources of problems somewhat exponentially increase as the baseline length increases. In a VRS/RTN scheme your **actual** baseline length is the actual distance to the nearest base station. The **virtual** base station that is mathematically created

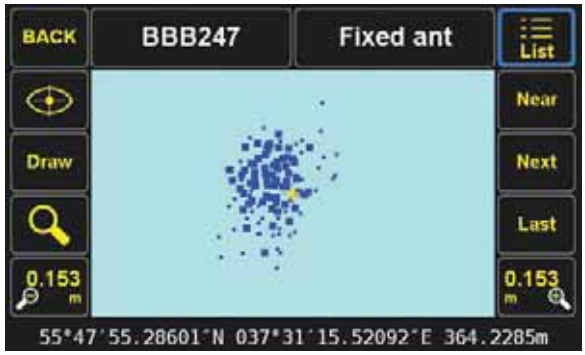

Figure 8 *Review screen shows cluster of 386 points*

Figure 9 *Detailed information on selected point (scroll to see all information)*

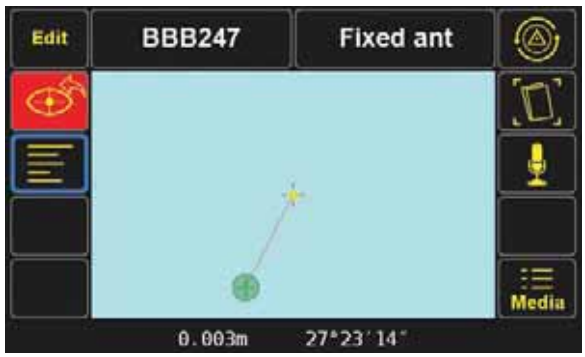

Figure 10 *Distance and direction from the current point to the selected point*

is not the actual length. We strongly recommend using your own base station near your job site in a Verified-Base RTK (VB-RTK) scheme.

In addition to providing you with the most reliable RTK solutions (especially true in remote areas where cell coverage is hit or miss), using your own base receiver allows you to easily tie your solutions to well-established IGS/NGS spatial reference systems through Javad's exclusive Data Processing Online Service (DPOS) and J-Field's user-friendly Base/Rover Setup. Note that post-processed results returned to the Triumph-LS using DPOS are dependent on the availability of orbital data from NGS and may require several hours. For further reading about DPOS, its integration into J-Field and the streamlined approach developed by Javad

for setting up the base and rover, please check out Shawn Billings' excellent article on VB-RTK on our website. Point your browser to: *http://www.javad.com/jgnss/javad/news/pr20150219.html*

Alternatively, if you don't have access to IGS-type stations to use DPOS, you can select an open area near your job site and use TRIUMPH-LS to obtain its position via RTN networks for about 5 minutes. You may repeat a couple of times for assurance. Then transfer this position to the TRIUMPH-1 or TRIUMPH-2 to use as the base station near your job site. The Base-Rover setup screen in the TRIUMPH-LS makes this job very easy.

Instantaneous Multipath charts

TRIUMPH-LS removes most of the multipath instantly on every epoch. Click on the Satellite icon to see the Signal Strength of satellites and then click the "+" key to see the multipath charts.

Figure 11 shows the amount of code phase multipath that TRIUMPH-LS has removed; relative to a fixed level. That is why negative numbers are in this figure. Units are in centimeter. Noting the signs in this figure, the amount of multipath in some satellites is in excess of 5.6 meters.

Figure 12 shows the amount of carrier phase multipath that TRIUMPH-LS has removed relative to a fixed level. Units are in millimeter. Noting the signs in this figure, the amount of multipath in some satellites is in excess of 4 centimeters.

SAT	EL	L1	P1	P2	L2C	L5	SAT	EL	L1	P1	P2	L2C	L5
GPS2	29↑	273	281	-76	--	--	BDU11	75↑	382	--	--	--	305
GPS6	44↑	55	201	-60	-5	189	BDU12	36↓	288	--	--	--	200
GPS12	70↑	183	190	-90	-94	--	GPS3	10	--	--	--	--	--
GPS14	25	281	317	-97	--	--	GPS29	3	--	--	--	--	--
GPS17	23↓	332	304	-74	6	--	GPS32	3	--	--	--	--	--
GPS24	53↓	117	566	67	-64	124	GLN7	3	--	--	--	--	--
GPS25	30↑	243	218	-42	-50	-34	GLN19	12	--	--	--	--	--
GLN1	10↑	305	229	-126	-404	--							
GLN8	16↓	26	87	-484	-617	--							
GLN9	32↑	359	301	-246	55	--							
GLN15	31↓	276	203	-93	-2	--							
GLN16	84↑	235	309	-133	-109	--							
GLN17	39↓	52	-84	-156	-52	--							
GLN18	69↑	190	168	-177	-184	--							
GAL12	88	680	-121	246	--	32							
SB127	25	488	--	--	--	318							
SB128	15	206	--	--	--	322							
QZ193	13↑	550	513	--	56	55							
BDU2	16	299	--	--	--	275							
BDU5	25	269	--	--	--	230							
BDU8	25↓	145	--	--	--	143							

Figure 11 *Code Phase multipath removed (cm)*

SAT	EL	AZ	L1	P1	P2	L2C	L5	SAT	EL	AZ	L1	P1	P2	L2C	L5
GPS2	29↑	154	7	7	2	--	--	BDU11	75↑	158	-6	--	--	--	-5
GPS6	44↑	98	11	9	2	2	-13	BDU12	36↓	60	-6	--	--	--	-14
GPS12	70↑	282	7	8	-2	-2	--	GPS3	10	26	--	--	--	--	--
GPS14	25	302	5	8	-4	--	--	GPS29	3	229	--	--	--	--	--
GPS17	23↓	58	6	9	-6	-2	--	GPS32	3	346	--	--	--	--	--
GPS24	53↓	198	1	4	13	1	-12	GLN7	3	297	--	--	--	--	--
GPS25	30↑	282	4	8	7	1	-32	GLN19	12	210	--	--	--	--	--
GLN1	10↑	34	1	4	-15	-23	--								
GLN8	16↓	344	12	15	17	25	--								
GLN9	32↑	316	0	2	-3	-6	--								
GLN15	31↓	142	5	5	0	1	--								
GLN16	84↑	266	2	2	-11	-18	--								
GLN17	39↓	44	-1	-4	-12	-10	--								
GLN18	69↑	188	-1	3	-1	-6	--								
GAL12	88	108	0	-26	0	--	-14								
SB127	25	160	7	--	--	--	-4								
SB128	15	130	8	--	--	--	-11								
QZ193	13↑	68	-3	-1	--	1	-19								
BDU2	16	132	-7	--	--	--	-17								
BDU5	25	154	-4	--	--	--	-7								
BDU8	25↓	54	-10	--	--	--	-20								

Figure 12 *Carrier Phase multipath remove (mm)*

Multipath Showcase

Graphs in the following examples show multipath effects in a 13.8 km baseline where about 1/3 of the rover sky was blocked by a tall building. This box shows horizontal (top) and vertical (bottom) offsets from the actual coordinates of the point (earlier surveyed for test).

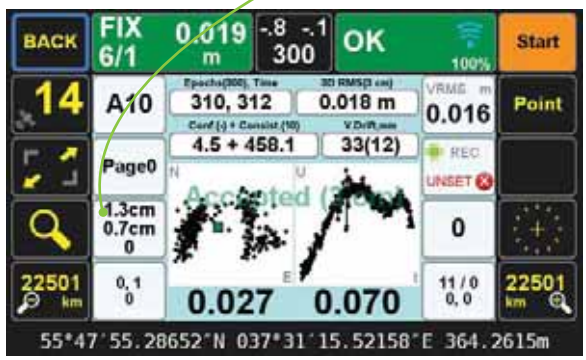

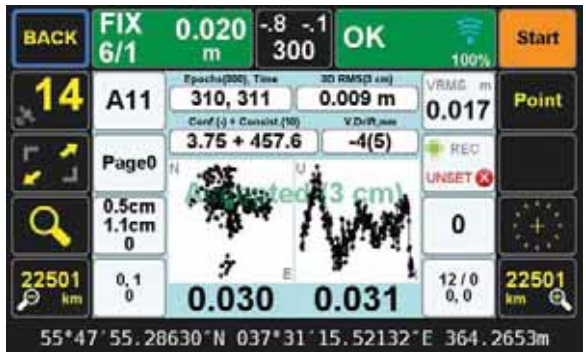

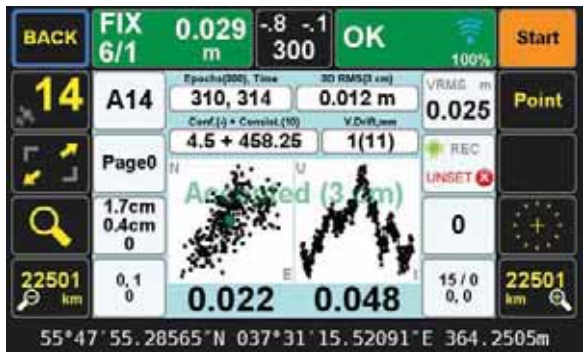

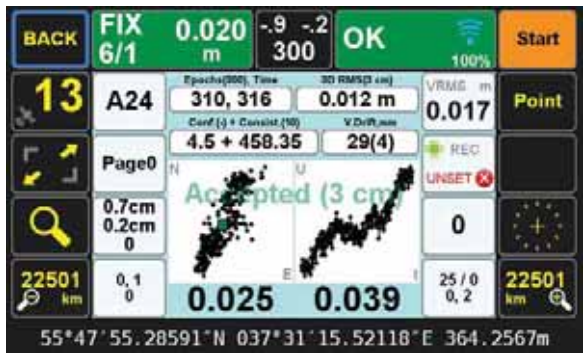

Javad Ashjaee, Ph.D.

original RTK positions, he simply clicks "**Undo**". This process is immune to base instrument height errors because the internal vectors between base to rover are related to the antenna, not the ground point. So, an accidental entry for the base height of 543' instead of 5.43' can be resolved by VB-RTK.

In addition to the advantages of having your RTK base station near your work area, which gives you much more accurate and faster fixes, especially in difficult areas, and saving you the RTN charges; perhaps most important of all, your work is now precisely related to one of the most accurate geodetic control networks in history - the NGS CORPS. Every rover point is only two vectors removed from the CORS (CORS to base, base to rover). This means that you can return again someday to find your monuments easily and accurately. This makes your records incredibly more valuable to both you and future surveyors. J-Field also has the unique ability to load and view every point you have ever surveyed from all the projects in its system. By combining this feature with a **distance filter** in its advanced set of filters, you can easily view all the points you have previously surveyed within a given distance of a point in your current project. Having an easily accessible record of nearby georeferenced coordinates is very beneficial as you may have previously located monuments in past surveys that are beneficial in your current project. J-Field allows you to easily copy these selected points into your current project, eliminating the need for you to resurvey them. All of this is available automatically on the world's most advanced RTK rover - **the Triumph-LS**.

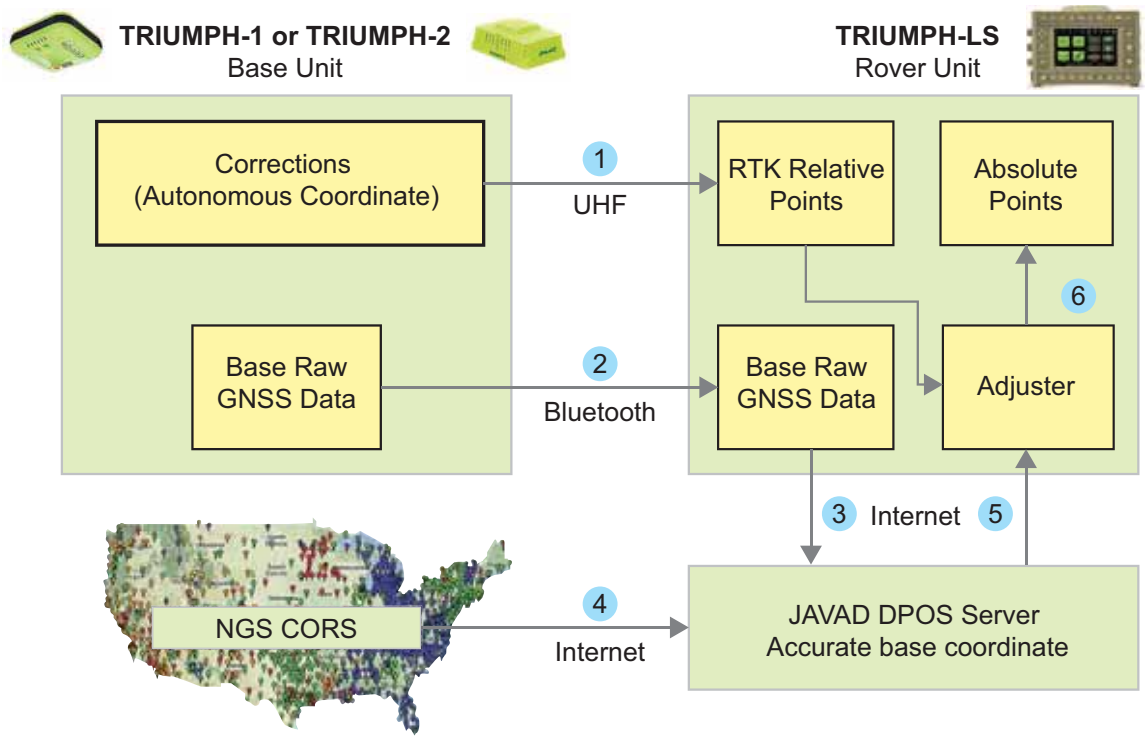

You do 1, the rest is automatic

Introducing

RAMS

Remote Assistance & Monitoring Services

JAVAD has gone and done it again! The brilliant minds at JAVAD GNSS have created yet another incredible first in surveying history: Remote Assistance & Monitoring Services (RAMS).

The RAMS Viewer is an elegant web interface. Using your own web browser, RAMS Viewer allows you to connect to your Triumph-LS from anywhere in the world when both your computer and Triumph-LS have access to the Internet.

RAMS is much more than just a remote data manager. Every function of J-Field that is available to the operator of the Triumph-LS that's in the field, is available to the remote viewer!

This incredible tool has many uses including facilitating live support by the PLS Support Team directly to Javad customers in the field, structural monitoring, training and other educational opportunities presented to large audiences in real time.

Using the Files tab, upload files to the Triumph-LS remotely from the office to the field... or right there on your desk in the office. Likewise you can download files wirelessly to the cloud or your own PC using RAMS Viewer.

Using the Status tab, quickly collect 18 screen shots in close succession showing your receiver's vital statics and bringing it all together at that very moment.

RAMS Server, the program running on the hosting computer, is at the heart of it all. This means you can set up RAMS Server locally on your own PC and keep it all in-house, or leverage the Internet using Javad's hosting server.

www.javad.com

A stand-alone positioning method for kinematic applications

In this study, an algorithm is proposed to improve the positional accuracy within a few decimeters using a single geodetic receiver with carrier phase data

M Halis SAKA
Associate Professor, Gebze Technical University, Department of Geomatics Engineering, Kocaeli, Turkey

Reha Metin ALKAN
Professor, Hitit University, Çorum, Turkey & Istanbul Technical University, Istanbul, Turkey

Alişir Özperçin
MSc Student, Gebze Technical University, Department of Geomatics Engineering, Kocaeli, Turkey

GNSS-based positions can be obtained in two general ways - Absolute (or Autonomous) Positioning and Differential (or Relative) Positioning. Absolute positioning, with only a single receiver, allows a meter level positioning easily and continuously. It has been widely used for several civil and military applications in real-time with only use of a single GNSS receiver. Although the absolute positioning accuracy has been significantly enhanced via the GNSS modernization studies, this accuracy is not regarded as sufficient for many surveying applications.

Over the past decade, a number of techniques have been introduced in literature to improve the positioning accuracy by using a single GNSS receiver. For example, in the 1980s, some researchers employed a method called 'smoothing' to create a pseudo-range/carrier phase combination that smoothes the pseudo-range data and could do point positioning at a meter or sub-meter level of accuracy, but it still did not meet the requirements of many surveying applications (Saka *et al.*, 2004).

Latest developments in GNSS data analysis and processing techniques offer some new approaches. A new method, called Precise Point Positioning (PPP), has arisen from the advent of widely available precise satellite orbits and clock data products provided from many organizations, such as International GNSS Service (IGS), Jet Propulsion Laboratory (JPL), NRCan and others. The PPP method provides positioning within a centimeter to decimeter level of accuracy using a single GNSS receiver data in static and kinematic modes (Zumberge *et al*., 1997; Kouba and Héroux, 2001; Choy *et al*., 2007; Huber *et al*., 2010; Alkan and Öcalan, 2013). Furthermore, for accurate PPP solutions, a number of corrections (e.g., carrier-phase wind-up, satellite antenna phase center, solid earth tide and ocean loading) should also be taken into account.

Although the PPP technique has been widely used and has become more popular, it has some drawbacks such as the necessity of long occupation time for convergence and the unavailability of PPP processing mode in common commercial GNSS processing software. The long convergence time restricts its usability in many cases where rapid solution is required and surveying efficiency is concerned (Liu *et al.*, 2013).

In our study, an algorithm is developed for precise positioning in dynamic environment utilizing dual-frequency GNSS carrier phase data collected only with a single geodetic-grade receiver. In this method, users should initiate the measurement on a known point near the project area for only a couple of seconds before starting the kinematic measurements. The technique employs iono-free carrier phase observations with precise orbit and clock products. The equation of the algorithm is given below;

$$S_m(t_{i+1}) = S_C(t_i) + [\Phi_{IF}(t_{i+1}) - \Phi_{IF}(t_i)] \quad (1)$$

where, $S_m(t_{i+1})$ is the phase-range between satellites and the receiver, $S_C(t_i)$ is the initial range computed from the initial known point coordinates and the satellite coordinates and Φ_{IF} is the ionosphere-free phase measurement (in meters) (Saka and Alkan, 2014). Tropospheric path delays are modelled using the Simplified Hopfield Model.

Figure 1: The Study Area

To accomplish the process, an in-house program was coded in MATLAB and some functions were adopted from Easy-Suite available at http://kom.aau.dk/~borre/easy (Borre, 2003). More detailed information about the handled algorithm can be found in Saka and Alkan (2013 and 2014); Saka *et al.*, (2015).

In this study, the usability of the introduced algorithm in near-shore kinematic applications is investigated. For this purpose, a test measurement was carried out in Istanbul, Turkey and the performance of the algorithm was assessed. In this paper, the test procedures and their results are briefly discussed.

Case study

In order to assess the performance of the introduced algorithm in a dynamic environment, a dataset from a kinematic test measurement was used. The data were collected from a kinematic test measurement in Haliç Bay (commonly known as the Golden Horn), Istanbul, Turkey in August 2009 (Figure 1).

In the test measurement, a geodetic-grade dual-frequency GPS receiver, Ashtech Z-Xtreme, was set up on a known point on the shore and a couple of epochs were recorded for initialization. The receiver was then moved to a vessel and data were collected for approximately 2.5 hours (Figure 2). The measurement was finalized on a known point on the shore.

While the kinematic measurements on the vessel were carried out, another GNSS receiver was set up on another geodetic point with known coordinates in ITRF reference frame on the shore and data were collected in static mode. The collected data by geodetic receivers, both on vessel and occupied on the shore, were processed by the Leica Geosystems commercial GPS processing software, Leica Geo Office (LGO). In this way, it is possible to obtain the reference trajectory with differential technique, i.e., known-coordinates of the vessel for each epoch that allows to perform precise assessment of the introduced approach.

Figure 2: Trajectory of the Vessel Along the Test Measurement

The coordinates of the vessel were calculated for each measurement epoch with the introduced method. As seen from Eq. 1, the process starts with the computing of distance between the observed satellites and the known point that measurements are initiated. After the first measurement, the change in the range between previous epoch and current epoch measured by the carrier phase is added to the previous range to determine the next phase-range. Then positions of the vessel are estimated for every epoch using phase-ranges (Saka and Alkan, 2014). In this study, with the purpose of obtaining more robust results, all coordinates were calculated once again inversely. As stated earlier, the test measurements ended up at a control point where coordinates were known precisely in ITRF datum. The process was run from last epoch to the first one and coordinates of the vessel were determined once again. The main purpose of this approach is to minimize the time-dependent error propagation. Furthermore, the calculated coordinates were also controlled. The average of estimated coordinates from two approaches was used as vessel coordinates. Positions of the vessel estimated from the introduced algorithm were compared with the known-coordinates epoch by epoch. The differences in north, east, positions and ellipsoidal heights are shown in Figure 3.

> The results produced in this study showed that decimeter level positional accuracy could be achieved with the introduced algorithm

The statistical comparison of the results as minimum, maximum, mean differences and root mean square of the error (RMSE) are summarized in Table 1.

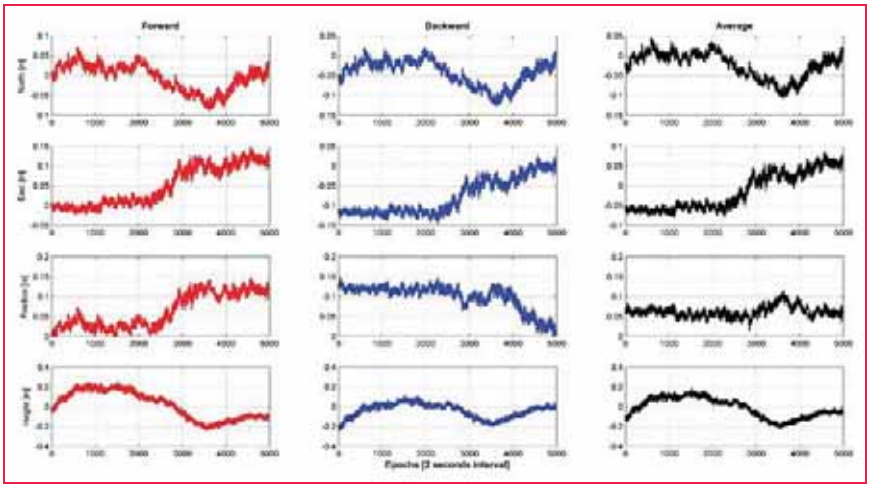

Figure 3: Differences between Known-coordinates and Introduced Solutions (left) Forward Solution (middle) Backward Solution (right) Average

Table 1: Statistical Comparison of the Results

	Position (m)				Height (m)			
	Max.	*Min.*	*Mean*	*RMSE*	*Max.*	*Min.*	*Mean*	*RMSE*
forward solution	0.15	0.00	0.06	± 0.04	0.25	-0.24	0.02	± 0.14
backward solution	0.15	0.00	0.10	± 0.03	0.12	-0.23	-0.04	± 0.07
average	0.11	0.02	0.06	± 0.01	0.18	-0.22	0.01	± 0.10

It is clearly shown in Figure 3 and Table 1 that the coordinates from the introduced method agree with the relative solution reaching to 11 cm and 22 cm for position and height respectively by the averaging of both estimated coordinates (i.e., calculated from first epoch to last epoch and from last epoch to first epoch). The differences were found relatively poor for the height components within about 2 dm or better accuracy. In general, the averaged-coordinates from the introduced method agree with the differential method within 1-dm or better level of accuracy for position and 2-dm or better level of accuracy for height.

Conclusions

In this study, an algorithm is proposed to improve the positional accuracy within a few decimeters using a single geodetic receiver with carrier phase data. The results produced in this study showed that decimeter level positional accuracy could be achieved with the introduced algorithm. This level of accuracy can be acceptable for a variety of surveying and mapping applications, including some marine applications, precise hydrographic surveying, dredging, attitude control of ships, buoys and floating platforms, marine geodesy, navigation and oceanography.

Acknowledgement

This paper is an extended and reviewed version of the study that was presented at the European Geosciences Union General Assembly 2015, Vienna, Austria, 12–17 April 2015.

References

Alkan, R.M. and Öcalan T. (2013). Usability of GPS Precise Point Positioning Technique in Marine Applications, *Journal of Navigation*, 66(4), pp. 579-588.

Borre, K. (2003). The GPS Easy Suite-Matlab Code for the GPS Newcomer,*GPS Solutions*, 7(1), pp. 47–51.

Choy, S.L., Zhang, K., Silcock, D. and Wu, F. (2007). Precise Point Positioning-A Case Study in Australia,*In Proc. of Spatial Sciences Institute International Conference (SSC2007)*, pp. 192-202, Hobart, Tasmania, Australia.

Huber, K., Heuberger, F., Abart, C., Karabatic, A., Weber, R. and Berglez, P. (2010). PPP: Precise Point Positioning-Constraints and Opportunities, XXIV FIG International Congress, Sydney, Australia, April 11-16.

Kouba, J. and Héroux, P. (2001). Precise Point Positioning Using IGS Orbit and Clock Products, *GPS Solutions*, 5(2), pp. 12-28.

Liu, Z., Ji, S., Chen, W. and Ding, X. (2013). New Fast Precise Kinematic Surveying Method Using a Single Dual-Frequency GPS Receiver,*Journal of Surveying Engineering*, 139(1), pp. 19-33.

Saka, M.H., Kavzoglu, T., Ozsamli, C. and Alkan, R.M**.** (2004).Sub-Metre Accuracy for Stand Alone GPS Positioning in Hydrographic Surveying, *Journal of Navigation*, 57(1), pp. 135–144.

Saka, M.H. and Alkan, R.M. (2013). An Approach for Decimeter-Level Positioning by Using Single Receiver in Hydrographic Applications, *Abstract Book of The 2nd International Conference on: Measurement Technologies in Surveying-GTP 2013*, pp. 35-36, Warsaw, Poland, 23–25 May.

Saka, M.H. and Alkan, R.M. (2014). Decimeter-level Positioning in Dynamic Applications with a Single GPS Receiver, *ActaGeodaetica et Geophysica*, 49(4), pp. 517-525.

Saka, M. H., Alkan, R.M. and Özperçin, A. (2015). An Approach for High-precision Stand-alone Positioning in a Dynamic, EGU General Assembly 2015, Geophysical Research Abstracts, Vol. 17, EGU2015-7378.

Zumberge, J.F., Heflin, M.B., Jefferson, D.C., Watkins, M.M. and Webb, F.H. (1997). Precise Point Positioning for the Efficient and Robust Analysis of GPS Data from Large Networks, *Journal of Geophysical Research*, 102(B3), pp. 5005-5017.

Assessing the quality of an UAV-based orthomosaic and surface model of a breakwater

This paper describes the conditions of the UAV flight and of the breakwater environment, conditions that were particularly hard, and presents the results of the quality control of the surface model made with the use of statistical methods

Maria João Henriques
Senior Research Officer, Applied Geodesy Division, Laboratório Nacional de Engenharia Civil, Lisbon, Portugal

Ana Fonseca
Senior Research Officer, Applied Geodesy Division, Laboratório Nacional de Engenharia Civil, Lisbon, Portugal

Dora Roque
Grant Holder, Applied Geodesy Division, Laboratório Nacional de Engenharia Civil, Lisbon, Portugal

José Nuno Lima
Research Officer, Applied Geodesy Division, Laboratório Nacional de Engenharia Civil, Lisbon, Portugal

João Marnoto
Director of the Geospatial Services unit, SINFIC, Amadora, Portugal

The breakwaters are built to protect infrastructure of ports. They are conceived and designed to withstand the most adverse and extreme weather conditions. The sea waves, the tides, the currents, winds, dynamics of underwater sediments and activities of the port, are some of the factors that lead to the degradation of breakwaters, and may restrict the activity of the port. One of the most insidious degradation is the removal of support materials that takes place beneath the blocks of protection on the surface. Quite often it is a localized process with slow progression and small effects on the surface of the breakwater, but that can be due to a major failure of a stretch of the structure and reduction of the functionality of the port.

When compared with structures like dams, bridges or large buildings, breakwaters are the structures much less monitored. As the deterioration of breakwaters usually doesn't put lives in danger and usually large structural modifications are a consequence of big storms that hit coastal areas, very few breakwaters are regularly monitored.

The monitoring of a breakwater, particularly the measurement of displacements, faces big challenges that have, in many cases, weak solutions. Marujo et al. (2013) has made a survey of the different monitoring techniques (expert judgment techniques and quantitative/automated techniques) available to monitor maritime and coastal structures. These include visual inspections (walking, waterborne, airborne, diving), close-up photography (terrestrial, waterborne, aerial and airborne), photogrammetry, videogrammetry, aerial photography (with normal or with unmanned aerial vehicles (UAV)), 'crane and ball' survey, topographic survey techniques (traditional and GNSS), multibeam and side scan sonar, Lidar, satellite images, InSAR methods and laser scanning.

Especially in breakwaters that protect small ports which don't generate large incomes, the monitoring displacements with aerial photography taken by a digital camera mounted on an UAV should be tested because, as being an inexpensive technique, it can represent an interesting alternative to other methods. This paper describes the first stage of a test, which is undergone, on the use of UAV techniques to monitor the displacements of the breakwater of Ericeira, a structure exposed to the north-west Atlantic waves. Since its rebuilt in the 2010s, this breakwater has been used to test new methodologies of monitoring like the use of 3D laser, multibeam techniques and UAV-based generation of surface model. This last one is the object of the studies performed by the authors of this paper, that deals with the assessment of the quality of an orthomosaic and of the surface model based in photos taken from an UAV, during a flight that faced difficult conditions, also reported in this paper.

The breakwater of Ericeira

Ericeira is a seaside resort, 35 km northwest of Lisbon, capital of Portugal, where fishing continues to

Figure 1: Reconstruction of the breakwater of the port of Ericeira

Figure 2: Breakwater of the port of Ericeira after the rehabilitation

play an important role in the local economy. In the past few years, Ericeira area has seen growing in its importance as a leisure resort due to the large number of quality surf breaks, seven, in just 4 km of coastline.

The port of Ericeira is mostly used by the local fisherman community. The advanced deterioration of the original protection of the quay (built in 1970s) was a consequence of the effect of the highly energetic north-westerly Atlantic Ocean waves on a under-dimensioned breakwater. A comprehensive study made by the National Laboratory for Civil Engineering (LNEC) in 2000, focused on the analysis of the status of pier under the perspective of its reconstruction and development of the port. The first stage of rehabilitation is already completed (Figures 1 and 2) and focused on rebuilding the breakwater and constructing new areas and buildings to support fishing activity.

The new rubble mound breakwater (RMB), which is longer and stronger, has created a wider area of sufficiently calm waters to allow safe operations of berthing, cargo transfer, vessels manoeuvre and protection of port infrastructures. The breakwater is 440 m long and 35 m wide. It consists of two straight lengths, angled at 147º to each other. The crest is 6.5 m wide and has an altitude of 9 m (referred to the hydrographic zero). The main elements of this breakwater are a core of finer material covered by big blocks (armor layer). Beneath the armor layer, a filter layer has been placed which is known as the underlayer, to prevent the finer material from being washed out through the armor layer.

Figure 3: Swinglet CAM and carrying case

Along the entire crest and on half of the leeside are two superstructures in concrete, being that the lowest one includes a quay. The most exposed slope of the breakwater (facing the northwesterly waves) is covered with tetrapods; the southwest extremity, which has a small lighthouse on the top, is covered with grooved cubes; the remaining areas are covered with large stones.

The UAV flight

The flight of the UAV airplane took place on February 9, 2013, after being delayed by a day due to strong winds in the area. It had to be carried out during high tide, not the best period of the day since many blocks were covered with water. The mix of these conditions (strong waves, wind, and high tide) made it impossible to find a good take-off/landing area nearby the breakwater. Ericeira village, on the top of the cliff that surrounds the port (see Figure 1), with a tight urban fabric, has no good areas either. The best one, a flat field with ground vegetation and no trees or bushes, was in the surroundings of Ericeira, nearly 1,200 m away from the port. It is necessary to state that this area was also chosen due to a clear sight to the area where the plane was going to operate in. On the slope between the take-off field (with at an elevation of about 100 m) and the port, there are several high buildings. For security reason, the altitude of the flight could not be set to a low value.

The photos were taken by a digital camera Canon IXUS 220 HS (3000×4000 pixels), mounted on the platform SenseFly Swinglet CAM (Figure 3), a very light (500 g) and small (80 cm wingspan) plane. The emission of data like battery level, speed of the wind, position of the UAV and a transmission that was made every 0.25 s to a control unit on land, would allow the monitoring of the flight. The control unit consists of the software eMotion (from Sensefly), installed on a laptop. This has an external radio antenna for communication. A more comprehensive description of the system can be found in Vallet et al. (2011).

EMotion was also used to programme the flight: To set the route, establish the height of the flight above ground, and to choose the points/area where to trigger the photos. In the flight above Ericeira breakwater, the following were set: i) the ground resolution, of 2 cm by pixel, ii) the area that needed to be covered, on a satellite view of the area downloaded from the internet, iii) the lateral overlap of the photos of 60%, iv) the longitudinal overlap of 90%. With this information, the software established automatically the flight eight (85 m), path (in the form of waypoints) and time interval between photos (a photo every two seconds). The flight plan was done at the office and transmitted to the airplane just before the flight. As explained before, it was impossible to find a good take-off area near the breakwater being that since the location chosen had a height of 100 m. For this reason, the flight over the breakwater was done at an altitude of

Figure 4: Flight path over Ericeira breakwater

Figure 5: Photo over the breakwater

185 m. As there is a strong connection between ground resolution and quality (Küng et al., 2011), the orthomosaic and the digital surface model generated from the photographs will have lower accuracy than initially expected.

During the flight there were problems with the transmission of data so the ground station received very few records from the airplane. When the UAV was over the breakwater, the ground station only received about 2% of the data expected, data that would have allowed to set an estimate on the location of the airplane (latitude, longitude, altitude), its attitude, speed, etc.

But, despite the communication problems and because the plane is completely autonomous, the flight was completed. The origin of these problems of communication might be related with radio interference caused by nearby communications antennae. Just before the flight over the breakwater it was performed another flight, 3 km southeast Ericeira, over a valley only with agricultural use. In this flight the only communication problems occurred when the airplane was behind hills and there was no line of sight to it. In Figure 4 we draw, on a GoogleMaps image, the programmed path of the flight (cyan lines) and the location of the centre of photographs

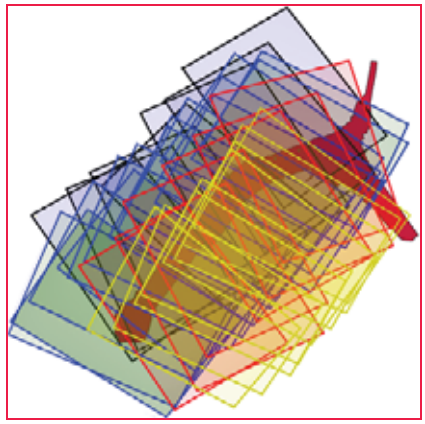

Figure 6: Span of the photos over the breakwater

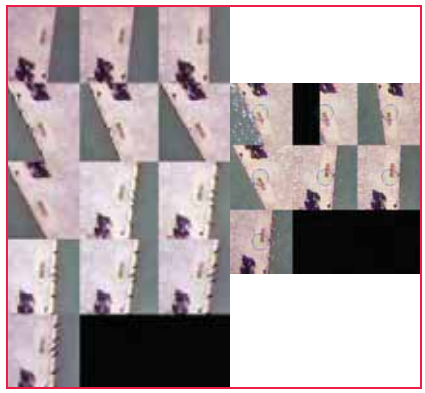

Figure 7: Automatic identification of a feature on 20 photos

(yellow dots), as received at the control station. From the 75 photographs taken, the ground station only received information about the flight in three of these. Figure 5 presents one of the photos taken.

Despite the bad conditions of the flight, with high northeast winds, we got a good coverage of the breakwater, as seen in Figure 6 where we represented, over the orthomosaic of the breakwater, the approximate span of each photo on the ground (in this study, only the breakwater area was considered).

During the flight the wind direction, and velocity, were not constant but the predominance was NW-SE direction. During the second and forth strips (blue and yellow polygons in Figure 6) the airplane flew in the NE direction, against the wind. One can see that its velocity slowed down because it took more photos. One can also see that it was at the beginning of the survey (black

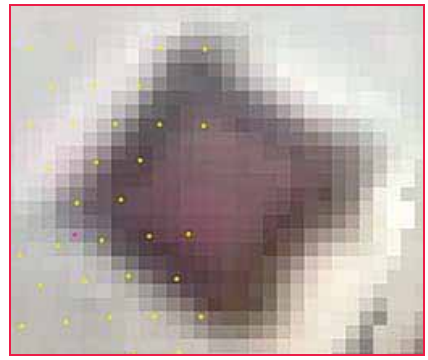

Figure 8: Manhole as seen on a photo. On the left side yellow points of the point cloud

Figure 9: Southwest corner of a manhole being coordinated

Figure 10: Coordinating a point near the lighthouse

polygons) that the wind presented more variations. Each spot of the breakwater was covered by at least five photos, being that some features are identified in

Figure 11: Orthomosaic. Location of the ground control points

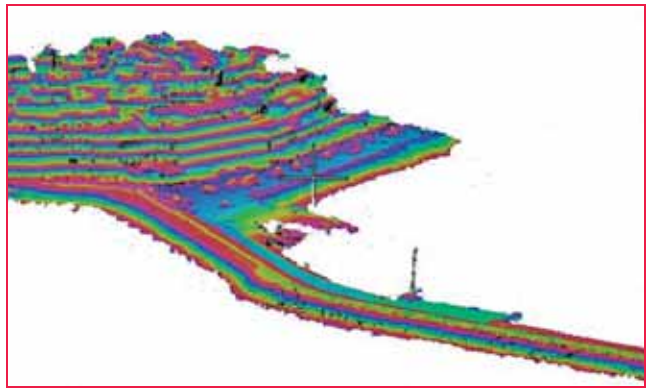

Figure 12: Point cloud. Colors of the points related with their altitude

Figure 13: Meshed surface that fits the point cloud (left image): it can be seen the lower level of the superstructure with several cars on it, parked by a vertical wall. On the right an extract of one photo, taken over the same area

21 photos (see example in Figure 7 of a feature that can be seen in 20 photos).

We determined the coordinates of several points (ground control points, GCP) of the superstructure of breakwater (Figure 11) by GNSS to reference the orthomosaic and the surface model and to assess planimetric and altimetric positional quality. We chose points that could be easily identified on the images (Figure 8), like the corners of the several square manhole covers placed along the superstructure (Figure 9), or the corners of the concrete base of the lighthouse (Figure 10). The points were coordinated using two Topcon choke ring antennae: one was placed on a tripod on the breakwater (reference station) and remained there during the surveying; the other was placed on top of a stick and on each point for three minutes. GNSS data was recorded at a period of 1 second. We calculated geodetic coordinates, in the ETRS89 reference frame, and cartographic coordinates, in the national coordinate system PT-TM06, using the software Pinacle and GNSS data of the nearest station of the Portuguese CORS Network.

Data processing

Despite the lack of information about the flight, the processing software PostFlight Terra 3D V1, also from Sensefly, was able to produce the orthomosaic and digital surface model.

The orthomosaic (Figure 11) is an orthogonal projection of the ground from which it is possibly to get only planimetric coordinates. It is the result of the combination of two photogrammetric processing tools: ortho-rectification (correcting imagery for distortion induced by elevation using elevation data and camera model information) and mosaicking (process of taking two or more separate images and 'stitching' them together into a single image). Information about height is necessary to build the digital surface model, which was derived from a point cloud also generated by the same software. The surface is described by a set of discrete points, independent of each other. Each one has only three attributes - the three coordinates. In Figure 12, we present the point cloud (perspective of the breakwater) where we assigned a color to each point based on its altitude. In this phase, for visualization purposes, we generated a triangle mesh from the point cloud (Figure 13).

Both products, generated only with very few data available from the flight, had large errors (almost 116 m in planimetry, in the south extremity of the breakwater), so we had to use some of the GCP to georeference the breakwater. We chose five points (green dots in Figure 11): one point near land, another near the end of the breakwater and two in the middle.

Such a large difference that is unusual in UAV orthomosaics, is the result of: i) lack of information about majority of the photos (coordinates of the centre of projection of the photos and airplane orientation); ii) in many photos the majority of the pixels has information about the water and this can't be used to stitch photos because it is impossible to find tie points; iii) small areas with tie points: the breakwater is a long and narrow structure that occupies a small area in each photo (photo in Figure 5 is a good example); iv) long areas with similar elements (monotonous tetrapods and stone blocks along a concrete strip). To surpass the problem, the only way was, as explained, to use some of the GCP as reference points. The points that we didn't use as reference points were used to assess the quality of the orthomosaic and of the surface model. In the next paragraph, the tests will be presented, and the

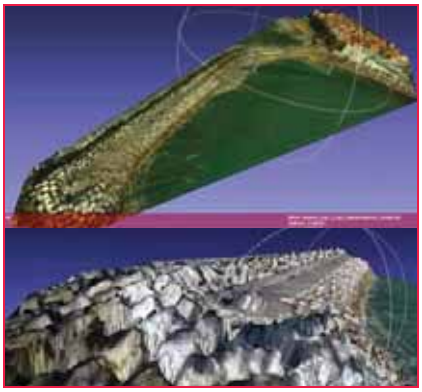

Figure 14: Orthomosaic on the surface model

following paragraph will include the data used and the results of the tests.

Statistics to test the differences of coordinates

We applied statistical tests to assess the quality of orthomosaic and surface model, tests that are usually used to evaluate the positional quality (Casaca 1999, Morrison 1990). We tested the accuracy and precision of the data. The data used are differences between GNSS and photogrammetric coordinates of the GCP. The GNSS coordinates, estimated with an error smaller than 1 cm, are more accurate than the photogrammetric coordinates obtained from the orthomosaic and the surface model, and therefore, will be considered as reference coordinates.

Let H (1,n), XY (2,n) and XYH (3,n) be matrices of the differences Δ between photogrammetric and GNSS coordinates:

$$H = [\Delta h_1 \quad \Delta h_2 \quad \cdots \quad \Delta h_n] \tag{1}$$

$$XY = \begin{bmatrix} \Delta x_1 & \Delta x_2 & \cdots & \Delta x_n \\ \Delta y_1 & \Delta y_2 & \cdots & \Delta y_n \end{bmatrix} \tag{2}$$

$$XYH = \begin{bmatrix} \Delta x_1 & \Delta x_2 & \cdots & \Delta x_n \\ \Delta y_1 & \Delta y_2 & \cdots & \Delta y_n \\ \Delta h_1 & \Delta h_2 & \cdots & \Delta h_n \end{bmatrix} \tag{3}$$

where n is the number of points, which can't be small.
The empirical average (scalar and vector) of the samples are determined by

$$m_H = \frac{1}{n}\sum_{i=1}^{n} \Delta h_i \tag{4}$$

$$\vec{m}_{XY} = \begin{bmatrix} m_X \\ m_Y \end{bmatrix} \tag{5}$$

$$\vec{m}_{XYH} = \begin{bmatrix} m_X \\ m_Y \\ m_H \end{bmatrix} \tag{6}$$

being that m_X and m_Y of (5) and (6) are determined from expressions equivalents to (4).

The corrected empirical variance of the samples are determined by

$$s_H^2 = \frac{1}{n-1}\sum_{i=1}^{n} (\Delta h_i - m_H)^2 \tag{7}$$

$$S_{XY} = \begin{bmatrix} S_X^2 & S_{XY} \\ S_{XY} & S_Y^2 \end{bmatrix} \tag{8}$$

$$S_{XYH} = \begin{bmatrix} S_X^2 & S_{XY} & S_{XH} \\ S_{XY} & S_Y^2 & S_{YH} \\ S_{XH} & S_{YH} & S_H^2 \end{bmatrix} \tag{9}$$

with the elements of the matrices presented in (8) and (9) determined by:

$$S_X^2 = \frac{1}{n\text{-}1}\sum_{i=1}^{n} (\Delta x_i - m_X)^2 \quad \therefore \tag{10}$$

$$S_{XY} = \frac{1}{n\text{-}1}\sum_{i=1}^{n} (\Delta x_i - m_X)(\Delta y_i - m_Y) \therefore \tag{11}$$

The matrices R of the empirical correlation are

$$R_{XY} = \begin{bmatrix} 1 & r_{XY} \\ r_{XY} & 1 \end{bmatrix} \tag{12}$$

$$R_{XY} = \begin{bmatrix} 1 & r_{XY} & r_{XH} \\ r_{XY} & 1 & r_{YH} \\ r_{XH} & r_{YH} & 1 \end{bmatrix} \tag{13}$$

with

$$r_{XY} = \frac{S_{XY}}{\sqrt{S_X^2\, S_Y^2}} \quad \therefore \tag{14}$$

where r is the correlation factor.

Under the hypothesis that distribution of the differences of coordinates are normal, the statistics

$$v_H = n\,\frac{m_H^2}{s_H^2} \in F\,(1;n\text{-}1;\omega) \tag{15}$$

$$v_{XY} = \frac{n\,(n\text{-}2)}{2(n\text{-}1)}\,\vec{m}^T\, S^{-1}\, \vec{m} \in F\,(2;n\text{-}2;\omega) \tag{16}$$

$$v_{XYH} = \frac{n\,(n\text{-}3)}{3(n\text{-}1)}\,\vec{m}^T\, S^{-1}\, \vec{m} \in F\,(3;n\text{-}3;\omega) \tag{17}$$

are distributed as random variables F de Snedcor, with the parameter of non-centrality ω.

The statistic

$$u_H = (n\text{-}1)\,\frac{s_H^2}{\sigma_H^2} \in \chi^2(n\text{-}1;\omega) \text{ with } \omega = \frac{\mu_H^2}{\sigma_H^2} \quad \therefore \tag{18}$$

is distributed as a random variable chi-square, with the parameter of non-centrality ω.

Testing the Accuracy

We characterize the accuracy of the photogrammetric coordinates by testing the centrality of the distribution of the positional errors of these coordinates. Under the null hypothesis (H0), the scalar v, from (15), (16) or (17) has a Snedecor's F distribution with f1 and f2 degrees of freedom; under the alternative hypothesis (HA), the scalar v has a non-central F distribution:

$$H0 \equiv v \in F\,(f1;f2) \quad ; \quad HA \equiv v \in F\,(f1;f2;\omega) \tag{19}$$

with f1=1, 2 or 3 when it is tested, respectively, altimetric, planimetric or 3D data. The degree of freedom f2 is equal to n-1. ω is a positive non-centrality parameter.

To test the null hypothesis against the alternative hypothesis, the variable of the test (v) is compared to the acceptance (RA) and critical (RC) regions:

$$RA = [0, q], \quad RC =]\, q, +\infty\, [\tag{20}$$

where q is the 0.95 quantile of the Snedecor's F distribution with f1 and f2 degrees of freedom.

Testing the Precision

We characterized the precision of the photogrammetric coordinates by testing the dispersion of the distribution of the positional errors of these coordinates. This test will allow us to assess if the orthomosaic/surface model is included in a pre-defined class of precision, class characterized by a tolerance (t_J), with a level of quality acceptable of, for instance, 0.95.

The variance σ_J^2 of each class "J" of precision is determined by the following expression:

$$\sigma_J^2 = \frac{(t_J)^2}{q} \tag{21}$$

where q is the 0.95 quantile of the chi-squared distribution with 1, 2 or 3

Table 1: Differences, in centimetres, between coordinates "UAV" (from the orthomosaic and the surface model) and coordinates GNSS

name	ΔX	ΔY	ΔH	name	ΔX	ΔY	ΔH	name	ΔX	ΔY	ΔH	name	ΔX	ΔY	ΔH
P1	-3.1	-3.8	-1.6	P5	1.1	-5.1	4.2	P16	1.7	-4.0	-4.3	Q44	-0.4	-10.3	7.4
P2	0.8	-3.6	6.4	P7	-2.8	-2.6	17.3	P18	-4.4	1.1	1.0	Q48	-2.4	-12.8	4.9
P3	3.1	-1.3	1.6	P9	-3.9	-7.8	11.3	P20	0.5	-13.8	1.9	Q49	8.6	-6.0	1.9
P4	0.1	0.2	1.3	P10	4.3	-14.0	15.4	Q10	12.3	-10.7	4.3	Q81	8.9	-9.1	14.0

degrees of freedom, depending on the coordinates (1D, 2D or 3D) being tested.

For instance, if it is considered three classes (J=I, II or III) with tolerances t_I=5 cm, t_{II}=10 cm; t_{III} = 15cm, the values of variances of each class when testing planimetric coordinates, would be σ_I^2=4.17 cm², σ_{II}^2=16.69 cm², σ_{III}^2=37.56 cm², since q=5.99.

In this test each component, X, Y and H are analysed in an independent way. Under the null hypothesis, the scalar u, from (18) has a chi-squared distribution with (n-1) degrees of freedom; under the alternative hypothesis, u has a non-central chi-squared distribution:

$$H0 \equiv u \in \chi^2\,(n\text{-}1); \quad HA \equiv u \in \chi^2\,(n\text{-}1;\omega) \qquad (22)$$

where ω is a positive non-centrality parameter. In equation (18), σ_H^2 will be replaced by σ_J^2, from the expression (21). The test will be performed as many times as the number of classes of precision established.

To test the null hypothesis against the alternative hypothesis, the variable of the test (u) is compared to the acceptance (RA) and critical (RC) regions:

$$RA = [0, q], \quad RC =]\,q, +\infty\,[\qquad (23)$$

where q is the 0.95 quantile of the qui-squared distribution with (n-1) degrees of freedom.

It was tested if each component was included in a chosen class of precision. To perform an analysis of the planimetric coordinates together (X and Y, as a whole) we will use a methodology adapted from the one presented by Mailing (1989). We will use a comparison of the ellipses with equal density of probability of the distribution of the planimetric inconsistencies with the corresponding circles of the planimetric tolerance. This test can be adapted to test the 3D coordinates.

Let λ be the smallest eigenvalue of the matrix of variance-covariance Σ^{-1}, matrix which is unknown. The condition

$$\frac{1}{\lambda} \leq \sigma_J^2 \qquad (24)$$

is necessary and sufficient for, given a probability level (1-α), the corresponding ellipse with equal probability density lies inside the circle of tolerance with radius:

$$t_J = \sqrt{q}\,\sigma_J \qquad (25)$$

where q is the probability quantile (1 - α) of a central chi-square distribution. It has two degrees of freedom when testing planimetric coordinates; three when testing 3D coordinates. Usually α=0.05.

According to Morrison (1990), the largest and the smallest eigenvalues of the matrix S^{-1} in the planimetric case (2×2 matrix) are

$$L_{max} = \frac{S_X^2 + S_Y^2 + \sqrt{(S_X^2 - S_Y^2)^2 + 4\,(S_{XY})^2}}{2\,[S_X^2\,S_Y^2 - (S_{XY})^2]} \qquad (26)$$

$$L_{min} = \frac{S_X^2 + S_Y^2 - \sqrt{(S_X^2 - S_Y^2)^2 + 4\,(S_{XY})^2}}{2\,[S_X^2\,S_Y^2 - (S_{XY})^2]} \qquad (27)$$

Knowing these eigenvalues is possible to build λ_*, an estimator of the smallest (λ) eigenvalue of the matrix Σ^{-1} and calculate the statistics w and the maximum likelihood estimator $\hat{\lambda}_0$ of λ.

$$\lambda_* = L_{min}\left[1 - \frac{L_{max}}{(n-1)(L_{min} - L_{max})}\right] \qquad (28)$$

$$w = \frac{\sqrt{n\text{-}1}}{L_{min}} \qquad (29)$$

$$\hat{\lambda}_0 = \frac{\sqrt{n\text{-}1} + \sqrt{n+7}}{2\,\hat{w}} \qquad (30)$$

The estimates $\hat{L}_{min}$ (27), $\hat{\lambda}_*$ (28) and $\hat{\lambda}_0$ (30) of the smallest eigenvalue λ can be used in the equation (24) to analyse if the level of tolerance can be accepted.

Results of applying the tests on the data

Ten points were used to assess the quality of the orthomosaic and the surface model. The planimetric coordinates were obtained from the orthomosaic using the software ArcGIS: the points were identified on the image and marked by a point. The attribute 'planimetric coordinate' of these points were transferred automatically to a text file. The height of these pointswere interpolated from the 2D barycentric coordinates. The differences between photogrammetric 'UAV' and GNSS coordinates are presented in Table 1.

The next step of the evaluation is to determine the empirical averages and variances (see values in Table 2).

With these values, we were able to perform the calculus of: i) statistics v_H, v_{XY} and v_{XYH}, and also of the statistics v_X and v_Y (Table 3) to test the accuracy, ii) statistics u and the eigenvalues of matrices to test the precision (Tables 4 and 5).

When v ≤q, the distribution of errors is central. In Table 3, it can be seen that only

Table 2: Empirical averages (m) and variances (S^2)

m_H= 5.4 cm	m_X = 1.5 cm	m_Y=-6.5 cm	(4)
S_H^2= 38.4 cm²	$S_{XY} = \begin{bmatrix} 23.9 & -7.6 \\ -7.6 & 24.0 \end{bmatrix}$ cm²	$S_{XYH} = \begin{bmatrix} 23.9 & -7.6 & 2.0 \\ -7.6 & 24.0 & -10.5 \\ 2.0 & -10.5 & 38.4 \end{bmatrix}$ cm²	(7) to (11)
	r_{XY}=-0.32	r_{XY}=-0.32, r_{XH}=-0.06, r_{YH}=-0.35	(12) to (14)

Table 3: Testing the accuracy

v_H=12.4; q=4.5; rejected	v_{XY}=13.1; q=3.7; rejected	v_{XYH}=9.0 q=3.4; rejected	(15) to (17) and (20)
v_X=1.6; q=4.5; accepted			
v_Y=27.9; q=4.5; rejected			

Table 4: Testing the precision. Each component *per se*

Class I t_I = 5 cm	Class II t_{II} = 10 cm	Class III t_{III} = 15 cm	Class IV t_{IV} = 20 cm	
u_X = 55.11	u_X = 13.78	u_X = 6.12	u_X = 3.44	(18) and (23)
u_Y = 55.31	u_Y = 13.83	u_Y = 6.15	u_Y = 3.46	
u_H = 88.44	u_H = 22.11	u_H = 9.83	u_H = 5.53	
q=7.26	q=7.26	q=7.26	q=7.26	

Table 5: Testing the precision of the planimetric and 3D coordinates

t_I = 5 cm; σ_I^2 = 4.2 cm^2 t_{II} =10 cm; σ_{II}^2 = 16.7 cm^2 t_{III} = 15cm; σ_{III}^2 = 37.6 cm^2 t_{IV} = 20cm; σ_{IV}^2 = 66.8 cm^2	t_I = 5 cm; σ_I^2 = 3.2 cm^2 t_{II} =10 cm; σ_{II}^2 = 12.8 cm^2 t_{III} = 15cm; σ_{III}^2 = 28.8 cm^2 t_{IV} = 20cm; σ_{IV}^2 = 55.1 cm^2	(21)
S_{XY} $\hat{L}_{Max}$= 0.061 cm^{-2} $\hat{L}_{Min}$= 0.032 cm^{-2} ⇒ $1/\hat{L}_{Min}$=31.56 cm^2 $\hat{\lambda}_*$ = 0.036 cm^{-2} ⇒ $1/\hat{\lambda}_*$=27.72 cm^2 $\hat{\lambda}_0$ = 0.035 cm^{-2} ⇒ $1/\hat{\lambda}_0$ = 28.20 cm^2 $\sigma_{II}^2 < 1/\hat{L}_{Min}, 1/\hat{\lambda}_*, 1/\hat{\lambda}_0 < \sigma_{III}^2$	S_{XYH} $\hat{L}_{Max}$= 0.070 cm^{-2} $\hat{L}_{Min}$= 0.022 cm^{-2} ⇒ $1/\hat{L}_{Min}$=45.20 cm^2 $\hat{\lambda}_*$ = 0.024 cm^{-2} ⇒ $1/\hat{\lambda}_*$=41.18 cm^2 $\hat{\lambda}_0$ = 0.025 cm^{-2} ⇒ $1/\hat{\lambda}_0$ = 40.39 cm^2 $\sigma_{III}^2 < 1/\hat{L}_{Min}, 1/\hat{\lambda}_*, 1/\hat{\lambda}_0 < \sigma_{IV}^2$	(27) to (30) and (24)

the positional errors of the X component have a central distribution. This is not a surprise after a simple analysis of the values of Table 1, where it can be seen that the majority of the differences of the components Y and H have the same sign.

According to the data presented in Table 4, the orthomosaic can be included in class III of dispersion because both statistics (u_X and u_Y) are smaller than q (the 0.95 quantile of the central chi-square distribution with 15 degrees of freedom). The component altitude, if considered independent, is classified as belonging to the class IV of dispersion.

To determine the eigenvalues of the matrix S_{XYH}, it was used the Excel addin Matrix.

To set the class of dispersion of the planimetric coordinates and of the 3D coordinates, it was used the three estimators of λ presented at the end of the last paragraph. In the last line of Table 5, the values presented are calculated for these three estimators. According to these and the classes chosen, the orthomosaic belongs to class III of tolerance; the surface model (that gathers planimetric coordinates with altitude) belongs to class IV of dispersion.

Conclusions

Several tests were presented that could be used to assess the positional quality in products used to represent the surface of the Earth. It was applied to analyse the quality of an orthomosaic and a surface model produced from photos of a breakwater. The photos were taken by a common digital camera mounted on an UAV airplane. The flight was done under bad conditions: strong wind, unknown position and attitude of the airplane due to the lack of communications.

The root mean square error of the photogrammetric 'UAV' coordinates is 10 cm in planimetry and 8 cm in height. The tests performed indicate that accuracy was not achieved while concerning the precision the orthomosaic that lies in Class III (15 cm) and the surface model in Class IV (20 cm).

These values are worse than the ones obtained from a very recent flight made with the same equipment over an area of 13.2 ha (the breakwater flight covered an area of 9.5 ha). In this larger area, in a city, it was possible to choose reference and control points all over it. Here, we were not limited to a narrow strip as in the breakwater study. Maybe this was the main reason for the achievement of better results.

References

Casaca,J. 1999. A Avaliação da Qualidade Posicional de Cartografia Topográfica em Escalas Grandes. Atas da II Conferência Nacional de Cartografia e Geodesia.

Küng, O., Strecha, C., Beyeler, A., Zufferey, J.C., Floreano, D., Fua, P., Gervaix, F. 2011. The accuracy of automatic photogrammetric techniques on ultra-light UAV imagery, Int. Arch. Photogramm. Remote Sens. Spatial Inf. Sci., XXXVIII-1/C22, 125-130, doi:10.5194/isprsarchives-XXXVIII-1-C22-125-2011.

Mailing, D. 1989. Elements of Cartometry. Pergamon Press.

Marujo,N., Trigo-Teixeira,A., Sanches do Valle,A., Araújo,M.A., Caldeira,J. 2013. An improved and integrated monitoring methodology for rubble mound breakwaters – application to the Ericeira breakwater. 6th SCACR – International Conference on Applied Coastal Research.

Morrison,D. 1990. Multivariate Statistical Methods. McGraw-Hill.

Vallet, J., Panissod, F., Strecha, C., Tracol, M. 2011. Photogrammetric performance of an ultra light weight swinglet "UAV", Int. Arch. Photogramm. Remote Sens. Spatial Inf. Sci., XXXVIII-1/C22, 253-258, doi:10.5194/isprsarchives-XXXVIII-1-C22-253-2011.

At a Glance

- A new three party agreement between Ordnance Survey (GB), Ordnance Survey Ireland (OSi) and Land and Property Services (LPS) Northern Ireland is set to improve access and availability of mapping services for customers and government users operating across the UK and Ireland.
- Raytheon-built GPS III system delivered
- Apple buys GPS firm Coherent Navigation
- MENA3D resseller of DroneMetrex for Mid-East and N. Africa
- Highway 407 ETR Selects Intergraph to Design Traffic Monitoring System
- Juniper Systems to Carry Cedar Tree Android Rugged Handhelds
- Airbus Defence and Space: 65th successful launch in a row of Ariane 5
- Euro Engineering, Italy Raises Research Value by Using SuperGIS
- DoT Completes 2014 Federal Radionavigation Plan
- US Air Force Opens Remote Sensing Systems Directorate
- Bluesky's New Mapshop Offers More Aerial Mapping Data
- Shallow Water Topography for South China Sea Islands by EOMAP
- Arithmetica simplifies CAD integration in Pointfuse
- ViaSat joins ESA's DeSIRE project
- Abia launches new geographic information system

RIEGL® VMZ

Hybrid Mobile Laser Mapping System

- fully integrated IMU/GNSS unit to support ***RIEGL* VZ-400, VZ-1000** and **VZ-2000** scanners for **mobile (kinematic)** data acquisition
- quick transition from mobile to terrestrial applications, and vice versa, without losing system calibration
- flexible installation options - vertical and horizontal setup
- image acquisition with fully integrated NIKON® DSLR camera and/or POINT GREY Ladybug5® camera
- easy system operation and data processing with ***RIEGL's* standard software packages** for static and mobile scanning applications

® registered trademarks

www.riegl.com

RIEGL®

RIEGL LMS GmbH, Austria | RIEGL USA Inc. | RIEGL Japan Ltd. | RIEGL China Ltd.

Coordinates

10 years before

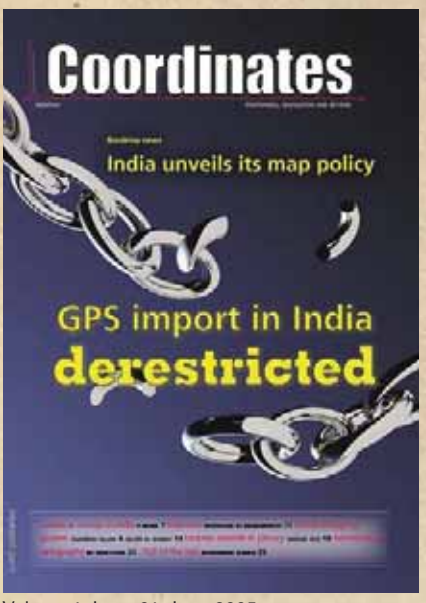

Volume 1, Issue 01, June 2005

Issues raised then...

Coordinates completes ten years... remembering the first issue

MANAGEMENT OF CHANGE

Cadastral surveys in India

A plea for centrally supported, orthophoto based, cadastral system and management of change

P MISRA

Recommendations

What is recommended in this paper is the technical aspect of cadastral surveys which is appropriate, modern, acceptable, practical and will provide a big push to the profession of cadastral surveys. The sound base will be given by the technology which eventually will reduce the ambiguity regarding records.

This technology can be practised in the model o f Public-Private-Participation (PPP). The State Government Departments need not spend huge money in procuring of equipment and instruments.

It is recommended that at initial stages, and in order to increase acceptability of the technology, the job should be done in some selected Taluks as Pilot Project. The technology can be transferred to States after adequate confidence is built up in State Cadastral Organizations.

The Survey of India should take a lead role in the introduction of technology, say, up to establishment of ground control by GPS. The resources generated by private sector in Geomatics can be harnessed through appropriate PPP model.

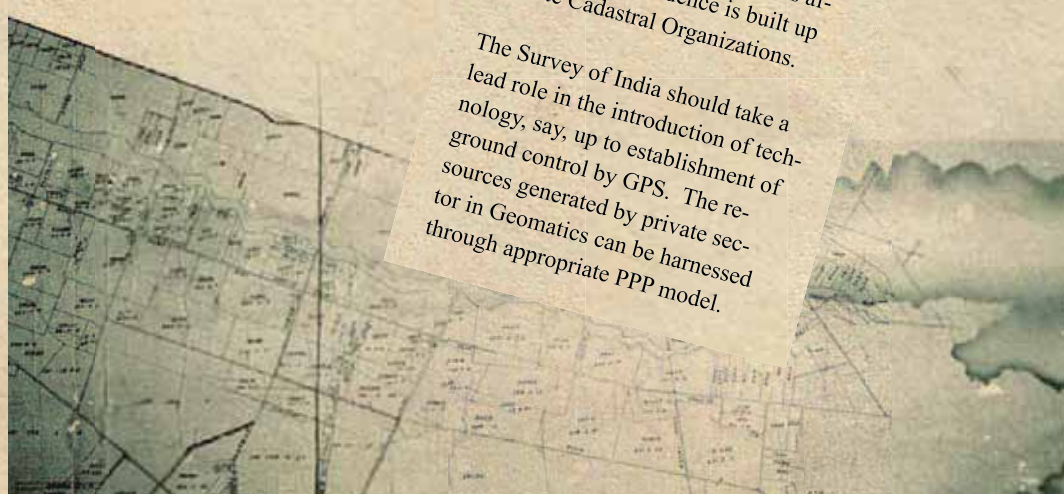

INTERVIEW

"Awareness is the key"

Prof V S Ramamurthy, Secretary, Department of Science and Technology (DST) emphasizes on awareness to promote positioning and navigation technologies the applicability of the technologies that makes a difference. Since July 1995, charge as Secretary to the Government of India, Department of Science and the Government of India awarded its prestigious 'Padma Bhusan, 2005' aw

Do you think that India should have its own satellite based position system?

Indian Space Research Organisation (ISRO) along with Airport Authority of India (AAI) has worked out a joint programme to implement the Satellite Based Augmentation System (SBAS) for the Indian region. The project called GAGAN (GPS Aided Geo Augmented Navigation) has been taken up to demonstrate the SBAS technology over the Indian region.

Talks regarding Indian Regional Navigation Satellite System" (IRNSS) are already in the air. In principle, there should be no issue on that, however, execution of such a plan will need huge investment of time and money.

Personally I feel that scientists should also keep on priority a research agenda of finding alternative ways of positioning and navigation even they have limited applications.

MOBILE MAPPING

Mobile Mapping Systems

In spite of the proven abilities and increasingly widespread adoption of MMS, there are a number of areas where significant improvements can still be made

CAMERON ELLUM AND NASER EL-SHEIMY

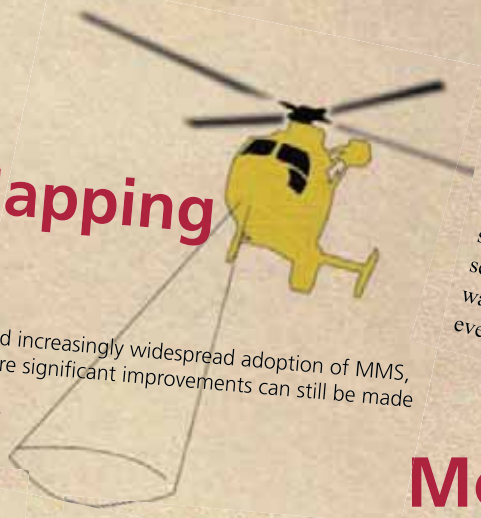

Challenges

In spite of the proven abilities and increasingly widespread adoption of MMS, there are a number of areas where significant improvements can still be made. Foremost among these is in the automated extraction of features from the remotely sensed data. Automated feature extraction has been one of the major research areas in mobile mapping technology since its inception. However, the techniques created so far have nearly all been ad-hoc solutions that work only with data from a single remote sensor, and for a limited number of features captured in specific environments from restricted sensor geometries. The techniques also typically require a moderate level of human monitoring. More advanced techniques of feature extraction that require less user input and interaction will open up even more applications for mobile mapping technology. Many of the developments in this area will require participation from researchers in robotics, artificial intelligence and computer vision. Closer collaboration with these researchers will undoubtedly benefit both the computer science and mobile-mapping communities.

Another area in MMS where there is room for improvement is in the sharing of data between the navigation and remotely sensed data processing streams. Currently, the sharing of data during processing is done at a rather superficial level: the results from the navigation processing are used to georeference the remotely sensed data, and then the mapping information of interest is extracted from the remotely sensed data. More advanced strategies where the sharing is done at the measurement level and/or in both directions could provide improved accuracy and reliability.

...are still relevant

Mobiles meddle in privacy

What are the objections to having location devices such as GPS? They may be misused with no protecion

GEORGE CHO

Privacy and legal protection

But such enhancements to law enforcement surveillance capabilities and market orientated capabilities raise serious privacy concerns. The third generation (3G) cell phones and web enables electronic devices are already available and everyone is eagerly watching for something to happen both in policy terms and in practice. The concern about further atrocities involving the use of electronic communication systems may prevail over the need for manageable e-business and personal data protection. Is the world moving towards a clamp down of human rights protection and data privacy protection? It is too early to tell.

GAGAN fully operationalized

The Indian Space Research Organization (ISRO) on 25 May 2015 announced the complete operationalisation of the GPS Aided Geo Augmented Navigation (GAGAN). The final operational phase of the system commenced on 19 May 2015 as it began broadcasting APV1 Certified signals.With this, India has become the fourth nation after the US, Europe and Japan to have inter-operable Satellite Based Augmentation System (SBAS). Also, GAGAN is the first SBAS system in the world to serve the equatorial region.

Earlier on 30 December 2013, Director General of Civil Aviation (DGCA) gave its nod for GAGAN for enroute operations (RNP 0.1) and subsequently on 21 April 2015 for precision approach services (APV 1). While the GAGAN Payload is already operational through GSAT-8 and GSAT-10 satellites, the third payload will be carried onboard GSAT-15 satellite scheduled for launch in October 2015. *www.jagranjosh.com*

New Airbus A350 Airliner fitted with EGNOS

The ESA-developed EGNOS system for sharpening the accuracy of satellite navigation across Europe has been adopted by a growing number of airports to enable satellite-guided landing approaches. The new Airbus A350 airliner, currently entering service, comes fitted with EGNOS as standard. This allows pilots to perform precision landing approaches guided by EGNOS or its US equivalent WAAS, offering vertical guidance down to a minimum of 60m before the pilot sights the ground to make the go/no-go decision on the final landing descent. The result is that the EGNOS-augmented signals are guaranteed to meet the extremely high performance standards set out by the International Civil Aviation Organisation (ICAO) standard, adapted for Europe by Eurocontrol, the European Organisation for the Safety of Air Navigation. A total of 131 airports in Europe offer some 225 EGNOS-based approach procedures. By 2020, 582 landing procedures are expected across 20 European countries. The largest international airports use Instrument Landing System (ILS) infrastructure, with radio beams offering a truly precision landing capability, including the ability to 'autoland' when visibility is at its worst. But ILS is expensive to install and maintain, so smaller regional airports often forego it. The same is true of many new or expanding airports.

Exelis, UrsaNav, the Dept. of Homeland Security and the U.S. Coast Guard enter into agreement

Exelis, UrsaNav, Inc., the Department of Homeland Security's Science and Technology Directorate (DHS S&T), and the U.S. Coast Guard have entered into a cooperative research and development agreement (CRADA) for testing and demonstration at former LORAN-C sites. These sites are the legacy ground-based radio navigation infrastructure of the decommissioned LORAN-C service that could be retained and upgraded to provide eLORAN low frequency service.

Under the CRADA, Exelis will use the former LORAN-C assets to put eLORAN signals in space for research, test and demonstration of the ability of eLORAN to meet precise positioning, navigation and timing (PNT) requirements of government and privately-owned critical infrastructure. *www.ursanav.com*

No imported components in construction of Glonass

JSC "Russian Space Systems" (RCC), together with ISS Reshetnev, plan to remove imported components in construction of GLONASS satellites. Production of the advanced GLONASS satellite "GLONASS-K" is scheduled to begin later this year.

According JSC CEO Andrew Tyulina, the company intends to stop the use of foreign electronic components as soon as possible. The plan is to have 80 percent of the satellites' electronic components payload be domestically produced by 2019.

The expected component supplier will be the largest designer and manufacturer of electronic components in Russia, Roselectronika, an entity that unites 112 companies, research institutes and design bureaus. The total investment in Roselectronika will exceed 210 billion rubles to 2020, including provision for modernizing industrial sites that produce electronic payloads for space.

Lotte World Tower to Use GNSS

Lotte world Tower, which is currently under construction in Jamsil, Seoul, will become the nation's first building to use the GNSS. This technology is currently used in the Burj Khalifa of Dubai and One World Trade Center in New York. The 2nd Lotte World Safety Management Committee held a conference recently for construction technology with the theme of "technology of measurement and a straightness management system for the Lotte World Tower skyscraper". *www.businesskorea.co.kr*

Centimeter-accurate' software-based GPS positioning developed

Now researchers at the University of Texas at Austin have developed a centimeter-accurate, software-based GPS-based positioning system, using existing smartphone GPS chips, which they claim is capable of drone package delivery down to a "specific spot on someone's back porch." It could also boost collision avoidance in cars and enable outdoor use of virtual reality headsets. The researchers also claim that when paired with a smartphone camera, it can build a 3D reference map of the surroundings, much in the same way Ford's LIDAR system and other autonomous vehicles do the same.

For now, the system, dubbed GRID, extracts carrier-phase measurements from low-cost antennas and operates outside the phone, but could eventually run on the phone's internal processor. Currently the system delivers both position and orientation information to less than one degree of measurement accuracy, which is more than enough for real-world VR use, 3D mapping, and collision avoidance systems. *www.extremetech.com*

INTERGEO®

Conference and Trade Fair for Geodesy, Geoinformation and Land Management

www.intergeo.de

Knowledge and Action for Planet Earth

15 – 17 September 2015
Stuttgart, Exhibition Grounds

INTERGEO®

along with

63rd German Cartographic Conference

Sponsors:

esri Deutschland

HEXAGON

Trimble

DVW DGfK

Host: DVW e.V.
Conference organiser: DVW GmbH and DGfK e.V.
Trade fair organiser: HINTE GmbH

RFP for GPS III launch services

The U.S. Air Force released a draft request for proposal (RFP) for GPS III Launch Services, including launch vehicle production, mission integration, and launch operations. The Space Exploration Technologies Corporation may well enter the competition.

On May 26 the Air Force Space and Missile Systems Center (SMC) and Air Force Program Executive Officer for Space announced the certification of Space Exploration Technologies Corporation's (SpaceX) Falcon 9 Launch System for national security space missions. It is now eligible for award of qualified national security space launch missions as one of two currently certified launch providers.

Sea Surface mapping with GNSS Radio Occultation

A new concept that involves mounting an instrument on the International Space Station and taking advantage of signals from navigation satellites could provide measurements of sea-surface height and information about features related to ocean currents, benefiting science and ocean forecasting.

In 2011 the European Space Agency (ESA) called for proposals to explore how the Space Station could be used to make scientifically valid observations of Earth. After reviewing and assessing numerous proposals, the result is to further develop the GEROS-ISS mission concept, which stands for GNSS reflectometry, radio occultation and scatterometry on board the ISS. GPS and Galileo satellites send a continual stream of microwave signals to Earth for navigation purposes, but these signals also bounce off the surface and back into space.

The idea is to install an instrument with an antenna on the Space Station that would capture signals directly from these satellites as well as signals that are reflected or scattered from Earth. This process could be used to calculate the height of the sea surface, and to measure waves — or "roughness" — that can then be used to work out the speed of surface winds.

Russian Glonass welcomed in Vietnam

Vietnam has been using GPS. If the negotiations succeed and Russia can place Glonass in Vietnam and three other countries, Cuba, Nicaragua and China, this will benefit Vietnamese users because it offers more choices for them. *http://english.vietnamnet.vn*

Russia, China Agree on Joint Exploitation of Glonass

The heads of Russia's Federal Space Agency and China's Satellite Navigation Office signed a joint statement on the joint exploitation of the BeiDou and Glonass. The document was signed by Igor Komarov and Wang Li in Moscow. *http://sputniknews.com*

Nicaragua approves Glonass

Nicaragua has approved the implementation of an agreement with Russia that authorizes the establishment of satellite ground stations in the Central American country. In 2012, Managua and Moscow inked an agreement to cooperate on space exploration and activities, including land installations for GLONASS. *www.presstv.ir*

The CALIBRA project

The CALIBRA project recently showcased a commercially applicable approach to mitigate the phenomenon's impact on high-accuracy GNSS positioning techniques. In two demonstrations, the project's newly developed algorithm was successfully tested in actual precision agriculture and offshore operations. Solar flares can cause ionospheric disturbance, a sudden increase in radio-wave absorption that often delays the propagation of signals and ultimately affects positioning. The problem has kept researchers busy for years.

The CALIBRA project team has been participating in this global research effort by focusing on Brazil, which is one of the most exposed regions due to its proximity to the magnetic equator. The project achieved three main milestones. First, the team confirmed that ionospheric scintillation and variations in total electron content (TEC) had a direct impact on the functioning of high accuracy GNSS techniques, such as Precise Point positioning (PPP) and real-time kinematic (RTK) positioning. Then a suitable metric was established to characterize these ionospheric disturbances. Finally, the project produced a short-term empirical model for forecasting TEC and scintillation. A regional TEC map was developed which proved advantageous for use in Brazil and, to counter scintillation, a number of approaches for the mitigation of this phenomenon were proposed and their benefit demonstrated.

A 'GPS' to Navigate the Brain's Neuronal Networks

In new research published by Nature Methods, scientists from the Hebrew University of Jerusalem and Harvard University have announced a "Neuronal Positioning System" (NPS) that maps the circuitry of the brain, similar to how a GPS receiver triangulates one's location on the planet. For more than a century, neuroscientists have tried to uncover the structure of the brain's neuronal circuits in order to better understand how the brain works. These brain circuits, which perform functions such as processing information and triggering reflexes, are composed of nervous system cells called neurons that work together to carry out a specialised function. Neurons send the messages to other neurons, or to target tissues such as skin and muscle that they innervate, via specialised wire-like processes called axons.

In the same way that we need to know the exact wiring of an electrical circuit to understand how it works, it's necessary to map the axonal wiring of neuronal circuits to understand how they function. Therefore a fundamental goal of neuroscience research is to understand the structural and functional connections of the brain's circuits. *ww.sciencedaily.com*

TI Asahi Co., Ltd.
International Sales Department
4-3-4 Ueno Iwatsuki-Ku, Saitama-Shi
Saitama, 339-0073 Japan
Tel.: +81-48-793-0118
Fax: +81-48-793-0128
E-mail: International@tiasahi.com

www.pentaxsurveying.com/en/

Authorized Distributor in India
Lawrence & Mayo Pvt. Ltd.
274, Dr. Dadabhai Naoroji Rd.
Mumbai 400 001 India
Tel.: +91 22 22 07 7440
Fax: +91 22 22 07 0048
E-mail: instmum@lawrenceandmayo.co.in

www.lawrenceandmayo.co.in

Mapping technique sheds new light on tropical forests

Scientists at the Woods Hole Research Center(WHRC) in Massachusetts, USA have developed vegetation height maps for the entire tropics at very fine spatial scales. These first-of its-kind high resolution maps can help researchers estimate forest cover, monitor biodiversity and wildlife habitats, and manage and monitor timber.

The WHRC researchers, led by senior scientist Josef Kellndorfer, combined two active remote sensing systems – radar and lidar – to create these maps. These active remote sensors send out pulses of electromagnetic waves – microwaves in the case of radar and light waves in the case of lidar - to map the earth's surface. Passive remote sensors, on the other hand, depend on the sun to illuminate parts of earth, and then detect the energy reflected or re-emitted by the different objects on earth.

Kellndorfer and his team combined more than 17,000 fine-scale radar images obtained by the Japanese ALOS satellite, with height measurements obtained by lidar on NASA's ICESat/GLAS mission, and developed continuous vegetation height maps for North and South America, Africa, and Asia for the year 2007. WHRC's pantropic maps are at a spatial resolution of 30 meters and can detect tree heights of up to 15 to 20 meters. This is an improvement over the previously existing vegetation height maps that were at coarser spatial scales, Kellndorfer said. *http://news.mongabay.com*

Delhi govt to use RS to check illegal construction

Delhi Government will use remote sensing satellite technology to check and map unauthorised constructions and encroachments in the city and that task forces led by sub-divisional magistrates have been formed to stop such activities. According to a senior official, the move came after the government decided to stop unauthorised construction in the city. *http://zeenews.india.com*

Vietnam, India cooperate in remote sensing technology

The Vietnamese Ministry of Natural Resources and Environment and the Indian Department of Space will promote cooperation in remote sensing and outer space technology via joint projects in human resources training and in applying remote sensing technology.

The two sides made the joint decision during working sessions between a delegation of the Vietnamese ministry, which made a three-day visit to India recently, and officials from India's Ministry of External Affairs, Department of Space, and Space Research Organisation.

The two sides reviewed preparations for establishing a centre for satellite tracking and data reception and processing for ASEAN – to be located in Vietnam, as part of the ASEAN-India cooperation framework. *http://english.vietnamnet.vn*

DigitalGlobe supports updated commercial remote sensing legislation

DigitalGlobe, Inc. has announced its support for the Commercial Remote Sensing Act of 2015, introduced in the U.S. House of Representatives on May 12 by Reps. Jim Bridenstine (R-OK) and Ed Perlmutter (D-CO). The Commercial Remote Sensing Act of 2015 is an important step toward necessary regulatory reform that will encourage growth in the U.S. commercial remote sensing industry, ensuring that the United States remains the world leader in this sector. The bill will provide for the collection of metrics around the U.S. Department of Commerce's regulatory workload and inform Congress about the Department's ability to meet statutory deadlines for adjudicating license applications. *www.digitalglobe.com*

KU awarded new FAA Center of Excellence designation

The University of Kansas in USA is among three universities across the state that are members of the new Federal Aviation Administration Center of Excellence for Unmanned Aircraft Systems, or UAS, which was awarded by the U.S. Department of Transportation in Washington, D.C. KU, Wichita State University and Kansas State University are members of the new center known as the Alliance for System Safety of UAS through Research Excellence, or ASSURE, which will play a key role in helping the FAA develop rules regulating commercial unmanned aerial systems. ASSURE, led by Mississippi State University, will provide the FAA and industry with research to maximize the potential of commercial unmanned systems with minimal changes to the current system regulating manned aircraft. *http://today.ku.edu*

Taiwan develops first indigenous RSI for FORMOSAT-5

The National Applied Research Laboratories has announced that the first optical remote sensing instrument (RSI) completely made in Taiwan that will be part of the payload for the FORMOSAT-5 satellite, marking a milestone in the nation's space technology development. The satellite is expected to be launched from Vandenberg Air Force Base in California in the first quarter of 2016 to replace FORMOSAT-2, which has been operating for over 10 years for Earth observation missions since its launch in 2004. *www.chinapost.com.tw*

Rapid Innovation Fund Award to the Remote Sensing Systems Directorate

The Space and Missile Systems Center Remote Sensing Systems Directorate was recently selected for a Rapid Innovation Fund award of $3 million to support Space Based Infrared System data exploitation innovations.

This award will be used to fund the Architecture for Real-time Overhead Persistent Infrared Wideband (ARROW) project, an initiative which enables the detection and tracking of dimmer and hard-to-detect objects to better protect the warfighter and the homeland. *www.spacedaily.com*

India is the world's top drone importer

The decision by India's National Disaster Response Force to use drones to help Nepal map the scale of devastation caused by last month's earthquake indicates how India has enthusiastically taken to these pilot-less aircraft -- the so-called eyes in the sky.

With 22.5 per cent the world's unmanned aerial vehicle (UAV) imports, between 1985 and 2014, India ranks first among drone-importing nations, followed by United Kingdom and France.

A total of 1,574 UAV transfers have taken place across the world between 1985 and 2014. Of these, 16 are armed UAVs, according to data provided by Stockholm International Peace Research Institute (SIPRI), an independent global conflict-research institute. *http://articles.economictimes.indiatimes.com*

Drones banned from Tokyo parks

The Tokyo Metropolitan Government has banned people from flying drones in metropolitan parks and gardens. Officials said it was based on an existing ordinance that bans "acts that cause a hindrance to management." The ordinance stipulates a fine of up to ¥50,000. *www.japantimes.co.jp*

Trimble Partners with Multirotor

Trimble has announced that it is partnering with UAS manufacturer MULTIROTOR service-drone, GmbH. The collaboration will allow Trimble to expand its existing UAS portfolio to provide its customers with additional solutions to choose from based on their aerial imaging project needs. *www.service-drone.com/en/*

eXom ready for take-off

senseFly has launched the eXom, quadcopter drone for mapping and inspection. Developed by experts working across numerous fields of robotics, this lightweight quadcopter offers professionals such as civil engineers and land surveyors the situational awareness, imaging flexibility and durability they need to complete challenging tasks safely, accurately and efficiently.

PrecisionHawk signs UAV research agreement with FAA

PrecisionHawk has entered into a Cooperative Research and Development Agreement with the Federal Aviation Administration to advance the research around UAVs across rural areas. PrecisionHawk will be the only UAV manufacturer, joining CNN and BNSF Railway, in the partnership forged under the Pathfinder programme, an operational concept validation set up by the FAA to help integrate commercial drones into the US national airspace, stated Michael Huerta, FAA Administrator.

Septentrio software and GNSS solution for the drone market

Septentrio has announced the launch of AsteRx-m UAS, a RTK –accurate GNSS receiver solution specially designed for the drone market. The UAS board is complemented by the release of GeoTagZ software suite; which works together with the UAS camera and image processing solution to provide cm-accurate position tagging of the images without the need for a real-time data link. *www.septentrio.com*

Daimler And Baidu Inc Team-Up

German automaker Daimler AG is increasing its ties with China's web service provider Baidu Inc to enhance its in-car software technology, for its luxury brands. Daimler. Daimler's Mercedes-Benz in China will support information and entertainment services from Baidu, where drivers and passengers will be able to access such services via vehicle's dashboard. *www.bidnessetc.com*

Ubimo Gets $7.5million

Ubimo incorporates additional data points, including weather and local events, to make ads more relevant and result in higher conversion rates.

Based in Tel Aviv, the startup recently closed a $7.5 million Series B led by Pitango Venture Capital, with participation from OurCrowd and YJ Capital (the venture capital arm of Yahoo Japan, which is investing for the first time in Israel).

Ubimo's software-as-a-service platform allows companies to manage ad placements by looking at factors that might influence each consumer's purchasing decisions, such as nearby venues, events, the weather, and neighborhood demographics such as the ages and gender of people most likely to patronize different services and businesses. *http://techcrunch.com/*

LED technology offers LBS

Philips has unveiled the first major install of its connected lighting system with LED-based indoor positioning for European hypermarket chain Carrefour.

The company said 2.5 kilometres of energy efficient LED lighting was installed at Carrefour hypermarket in Lille, France, which can transmit a location signal to a shopper's smartphone, triggering an app to provide location-based services. The technology allows Carrefour to provide new services to customers, including in-store navigation and promotions. *www.talkingretail.com*

Galileo update

Both New Galileo satellites now transmitting

Signals from both Galileo satellites launched March 27 are now transmitting signals.

Researchers at Université de Liège and at the German Aerospace Center (Deutsches Zentrum für Luft- und Raumfahrt, or DLR) reported on May 21 that the first of the full-operational-capability (FOC) satellites had begun transmitting standard L-band signals. The satellite, designated Galileo 8, is using pseudorandom-noise-code identifier 22.

The first E1 and E5 signals from Galileo 8 were received at an International GNSS Service Multi-GNSS Experiment tracking station in Windhoek, Namibia, at about 11:32 UTC on May 21. The satellite's signals were subsequently tracked by a station in Wettzell, Germany, and then by others.

The other satellite, Galileo 7, began transmitting standard L-band signals on May 25. The first E1 and E5 signals from Galileo 7 were received around 17:00 UTC. The satellite is using PRN code 26.

The signals will be set unhealthy for use until satellite commissioning is completed.

Galileo 7 is also known as GSAT0203, FOC-FM3 and as NORAD object 40544. Galileo 8 is also designated GSAT0204, FOC-FM4 and NORAD object 40545.

Eurocontrol, GSA Start Working to Better Implement SatNav in ATM

Following the signature of a framework partnership agreement on April 8, on April 20 Eurocontrol's Director General Frank Brenner visited the European GNSS Agency's (GSA) headquarters in Prague where, accompanied by his colleague, Adriaan Heerbaart, director of the Pan-European Single Sky, he met with GSA Executive Director, Carlo des Dorides. During this meeting they discussed key topics such as the aviation-specific environment and its requirements; the exploitation of EGNOS and Galileo; security for critical aviation systems; and future cooperation.

The teams discussed six work packages in depth, agreeing on priorities, timeframes and deliverables. These work packages cover aviation users' needs to support the definition of mission level requirements for EGNOS; the operational introduction of European GNSS services (EGNOS and Galileo) for aviation; advice on Regulatory and Standardization aspects, including spectrum; support to European GNSS Development and Exploitation Activities; coordination of R&D for GNSS in aviation; and the inclusion of EGNOS and Galileo in future GNSS user terminals for aviation.

Both teams described the progress meeting as a success to begin articulating secure and safe implementation policies for European satellite-based navigation in the aviation sector. *www.aviationtoday.com/*

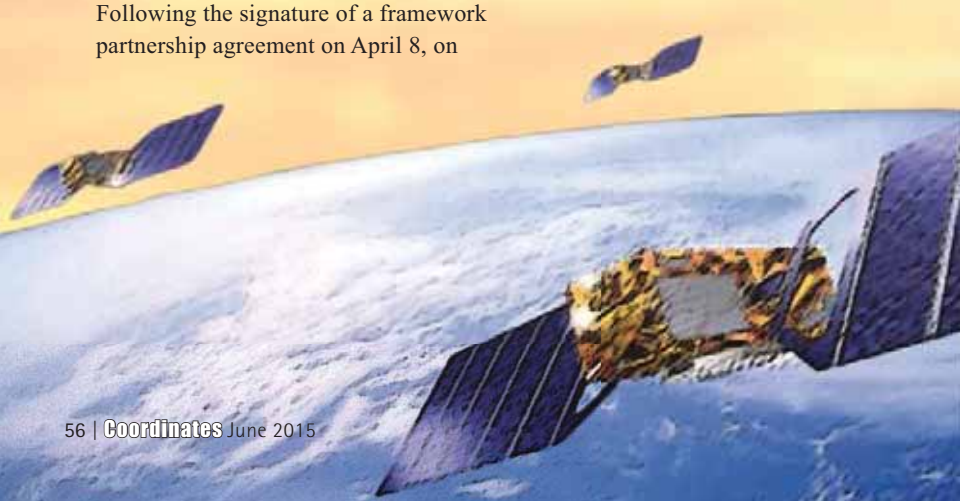

Uber's SOS button will send live GPS updates

Uber added an "SOS" button to its app in India. Starting in the city Kolkata and potentially rolling out elsewhere, activating the SOS button will now send live GPS updates to local police, provide police with information on the driver, and send details on the passenger reporting the issue, in addition to initiating a phone call with the police as it initially did. That information, which should enable police to track an Uber vehicle, will appear on a display that Uber installs for the local police.*www.theverge.com*

Delhi's wheels get GPS cover

Commuters in Delhi will shortly get to see the public vehicles operating with GPS. The government has approved mandatory GPS to all public transport vehicles, effective from June 1. The transport department had been extending the deadlines regarding the GPS and also announced that vehicles would need it in order to get their fitness certificate. *http://metroindia.com*

CMS V500 Cavity Monitoring System by Teledyne Optech

Teledyne Optech released the CMS V500, a complete redesign of its highly popular Cavity Monitoring System that introduces a live video feed, cable-free operation, and other critical new features that improve safety and efficiency in underground mining. It has been the ideal scanning solution for dangerous and inaccessible cavities in underground mining operations for years, improving safety by letting operators stand clear as the sensor head surveys. The accurate 3D data collected by the CMS improves mine operation efficiency by providing accurate insight into the mine's actual structure and the results of blasting, and increases mine profitability by verifying actual cavity size and orientation.

KCS TraceME

LoRa ™ Internet of Things

KCS has extended their successful TraceME product line with an advanced module, targeted for worldwide mobility in the Internet of Things era. The latest development of the TraceME GPS/GPRS Track and Trace module will combine the RF location based positioning solution with the LoRa™ technology. This combination offers 'smart objects' being even smarter, since LoRa™ enables long range, battery friendly communication in a wide variety of (M2M) applications. Supporting GPRS/SMS and optional 3G, Wi-Fi, Bluetooth LE, ANT/ANT+ and iBeacon™ provides easy integration with existing wireless networks and mobile apps. Other variants in the high/mid-range and budget-line will follow soon.

ANTI-THEFT module based on RF

KCS TraceME product line offers an intelligent location based positioning solution for indoor and anti-theft applications.The solution is based on RF with an intelligent algorithm of measuring the propagation time of transmitted (proprietary protocol) signals. Unique features are: minimum size (46x21x6.5mm), weight (7 grams for fully equipped PCB) and a standby battery lifespan of more than 10 years.'Listen before talk' algorithm makes it practically impossible to locate the module, which secures the valuable vehicle or asset. Supporting GPRS/SMS and optional 3G, Wi-Fi, Bluetooth LE, ANT/ANT+ and iBeacon provide easy integration with existing wireless networks and mobile apps.

www.Trace.ME

All trademarks mentioned herein belong to their respective owners

Integrated statistical and geospatial data vital for public information infrastructure

Integration of statistical and geospatial data is key to delivering a public information infrastructure that supports evidence-based decision making. At their first joint meeting, representatives from UN-GGIM: Europe and the European Statistical System (ESS) set out a committment to using geospatial information to link and match together data from multiple sources. This integration will not only meet user demands for statistical information with higher geographical detail but will also significantly speed up its delivery.

Bengt Kjellson, Chair of the UN-GGIM: Europe Executive Committee explained that its aim is to ensure a joint working relationship between National Mapping, Cadastral and Land Registry Authorities and National Statistical Institutes in the European UN Member States, the European Institutions and associated bodies. The meeting was held in Luxembourg and hosted by Eurostat. *www.un-ggim-europe.org*

Updated Global Mapper LiDAR module now available

Blue Marble has announced the release of Global Mapper LiDAR module version 16.2. Released in conjunction with Version 16.2 of Global Mapper, the latest version includes numerous functional enhancements and performance improvements that have been designed to help streamline the processing of LiDAR data. *www.bluemarblegeo.com/*

OS becomes a Strategic Member of the OGC

Ordnance Survey (OS) has announced that it has raised its Open Geospatial Consortium (OGC) membership level to become the first Strategic Member outside of the USA. As a strategic member OS will use their skill and expertise to drive a collective and unified approach to promoting interoperability for the geospatial industry. The new membership will also allow OS to represent Europe, at a strategic level, to improve the quality of standards globally and to enable the industry to continue to innovate and grow.

Cadastre 2034: Powering Land and Real Property

Cadastre 2034: Powering Land and Real Property is a national strategy for Cadastral Reform and Innovation for Australia. It has been prepared by the Permanent Committee on Cadastre; a Subcommittee of ISCM. The strategy captures the trends and articulates the vision of what we believe the community will require of our cadastral system by 2034. It identifies where current information falls short of today's consumer expectations, and considers the user scenarios that could trigger changing needs in the future. Cadastre 2034 has been developed with input from a New Zealand perspective and Trans–Tasman collaboration remains an important feature of this strategy. *www.icsm.gov.au/*

Mumbai starts GIS mapping of electoral wards

Brihanmumbai Municipal Corporation in India has started preparing heavily for the 2017 civic polls. The civic body is currently in the process of marking the boundaries of all the 227 electoral wards on google earth, as per the directions from the state election commission. As part of the plan, enumeration blocks will also be GIS mapped and in each block, the population as per the latest 2011 census will be marked. The herculean task will be undertaken by the election department of the BMC, with the help of the civic IT department and the medical officer (health) of all the 24 administrative civic wards, following which, it will be submitted to the state election commission. *www.dnaindia.com*

ArcGIS 10.3.1

Esri has released ArcGIS 10.3.1, bringing new capabilities:

- **Smart Mapping** is an innovative approach for creating maps that is available through ArcGIS Online. You can quickly style the features of your map to create useful and visually stunning maps every time.
- **3D Web Scenes** allow you to view, create, and share 3D web scenes in your browser. Available in ArcGIS for Server and Portal for ArcGIS, you can share these scenes within your own infrastructure, and if you choose to, share them publically.

IIC Technologies and DAT/EM Systems strengthen partnership

A long-time user of DAT/EM products, IIC Technologies has now extended its investment to 100 licenses of DAT/EM software as a part of their commitment to use quality tools to efficiently and cost-effectively serve their clients on a wide variety of projects.

Papua New Guinea: Monitoring forests with new Fire Watch website

Supported with a grant by the European Union, Papua New Guinea (PNG)'s new Fire Watch website uses the latest satellite imagery and image processing techniques, to advance an understanding of what is going on in PNG's forests in 'real time'. The Fire Watch website shows every location where a fire is burning, records where and when fires occur in PNG's forests and automatically uploads the information onto the site as it happens. Moreover, high resolution satellite images and maps of PNG can be viewed interactively with the locations of each fire. The website also features an archive of past locations, including time and date, of all fires detected across PNG since the mid 1990's. The Fire Watch website allows users to generate and print their own maps of fire locations in Papua New Guinea. The site is public and available free of charge to all users. *http://fire.pngsdf.com*

Mobile Surveying with High-Precision GPS and Advanced Mapping Features

TerraGo Edge Version 3.6 provides advanced support for EOS and SXBlue High-Precision GNSS receivers on iOSTM and AndroidTM, adds new mobile surveying features, new basemap sources and integration with Google EarthTM.

Trimble introduces BD935-INS module with precision GNSS

The Trimble BD935-INS is part of the company's GNSS OEM portfolio and augments real-time positioning with 3-D orientation. It is designed for applications that require orientation as well as RTK in a single package.

The module features triple frequency for both GPS and GLONASS constellations, as well as dual frequency for BeiDou and Galileo. It delivers RTK initialisation for 1–2cm positioning. For applications that do not require centimetre accuracy, the BD935-INS integrated GNSS-Inertial engine delivers GNSS and DGNSS positions in GNSS-denied environments such as urban canyons, tunnels, heavy canopy and more.

IFEN's v3.0 of SX3 GNSS Software Receiver

IFEN has launched the latest software release, v3.0, for its SX3 GNSS Software Receiver Generation with following features:

- Real-time P-code generator and P-code aiding for GPS L1/L2 cross-correlation
- Full dual-antenna support for SX3 Black Edition
- KML file output for Google Earth real-time visualization
- Better performance through switch from 32-bit to 64-bit version
- Support of new SX3 RF front-end with up to 12 IF streams

IFEN's SX3 multi-GNSS software receiver now tracks all known and in future upcoming GNSS signals in view in real-time on a standard laptop (up to 1,000 channels in parallel on a core i7 desktop PC).

Fugro wins DeepOcean fleet contract

Fugro has been awarded a contract by DeepOcean for the provision of precise satellite positioning for their entire fleet. The contract is valid for three years and also includes the new vessels in DeepOcean's continuously expanding fleet. DeepOcean is one of the world's leading providers of services and technologies for the subsea industry.

NovAtel chooses FileCatalyst Direct to send Large Files Fast

Unlimi-Tech Software, Inc., creator of FileCatalyst, has announced that NovAtel Inc has chosen FileCatalyst Direct for their high-speed file transfer requirements. With the implementation of FileCatalyst Direct, NovAtel employees are now able to transfer their large datasets across the globe quickly and securely. *http://www.prweb.com*

Hemisphere GNSS release Athena

Hemisphere has designed its new core engine to maximize the company's ability to excel at the rigorous GNSS requirements of multiple market segment customers in Machine Control, Survey and GIS. The release of Athena is a significant milestone for Hemisphere but just the first piece of a wave of new technologies being delivered into the market by Hemisphere in 2015. Athena excels in virtually every environment where high-accuracy GNSS receivers can be used.

New Thuraya Sat Phone comes with GPS, BeiDou and Glonass

Thuraya Telecommunications Company has launched a new satellite phone, the Thuraya XT-PR, featuring built-in GNSS with GPS, BeiDou and Glonass. It has a talk-time of up to 9 hours, it is water splash, dust and shock resistant, and features a hardened Gorilla glass display.

Forsberg Acquires Raven's StarLink GNSS Product Line

Forsberg Services Ltd. has acquired the StarLink product line from Raven Industries. StarLink includes inline amplifiers, coaxial down/up converters and fiber-optic link systems to enable and support extended cable runs

for GNSS in navigation and time synchronization applications.

Forsberg Services Ltd. is a European navigation systems integrator and OEM component supplier based in Lancaster, U.K. *www.forsbergservices.co.uk*

Topcon's GNSS network expands to Latin America

Topcon Positioning Group has announced the expansion of the TopNETlive GNSS reference station network into Latin America. In conjunction with hosting partners, new service will be provided in Mexico, Peru, the Dominican Republic, Bolivia, Guatemala, Colombia and Panama. It is designed to deliver high-accuracy GNSS correction data to rovers for surveying, construction, GIS mapping and agricultural applications.

eCognition Suite 9.1 by Trimble Geospatial

Trimble Geospatial has announced a new version of the Trimble® eCognition® software suite. It offers additional workflows to increase efficiency and quality of deliverables for Remote Sensing and GIS experts. This release includes capabilities to more efficiently generate intelligence from images and point clouds acquired by aerial, space borne, UAS-based or mobile mapping platforms. *eCognition.com*

Kenya Land Survey Efforts Aided with Spectra Precision Equipment

The Kenya Department of Surveys has acquired eight Focus 30 total stations and an additional eight Epoch 50 GNSS receivers as part of an ongoing major effort to adjudicate land and prepare deeds. According to the Lands Cabinet Ministry, until recently 67 percent of Kenya had yet to be adjudicated even as the work was supposed to be completed within 20 years after it was commissioned in 1957 by the British colonial government. To rectify the problem the government of President Uhuru Kenyatta two years ago began a major new push to produce three million titles by 2017. Recently, it was announced by the Land Surveys Department that 800,000 title deeds had been prepared and are being distributed.

RTK V6+ six engines plus one support by JAVAD GNSS

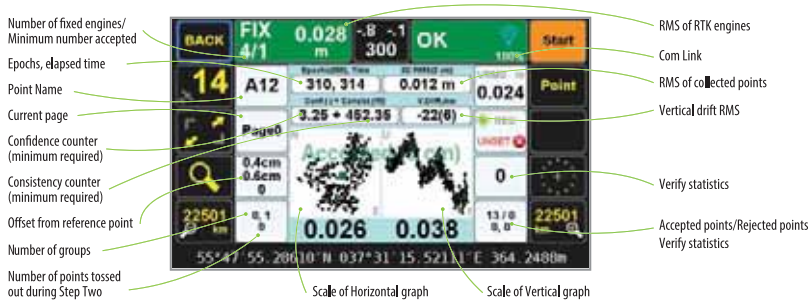

Auto Verify... Auto Validate...

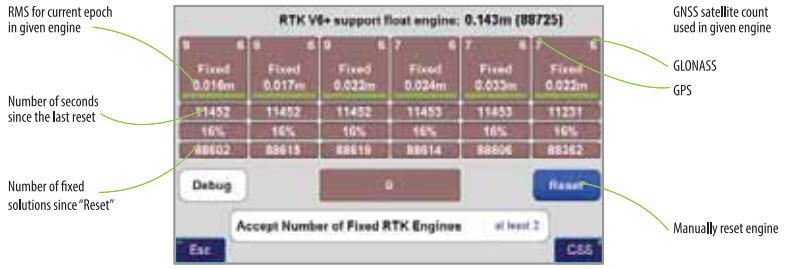

This vigorous, automated approach to verifying the fixed ambiguities determined by TRIUMPH-LS gives the user confidence in his results and saves considerable time compared to the methods required to obtain minimal confidence in the fixed ambiguity solutions of other RTK rovers and data collectors on the market today. The methods required by other systems are not nearly so automated, often requiring the user to manually reset the single engine of his rover, storing another point representing the original point and then manually comparing the two by inverse, all to achieve a single check on the accuracy of the fixed ambiguities. Acquiring more confidence requires manually storing and manually evaluating more points. Conversely, J-Field automatically performs this test, resetting the multiple engines, multiple times (as defined by user), provides an instant graphic display of the test results, and produces one single point upon completion. *www.javad.com*

AAM Group expands its operations to India

AAM Group has announced their expansion into India during a recently held ceremony held in Delhi. According to Mr. Mark Freeburn, Global CEO, AAM Group, "AAM is the largest geospatial mapping business in our Region which spans Africa, Asia and the Pacific. Creating AAM India furthers our aspirations and capabilities in Asia, with offices in India, Singapore and Malaysia. The new entity will focus its energies to provide excellence in data acquisition, processing and delivery across the geospatial spectrum. We will provide 3D City models,similar to the AAM produced models for Singapore, Sydney and Hong Kong, to broad area geospatial informationat a state wide level to assist with infrastructure, urban design planning, and the National Land Records Modernization Programme. We plan to work with other Indian geospatial companies to provide a new level of technology to support India's growth".

ION GNSS+ 2015

GNSS + Other Sensors in Today's Marketplace

The 28th International Technical Meeting of the
Satellite Division of The Institute of Navigation

September 14 – 18, 2015
Tutorials: Sept. 14 – 15
Tampa Convention Center / Tampa, Florida

SYSTEMS AND APPLICATION TRACKS
Mass-Market Applications
High Performance & Safety-Critical Applications
System Updates, Plans and Policies

PEER-REVIEWED TRACKS
Multisensor Navigation and Applications
Algorithms and Methods
Advanced GNSS Technologies

And, featuring the popular **Indoor Location Panel and Demonstrations**

The world's largest technical meeting and showcase of GNSS technology, products and services.

Register today! www.ion.org

Exhibitors—reserve your booth today! Space is limited.

SUBSCRIPTION FORM

YES! I want my Coordinates

I would like to subscribe for (tick one)

☐ 1 year	☐ 2 years	☐ 3 years
12 issues	24 issues	36 issues
Rs.1800/US$100	Rs.3000/US$170	Rs.4300/US$240

SUPER saver

First name .....

Last name .....

Designation .....

Organization .....

Address .....

.....

City ..... Pincode .....

State ..... Country .....

Phone .....

Fax .....

Email .....

I enclose cheque no. .....

drawn on .....

date ..... towards subscription

charges for Coordinates magazine

in favour of **'Coordinates Media Pvt. Ltd.'**

Sign ..... Date .....

Mail this form with payment to:

Coordinates
A 002, Mansara Apartments
C 9, Vasundhara Enclave
Delhi 110 096, India.

If you'd like an invoice before sending your payment, you may either send us this completed subscription form or send us a request for an invoice at iwant@mycoordinates.org

MARK YOUR CALENDAR

June 2015

ESNC & Copernicus Masters 2015
15 April to 13 July
www.esnc.eu, www.copernicus-masters.com

The Commercial UAV Show Asia 2015
30 June - 1 July
Singapore
www.terrapinn.com/exhibition/commercial-uav-asia/index.stm

July 2015

IGNSS 2015
14-16 July
Queensland, Australia
www.ignss.org

Esri User Conference
20 – 24 July
San Diego, USA
http://www.esri.com/events/user-conference

13th South East Asian Survey Congress
28 – 31 July, Singapore
www.seasc2015.org.sg

August 2015

The Fifth Session of the UN-GGIM
3-7 August
United Nations Headquarters, New York, USA
http://ggim.un.org

CPGPS MIPAN'2015
26 and 28, August
Xuzhou, Jiangsu, China
www.cpgps.org/new_site/news2015.php

UAV-g 2015
30 August - 2 September
Toronto, Canada
www.uav-g-2015.ca

ESA/JRC International Summer School on GNSS 2015
31 August - 10 September
Barcelona, Spain
http://congrexprojects.com/2015-events/15m21/registration

September 2015

GIS Forum MENA
6 – 9 September
Abu Dhabhi, UAE
http://gisforummena.com

InterDrone
9-11 September 2015
Las Vegas, USA
http://www.interdrone.com/

ION GNSS+
14-18 September
Tampa, Florida, USA
www.ion.org

INTERGEO 2015
15 – 17 September
Stuttgart, Germany
www.intergeo.de/intergeo-en/

October 2015

Surveying & development regional conference
03-06 October
Sharm El-Sheikh, Egypt
www.sd2015-eg.org/

Commercial UAV Expo
5 - 7 October
Las Vegas, Nevada, USA
www.expouav.com

DIGITAL EARTH 2015
October 5-9
Halifax, Canada
www.digitalearth2015.ca

20th UN Regional Cartographic Conference for Asia and the Pacific
5-9 October
Jeju Island, Republic of Korea
http://unstats.un.org/unsd/geoinfo/RCC/

Intelligent Transportation Systems: 22nd ITS World Congress
5 - 9 October
Bordeaux, France
http://itsworldcongress.com

Geo Empower Africa Summit
6 - 7 October
Johannesburg, South Africa
http://itc.flemінggulf.com/geo-empower-africa-summit

36th Asian Conference on Remote Sensing
19 - 23 October
Manila, Philippines
www.acrs2015.org

2015 IAIN World Congress
20 – 23 October
Prague, Czech Republic
www.iain2015.org

Joint International Geoinformation Conference
28 - 30 October
Kuala Lumpur, Malaysia
www.geoinfo.utm.my/jointgeoinfo2015/index.html

November 2015

ISGNSS 2015
16 - 19 November
Kyoto, Japan
http://www.isgnss2015.org/

Drone World Expo/MAPPS Conference
17 - 18 November
San Jose, CA United States
www.droneworldexpo.com

December 2015

9th International Symposium on Mobile Mapping Technology (MMT 2015)
9 - 11 December
UNSW, Sydney, Australia
www.mmt2015.org

StarFire 5cm accuracy
available anywhere on the Earth's surface,
land or sea.

5 cm

WHO NEEDS A BASE STATION WHEN YOU HAVE STARFIRE?

STARFIRE
Precise Point Positioning (PPP)

Watch the StarFire story at www.navcomtech.com/starfire

www.navcomtech.com
NAVCOM
A John Deere Company

We have you covered

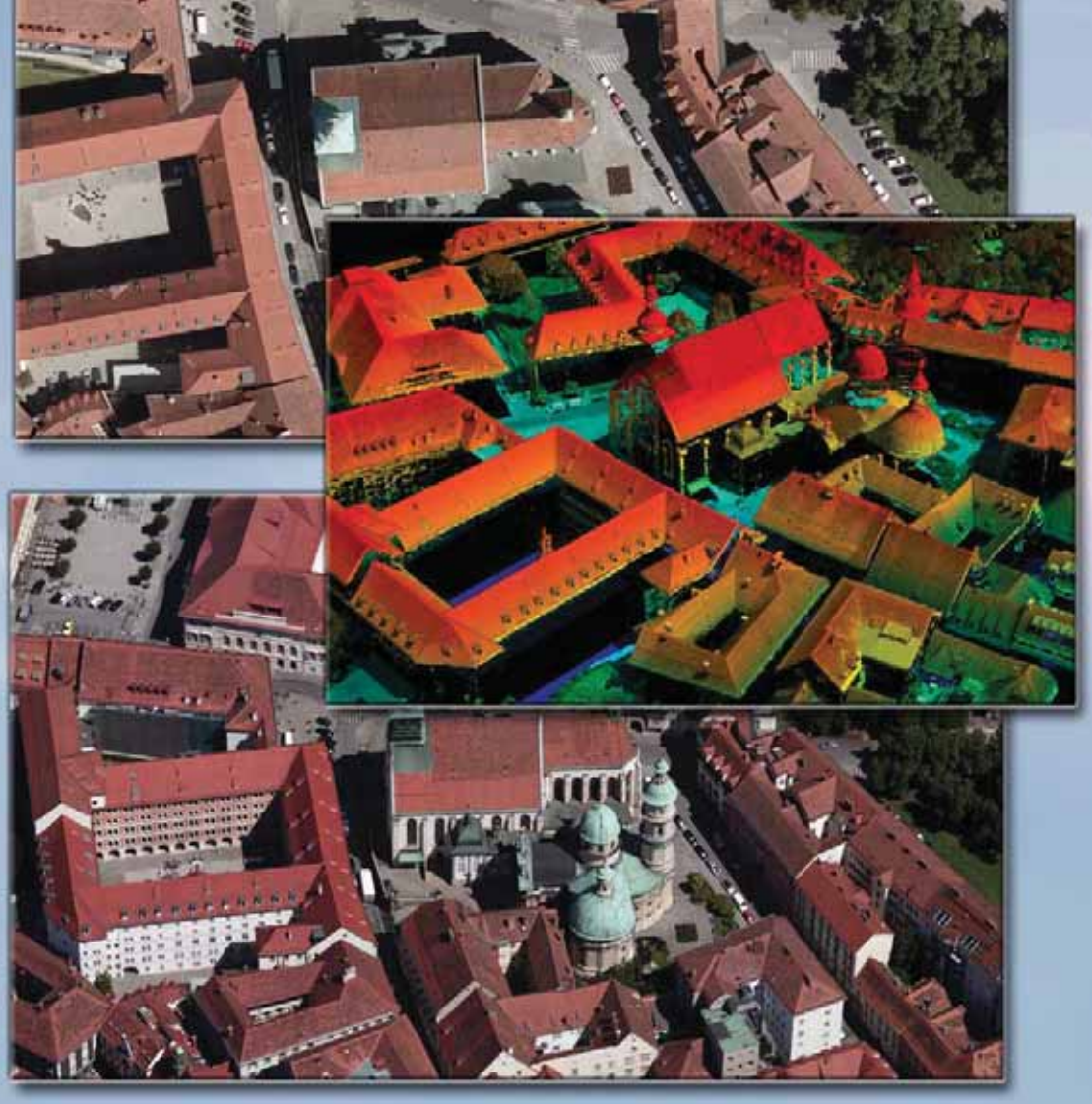

from all angles.

Need a large format camera system for low-altitude, corridor missions? High-altitude ortho collections? Something in between?

Need to be able to collect oblique imagery? How about oblique and nadir imagery in panchromatic, color and near-infrared all in the same pass?

Need a software system that will allow you to take that aerial imagery and create point clouds in LAS format, digital surface models, and orthomosaics? **No problem.**

The UltraCam series of large format photogrammetric digital aerial sensors includes systems of varying image footprints and focal lengths. Whether you need multi-spectral nadir imagery or obliques—or both from the same camera—we have a system for you.

Meanwhile, our highly automated UltraMap photogrammetric workflow software enables you to process UltraCam data to Level 3, radiometrically corrected and color-balanced imagery, high-density point clouds, DSMs, DSMorthos and DTMorthos.

We've got you covered.

iFlyUltraCam.com ULTRACAM Microsoft

©2015 Microsoft Corporation. All rights reserved. Microsoft, UltraMap and UltraCam Osprey, Eagle, Falcon and Hawk are either registered trademarks or trademarks of Microsoft Corporation in the United States and/or other countries.